

INVESTIGATION OF HORIZONTAL CRUSTAL MOVEMENTS
IN ICELAND USING A MODULATED LIGHT-BEAM DEVICE

A thesis submitted

by

RODNEY WILLIAM CALVERT, B.A.

for the

Degree of Doctor of Philosophy

of

The University of London

October, 1969.

Department of Geophysics,
Imperial College,
London, S.W.7.

ABSTRACT

Horizontal movements of the earth's crust have been investigated using a Mekometer, a modulated light-beam distance measuring device, developed at the United Kingdom's National Physical Laboratory, Teddington, by K.D. Froome and R.H. Bradsell. The Mekometer, which times the return flight of a light pulse from itself to a target reflector, has a range of up to three kilometres, and a sensitivity of 0.1 mm, or 1 part in 10^7 , whichever is the greater. The accuracy is normally limited by uncertainty of the refractive index of the air along the light path. Methods have been developed to increase this accuracy.

The measurements were made in Iceland to provide information concerning the tectonic movements associated with mid-ocean ridges. In one of the areas studied a shear strain with a maximum extension of 5.0 parts per million per year, in a direction 53° east of north has been measured. The orientation of the stress field suggested by this strain is consistent with the surface cracks observed in the area. Possible origins of this stress field are also discussed.

ACKNOWLEDGEMENTS

The author sincerely wishes to thank all those who have helped and contributed towards this project.

Foremost among these are K.D. Froome and R.H. Bradsell who lent their valuable Mekometer for the work, and shared a keen interest in the results. Under their supervision I spent a very pleasant period at the National Physical Laboratory assembling another Mekometer. The experience thus gained proved extremely useful in conducting successful field operations. R.H. Bradsell, who was a frequent visitor to Iceland and took some of the early readings, also gave guidance throughout the work, especially on electronic problems.

This work owes much to those who worked so hard and cheerfully collecting the data in Iceland, often under arduous conditions. They were Colin Andrews, Bob Bradsell, James Brander, Chris St. John, John Piper, Bob Selby, Gerry Wothington and my wife Rosemary who set a standard in book keeping and precise meteorology, and later assisted with some of the drawings. It is due to these members of the various expeditions that such an ambitious field programme was possible.

I should also like to thank Agust Bodvasson, the head of Landmaelingar Islands, the Icelandic Geodetic Survey, who was our official sponsor in Iceland, appointed by the Icelandic National Research Council. Both he and Agust Gudmundson, also

of Landmaelingar, took great trouble to ensure our early work was a success. Landmaelingar recommended the design of the geodetic pillars and assisted with some of the early building.

I should also like to acknowledge the help of Professor R.G. Mason, my supervisor, who suggested the work, has given encouragement throughout and suggested many improvements to the final text.

The author was supported throughout this work by a generous studentship awarded by Royal Dutch Shell, for which he is very grateful.

This work could not have taken place without a substantial grant from the Natural Environmental Research Council.

Finally I am very grateful for the prompt and careful typing of the thesis by Mrs. Julia Kelland.

R.W. Calvert.

October, 1969.

CONTENTS

	Page
CHAPTER 1 INTRODUCTION	8
1.1 The Theories of Continental Drift and Sea-Floor Spreading.	8
1.2 Previous Work.	15
1.3 The Present Work.	16
CHAPTER 2 THE MEKOMETER	22
2.1 The Modulation Principle.	25
2.2 The Optical System.	29
2.3 The Electronic System.	30
2.4 The Refractive Index Compensation.	40
2.5 Other Distance Measuring Instruments.	41
2.5.1 The AGA Geodimeter, Model 6.	41
2.5.2 The Tellurometer Model NRA-101.	42
2.6 Advantages and Disadvantages of the Mekometer over other Systems.	44
2.7 Possible Modifications for Geophysical Use.	45
2.7.1 Increasing the range.	45
2.7.2 Making the frequency more certain.	46
2.7.3 Atmospheric refractive index determination.	47
CHAPTER 3 THE CORRECTIONS	49
3.1 The Theory of the Atmospheric Corrections.	49
3.1.1 The effective wavelength.	50
3.1.2 The dispersion of the atmosphere.	50
3.2 The Frequency measurement of the Mekometer.	52
3.2.1 Description of WILLEM.	57
3.3 Obtaining the Atmospheric Corrections.	58
3.3.1 Pressure.	58
3.3.2 Humidity.	59
3.3.3 Air temperature.	59
3.3.3.1 Description of temperature probes.	60
3.4 The Geometrical End Corrections.	68

3.4.1	The reflector calibration.	68
3.4.2	Geometrical corrections at the Mekometer end.	71
3.4.2.1	The tiltmeter.	71
3.4.3	Geometrical corrections at the reflector end.	73
3.5	The 48 Hour Watch as a Check on the Atmospheric Corrections.	79
CHAPTER 4	PRACTICAL CONSIDERATIONS	87
4.1	Description of the Pillars.	89
4.2	The Laying out of the Networks.	92
4.3	Field Procedure for Measurement.	94
4.3.1	Mekometer operation.	98
4.3.2	Problems likely to be met with in the field.	103
4.3.2.1	Wind.	103
4.3.2.2	Rain.	104
4.3.2.3	Intense cold.	104
4.3.2.4	Background light.	105
4.3.2.5	Prolonged sunshine.	105
CHAPTER 5	THE RESULTS AND THEIR ERRORS	107
5.1	The Computing of the Results.	107
5.2	The Line Lengths.	111
5.3	Estimation of the Various Errors.	133
5.3.1	Errors due to cavity phase settings.	133
5.3.2	Errors due to errors in pressure measurement.	135
5.3.3	Errors due to errors in humidity measurement.	136
5.3.4	Geometrical errors.	136
5.3.5	Errors due to uncertainty in air temperature.	137
5.3.5.1	The equilibrium states of the atmosphere.	139
5.3.5.2	Ray bending.	141
5.3.5.3	Causes of the random scatter in the observed readings.	143
5.3.5.4	Systematic temperature errors.	146
5.3.6	Errors due to equipment faults and operator mistakes.	153
5.4	Determination of the Rates of Movement.	156

CHAPTER 6	INTERPRETATION AND CONCLUSIONS	163
6.1	Reykjanes Interpretation.	163
6.1.1	Fitting a shear.	163
6.1.2	The shear fit results.	167
6.1.3	Interpretation of the faulting.	169
6.2	Generalisations from the Reykjanes Results.	177
6.3	Interpretation of the Thingvellir Results.	184
6.4	The Horizontal Tectonics of Iceland.	186
6.5	The Origins of Iceland.	190
6.6	Conclusions.	191
REFERENCES		193

CHAPTER 1

INTRODUCTION

1.1 The Theories of Continental Drift and Sea-Floor Spreading.

In recent years the theories of continental drift and sea-floor spreading have become widely accepted as providing the best explanation of global tectonics. Work on the magnetic anomalies caused by ocean crust has furnished estimates of how the motion has taken place over the last few million years. The work described in this thesis was aimed at providing information about how the processes are taking place at the present time.

The idea of sea-floor spreading was first put forward by A. Holmes (1944). The theory was enlarged upon by Dietz (1961) and Hess (1962), and since then much new evidence has been put forward to support these ideas. A brief summary of the theories is given here, a fuller version of the present ideas is given by Isacks, Oliver and Sykes (1968).

The surface of the earth is thought to be composed of a strong rigid layer, the lithosphere, which is up to 100 km in thickness. Beneath the lithosphere lies the asthenosphere which has no strength on the geological time scale. It is made up of plastic rock which may creep and flow.

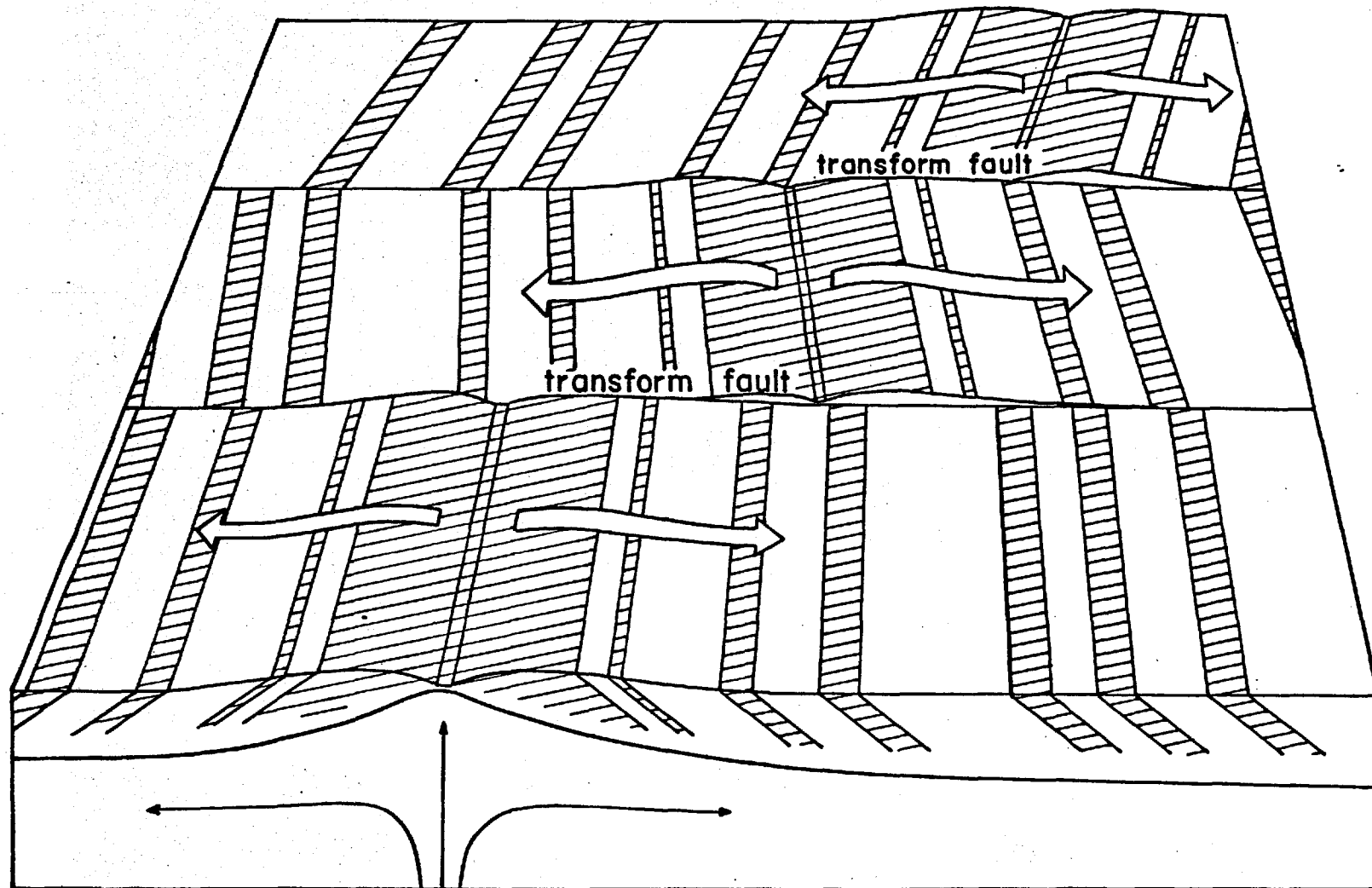
The lithosphere is divided into blocks of varying size which are thought to be floating on the asthenosphere. The boundaries of these blocks are the zones of seismic activity in the earth, i.e. the ocean ridges, the island arc and trench systems and the major strike-slip faults. The differing tectonic features found on the earth are the results of various relative movements of these blocks.

Where the blocks move apart ocean ridges are formed. For example, the Mid-Atlantic Ridge is caused by the separation of the Americas from Africa and Europe. Where the blocks are moving together one underthrusts the other to produce a trench and island arc when the two blocks are oceanic, or an ocean trench and coastal range if one block is continental. An example of the former is the Japanese island arc with its associated trench, and of the latter, the Andes bordering South America. Where the blocks are moving alongside each other major strike-slip faults occur of which the most famous is the San Andreas fault system.

A strength of the theory is that it is supported by evidence from widely differing fields of experiment. The theory of sea-floor spreading suggests that new crust is formed at an ocean ridge and then carried away from the ridge, as on a conveyor belt, as more crust is generated. Early evidence for this was the increasing age of oceanic islands with their distance from ridge axes.

The most spectacular evidence in support of the theory came from the characteristic ocean floor magnetic anomalies which were first reported by Mason and Raff (1961). These magnetic anomalies are long strip-like anomalies parallel to the

A BLOCK OF OCEAN RIDGE SHOWING TRANSFORM FAULTS



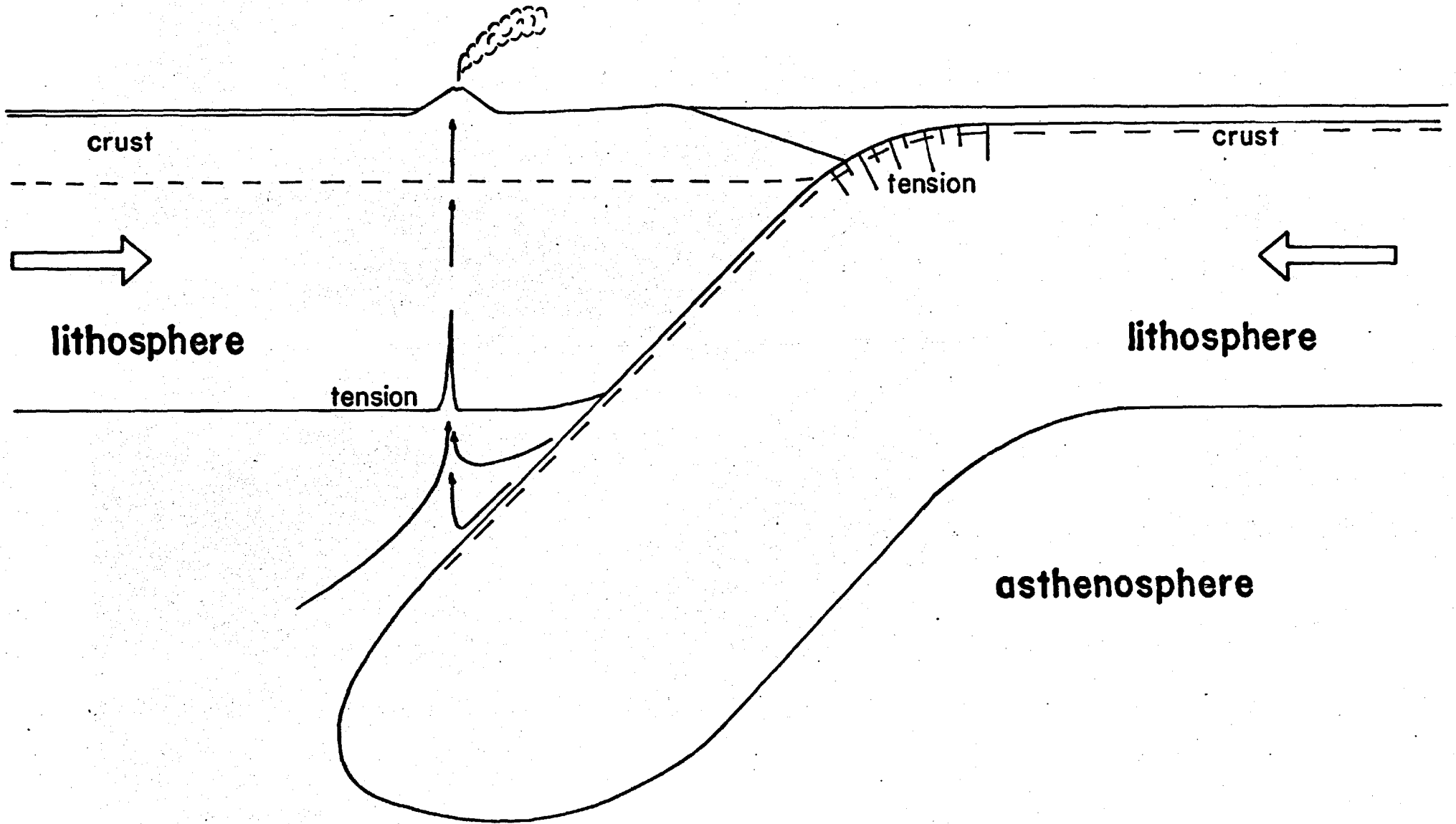
magnetization
▨ normal
□ reversed

ocean ridge and symmetrical about it. They were explained by Vine and Matthews (1963) as being due to normally and reversely magnetised crust being formed between geomagnetic reversals. Experiments carried out on rocks to find their directions of magnetisation have shown that some are magnetised in the opposite direction to that expected. It is thought that the earth's magnetic field has two stable states, one normal as at present, and another reversed, which is a field of the opposite sense. From various dating experiments the periods of normal and reversed field have been firmly established for the last 10 million years and less well for older periods.

Vine and Matthews showed that by assuming a constant spreading rate the linear magnetic anomalies could be explained in sense and magnitude by crust being magnetised in the prevailing earth's magnetic field as it formed. The magnetised crust was then transported from the ridge rather like a recording on a magnetic tape.

Large off-sets of the magnetic pattern have been noticed along fault zones. Some of these off-sets suggested transcurrent faulting with displacements of up to thousands of kilometres. Seismic evidence however suggested that displacements were taking place in an opposite sense to those indicated by the off-sets of the magnetic anomaly. This problem was solved by Wilson (1965) who postulated the transform fault. The latter is formed wherever the ocean ridge is off-set. Each branch generates crust in the normal way causing a counter current between the two branches.

A PROFILE OF AN ISLAND-ARC



The mechanism of crust generation is thought to be by dyke injection and fissure eruptions. This has been supported by work in Iceland (Walker, 1965).

More recent support for the new theory of global tectonics has come from seismology. Fault plane solutions have been carried out for earthquakes from many parts of the world. It has been shown by Le Pichon (1968) that the slip vectors derived from these studies are compatible with the motion of large rigid blocks of the earth's crust.

Other evidence from many disciplines supports the idea of continental drift and sea-floor spreading. Floral and faunal evidence suggests that the Americas and Europe and Africa were once joined. The coastlines of the two land masses can also be made to fit together closely (Bullard, 1965). It has been shown that the ocean sediments are thicker away from the ridge axes (Ewing, 1964). The ages of the oldest fossils on the ocean bed also increase away from the ocean ridge (Funnel, 1969).

The theory of the formation of island arcs and their associated deeps by one block of lithosphere underthrusting another also seems to fit the evidence very well. The island arcs are marked by high isostatic gravity anomalies. The islands or continental margins are notable for evidence of severe compression normal to the arcs.

The island arcs are also notable as being sources of deep focus earthquakes. The fault plane solutions and focal position of these earthquakes are consistent with one slab of lithosphere underthrusting another. Seismic refraction studies

of island arcs also support this structure (Badgley, 1965). Graben-like structures are found at the position of downwarping caused by the local tension on the seaward slope of the trench.

The strike-slip motion of the plate boundaries is best characterised by the San Andreas fault. This seems to be a vast transform fault connecting ridges off Oregon with those in the Gulf of California (Isacks, 1968). Displacements of up to 500 km have occurred along this fault. Most of the earthquake activity is confined to the upper 5-10 km so that at depths of 20 km the deformation must be by plastic creeping.

Little is known at present about the driving mechanism for these movements. It has been suggested that the motion is due to large scale convection currents within the earth's mantle (Bott, 1967). The shape of the required convection cells however seems rather unlikely if the convection cells are to penetrate to great depth. To overcome some of the difficulties the movements have been postulated as arising from currents caused by the interaction of a proposed asthenosphere with the lithosphere. The asthenosphere is supposed to lie between 100 km and several hundred kilometres beneath the earth's surface. It coincides with a layer which strongly attenuates seismic S-waves. Some light should be thrown on the problem by global gravity trends being established from satellite data.

1.2 Previous Work.

The direct measurement of some crustal movements has already taken place, mostly in California along the great San Andreas fault system. Extensive work has been carried out by the State of California's Department of Water Resources (1968), who have a practical interest in the movements along the San Andreas fault zone.

Their work was started in 1959 based upon measuring the lengths of isolated lines across the fault zone. During the period 1965 to 1967 further lines were added, many in the form of closed figures. The measurements were made using a Geodimeter M2A, a light beam distance measuring device. These measurements have shown that side-slip movement is taking place along the San Andreas fault at a rate of about four centimetres a year. The individual lines were 8-20 miles long and measured with an accuracy better than two centimetres.

In the Dixie Valley-Fairview Peak area of Nevada (Meister, 1968) strains of up to 3×10^{-4} have been measured by the conventional methods of geodetic surveying. These strains occurred during four earthquakes in 1954. Near the fault, the extension was generally greater than the compression and at right angles to it. The fault line was approximately at 40 degrees to the direction of maximum compression. This work was carried out using a theodolite on a triangulation network.

Repeated measurements have also been made in Japan by Kasahara et al (1968) using a geodimeter on specially built base lines. Their networks, consisting of three lines meeting at a point, were built to monitor the horizontal deformation

associated with the very strong Matsushiro earthquake swarm. The lines were about three kilometres in length and measured with an accuracy quoted as "probably about ± 10 mm". Repeated measurements have been made since October 1965. The deformations reached a climax in October 1966 when one of the networks showed changes in the three lines of +116 cm, +72 cm and -22 cm. The strain ellipse postulated agreed with the polarity of P-wave first arrivals noted at nearby seismic stations. During the phase of decaying seismicity the lines recovered slightly and by March 1968 had recovered by approximately 10 per cent. Ground fissures suggested that the original movements had taken place by means of left lateral strike-slip faulting.

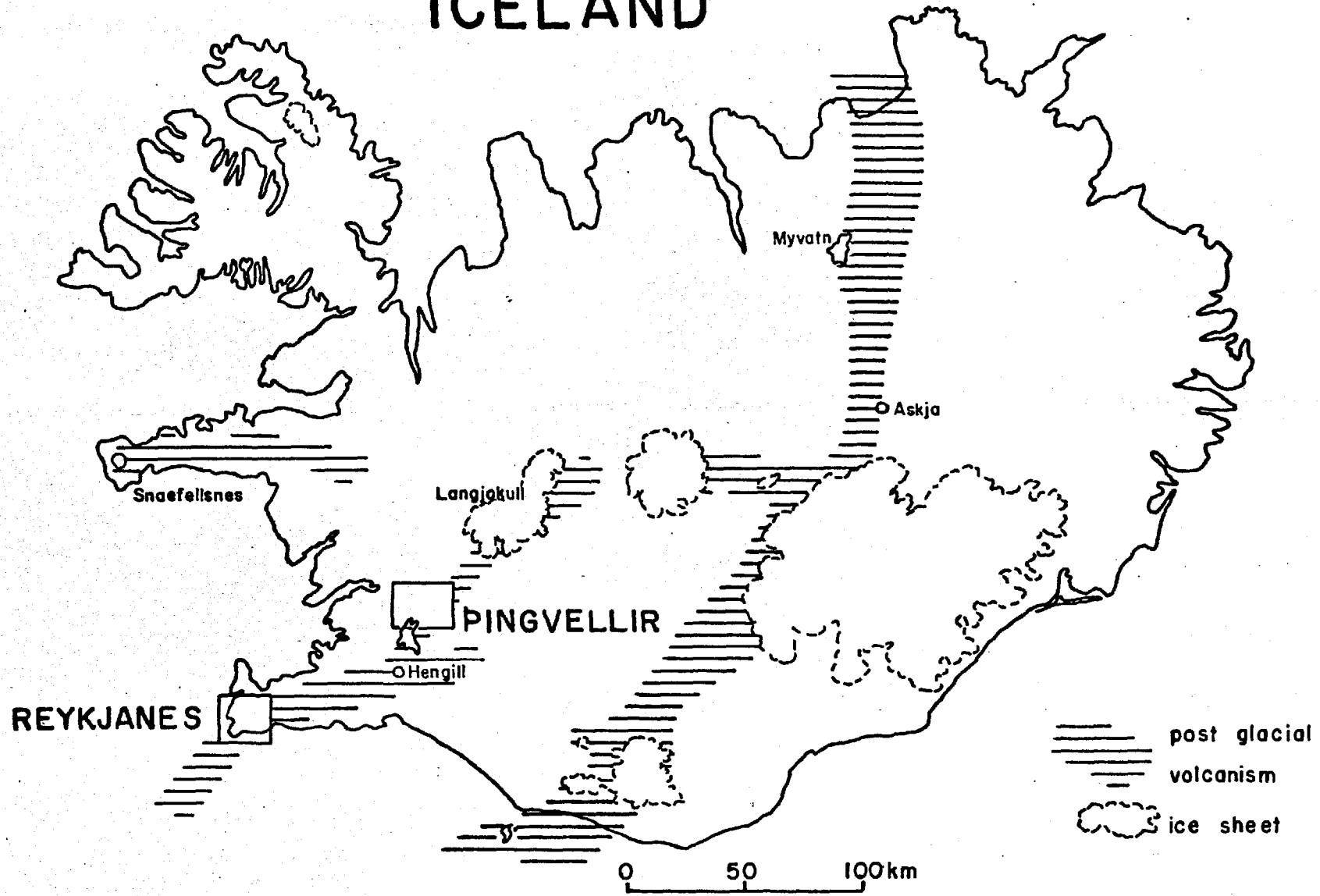
Some similar work has also been carried out in Iceland. A network in the Myvatn area, in the north of Iceland, was constructed and first measured in 1938 by Niemczyk. This was remeasured in 1965 by Gerke (1967) who found that the errors in the earlier measurements were so large that no movements could be detected.

In 1967 Decker (1968) made geodimeter traverses across both of the active zones in southern Iceland and measured some lines on Askja, a volcano in central Iceland. As yet this survey has not been repeated.

1.3 The Present Work.

As yet no direct measurement of the horizontal strain associated with ocean ridges has been reported. Apart from the work on the San Andreas fault system, the deformations measured in both America and Japan have been associated with

ICELAND



violent earthquake swarms resulting from stress build-up in the crust and lithosphere. On ocean ridges however, the crust and lithosphere are greatly thinned making stress build-up and major earthquakes less likely. Of 175 earthquakes with a magnitude greater than or equal to 7.9 reported by Richter (1958) only five originated in the world rift system. Nearly all the large earthquakes on the rift system seem to occur along the major transform faults.

Since the crust is so thin over ocean ridges any movements should be closely connected with convection currents or movements in the asthenosphere. The most favourable place to study the movements across an ocean ridge seems to be Iceland. Iceland is unique in being astride a typical section of ocean ridge; it exhibits many of the features expected of sea-floor spreading.

Iceland extends outside the active zone of the mid-Atlantic ridge to the east and to the west. It is divided by an active zone running from north-east to south-west which has a characteristic graben structure. In the southern half of Iceland the zone divides into two branches. The island is nearly entirely made up of basalt in the form of gently dipping lava piles and central volcanoes. Recent activity is well marked by the characteristic palagonite formations formed during the last ice age, and better still by the narrow zones of post glacial activity.

The older rocks are found to the east and west of Iceland with the younger rocks in the central zone. The post glacial activity has taken the form of sometimes large fissure

eruptions and the formation of open fissures. These features are largely parallel and are suggestive of tension across the zone.

The older lavas gently dip towards the active zone (Walker, 1965) and were erupted through dykes which are mostly parallel to present day fissures. As a result of extensive work in the eastern part of Iceland Walker suggested that crustal drift in Iceland was taking place by the forcing apart of east and west by dyke injection at the centre. The open fissures were visualised as being due to dykes which had not reached the surface.

Since the active zones mark the boundaries of the blocks of crust in Iceland, the relative movements between the blocks can be determined by studying the deformations occurring in these active zones. The aim of the present work was to study the deformations taking place, or at least develop a method by which the deformations might be measured.

Since these active zones are at least a few kilometres wide the problem is one of accurate surveying. As the aim was to measure movements over periods of only a few months or less the expected strains were very small, of the order of 10^{-6} . Distance measurements of this accuracy have recently been made feasible in the field by the development of electromagnetic distance measuring instruments. These instruments measure the times of flight of electromagnetic pulses along the line to be measured. Their accuracy is theoretically limited by a knowledge of the refractive index of the air along the measured lines.

The most advanced of these instruments over the range of 50 m to 2 km is the Mekometer developed at the National Physical Laboratory, Teddington by Froome and Bradsell (1966). The Mekometer has a sensitivity of 0.1 mm or 1 part in 10^7 , and an accuracy normally limited by uncertainties of the atmospheric temperatures. This instrument is not yet commercially available, but a prototype was kindly loaned to us by N.P.L.

The first field season in Iceland was from June until October 1967. During this period two geodetic networks were set up in the south-west of Iceland at Reykjanes and Thingvellir, and some preliminary measurements made. These networks consisted of concrete pillars laid out in rigid triangulation grids. The points of reference were the centres of mounting plates cemented into the tops of these pillars.

The second period of measurements was during the last week of March 1968. The third field season was from July until September 1968, during which time the Reykjanes network was extended and completely measured, and the Thingvellir network partially measured. The fourth field season was from March until May 1969, when both networks were completely measured. The results from these four surveys are discussed in this thesis and the work continues.

Significant movements of the order of five parts per million per year have been detected. In many cases these strains are associated with surface cracks, so an attempt has also been made to relate these observed deformations and cracks to the pronounced fissure patterns seen elsewhere in Iceland.

The range and sensitivity of the Mekometer are such that it was found convenient to use a modulation wave-length approximately two feet long. For simplicity of operation for the general user it was decided to make the instrument read distances directly in feet. Throughout this thesis therefore Mekometer readings and results are quoted in feet.

CHAPTER 2

THE MEKOMETER

Much of the information contained in this chapter is taken from papers published by Froome and Bradsell by kind permission (Froome and Bradsell 1966; Bradsell 1966; Froome and Bradsell 1968).

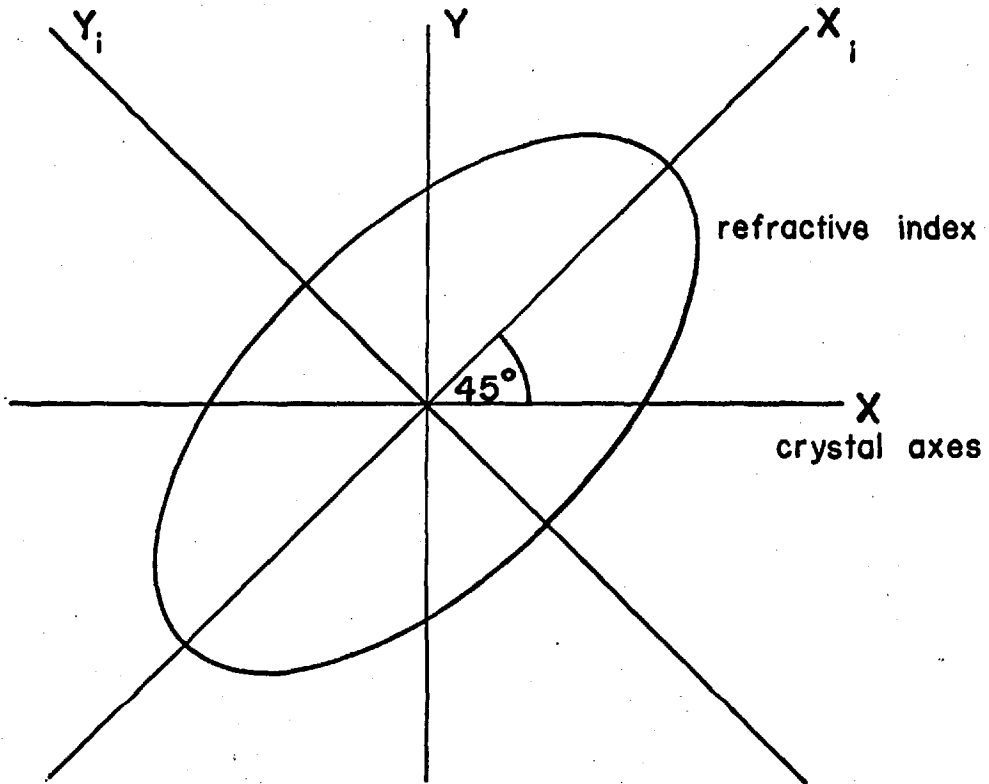
The Mekometer is a distance measuring instrument designed and made at the National Physical Laboratory by Dr. K.D. Froome and Mr. R.H. Bradsell. It can measure with an accuracy up to 0.1 mm and operate over distances of up to three kilometres. It uses a modulated light beam and counts the number of wavelengths between itself and a target reflector.

The Mekometer was not designed for geophysical use but for civil engineering projects and short range surveying, for example in towns. It has been used for laying out the existing and proposed radio telescopes at Cambridge. It has been used to lay out the new storage ring and particle accelerator at C.E.R.N. in Switzerland. The new railway tunnel for Heathrow Airport has also been surveyed by the Mekometer. For projects such as these the Mekometer produces answers as good as, if not better than, by taping, in a fraction of the time, at a fraction of the cost. It is extremely costly to lay invar tapes across runways or through built-up areas.

It is impossible to lay tapes from receiver to receiver on a radio telescope array, as the points to be measured are high off the ground. Because of its high accuracy the Mekometer now makes feasible measurements of dam deformation and rock creep, which could only be indirectly inferred previously.

The commercial applications of this instrument are limitless. Where accurate work previously had to be done by taping, it can now be done by Mekometer. This makes surveying by traverse much easier than before; triangulation is impossible in tunnels, built-up areas and mines. Triangulation networks can also now be surveyed more accurately by trilateration than by theodolite.

Because of this wide range of applications and possible users the Mekometer has been designed to be as simple to use as possible. By referring distances to a compensating reference cavity the need for refractive index corrections is eliminated, except in extreme conditions, or where the highest accuracy is required. The distance is obtained directly in feet without any need for calculation except perhaps to subtract a two feet end correction. The Mekometer is light and portable, being divided into the instrument itself and a power supply and battery unit. The two units each weigh about 5.5 kg (12 lbs). The power consumption is only about 16 watts, enabling an average day's work to be done using the internal battery.



Polar diagram of refractive index in X-Y plane of modulating crystals

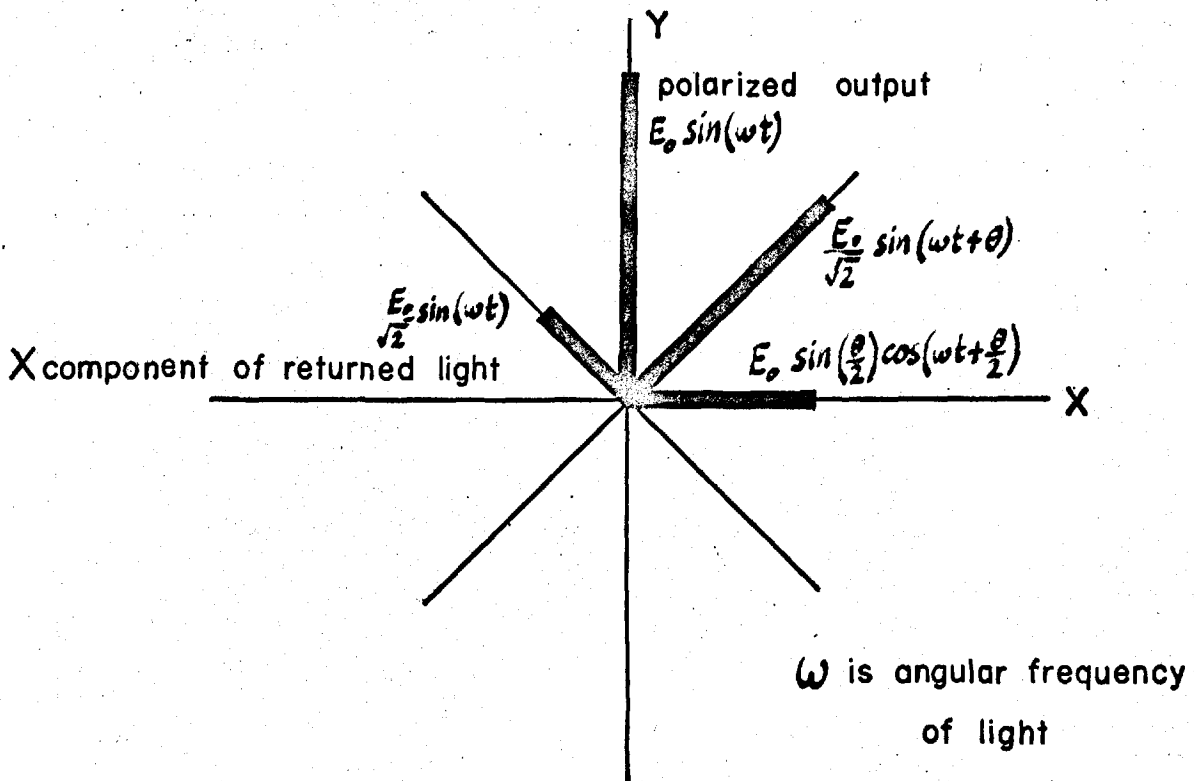


Diagram showing components of electric vectors and returned light

2.1 The Modulation Principle.

The heart of the Mekometer is the modulation system. The light beam is modulated at just under 500 MHz to give a modulation wavelength of two feet. Modulation is achieved by means of KDP (potassium dihydrogen phosphate) crystals which exhibit a linear electro-optic effect (Pockels effect).

KDP is a uniaxial crystal having two equal refractive indices. The indicatrix thus has the equation

$$\frac{1}{n^2} (x_i^2 + y_i^2) + \left(\frac{z_i}{n_c}\right)^2 = 1$$

For an electric field in the Z direction the refractive indices become

$$n_{x_i} = n_o + \frac{1}{2} r E_z$$

$$n_{y_i} = n_o - \frac{1}{2} r E_z$$

$$n_{z_i} = n_c$$

where r is an electro-optic constant.

The crystal axes are in fact at 45° to the axes of the indicatrix, thus if plane polarised light is propagated along the Z axis with its plane of polarisation parallel to the X or Y crystal axes there will be a phase difference θ between the x_i and y_i components given by

$$\theta = \frac{2\pi d}{\lambda} (n_{x_i} - n_{y_i})$$

where d = the thickness of the crystal

λ = the wavelength of light.

This will in general give elliptically polarised light (plane polarised for $\theta = 0^\circ$ and circularly polarised for $\theta = 90^\circ$).

Substituting for n_{x_i} and n_{y_i} , we get

$$\theta = \frac{2\pi r V}{\lambda}$$

where $V = E_z d$, the voltage across the crystal.

The phase difference along the optic axis is thus a function of V only. If the applied field is alternating, the phase difference is

$$\theta_1 = \frac{\pi V}{V_m} \sin(\omega t)$$

where $V_m = \frac{\lambda}{2r}$ is the value of voltage (30 kv) which will produce maximum electro-optic effect, i.e. produce plane polarised light perpendicular to the initial plane, i.e. $\theta = \pi$

If the light is now allowed to travel to a reflector and then return through the crystal where will be an additional phase difference of

$$\theta_2 = \frac{\pi V}{V_m} \sin\left(\omega t + \frac{2\pi\delta}{L}\right) + e$$

where δ = length of light path to reflector

L = modulation wavelength in air

e = any additional ellipticity added along the light path, e.g. by the reflector.

The total phase difference θ is equal to $\theta_1 + \theta_2$

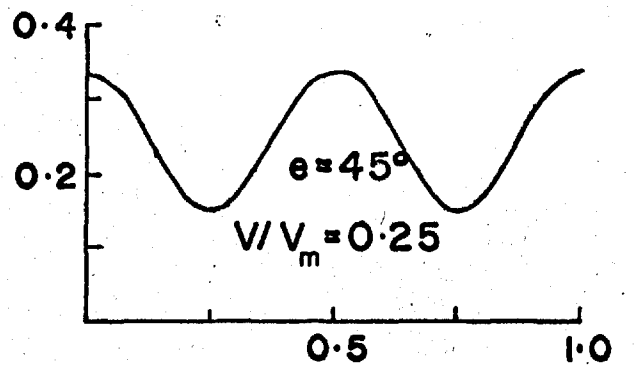
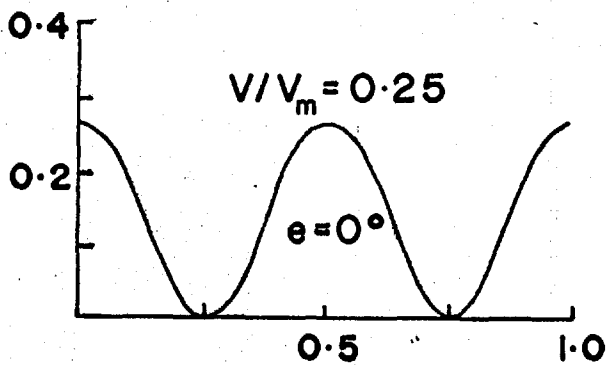
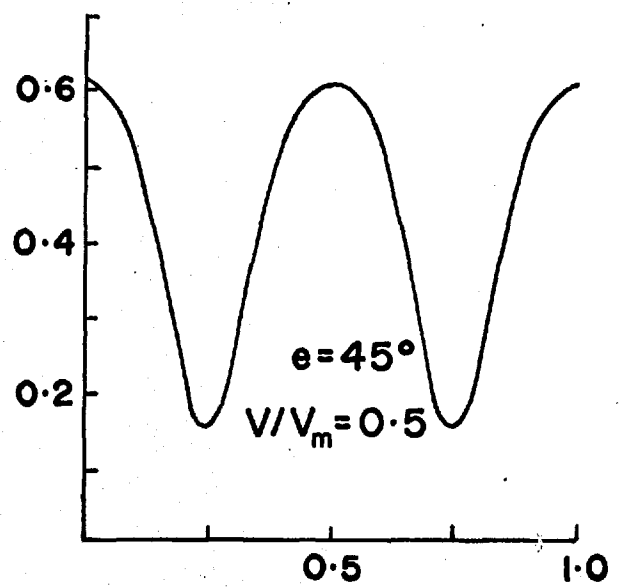
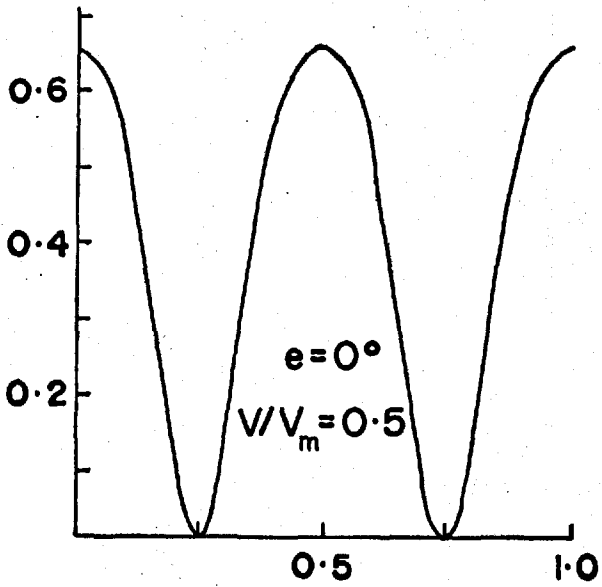
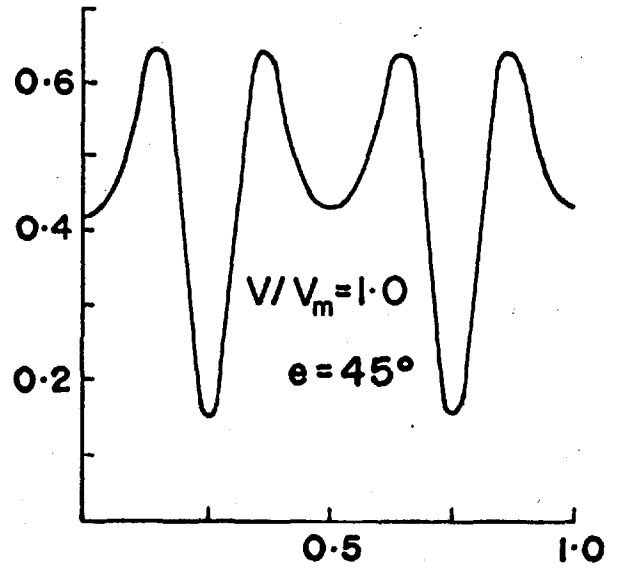
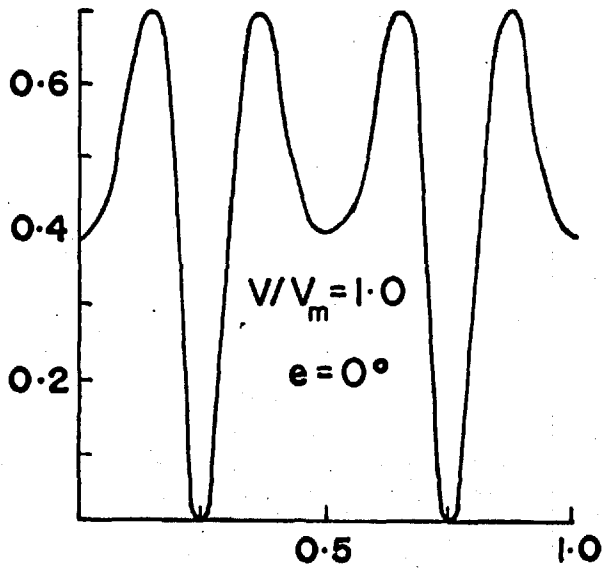
i.e.

$$\theta = \frac{2\pi V}{V_m} \sin\left(\omega t + \frac{2\pi\delta}{L}\right) \cos\left(\frac{2\pi\delta}{L}\right) + e$$

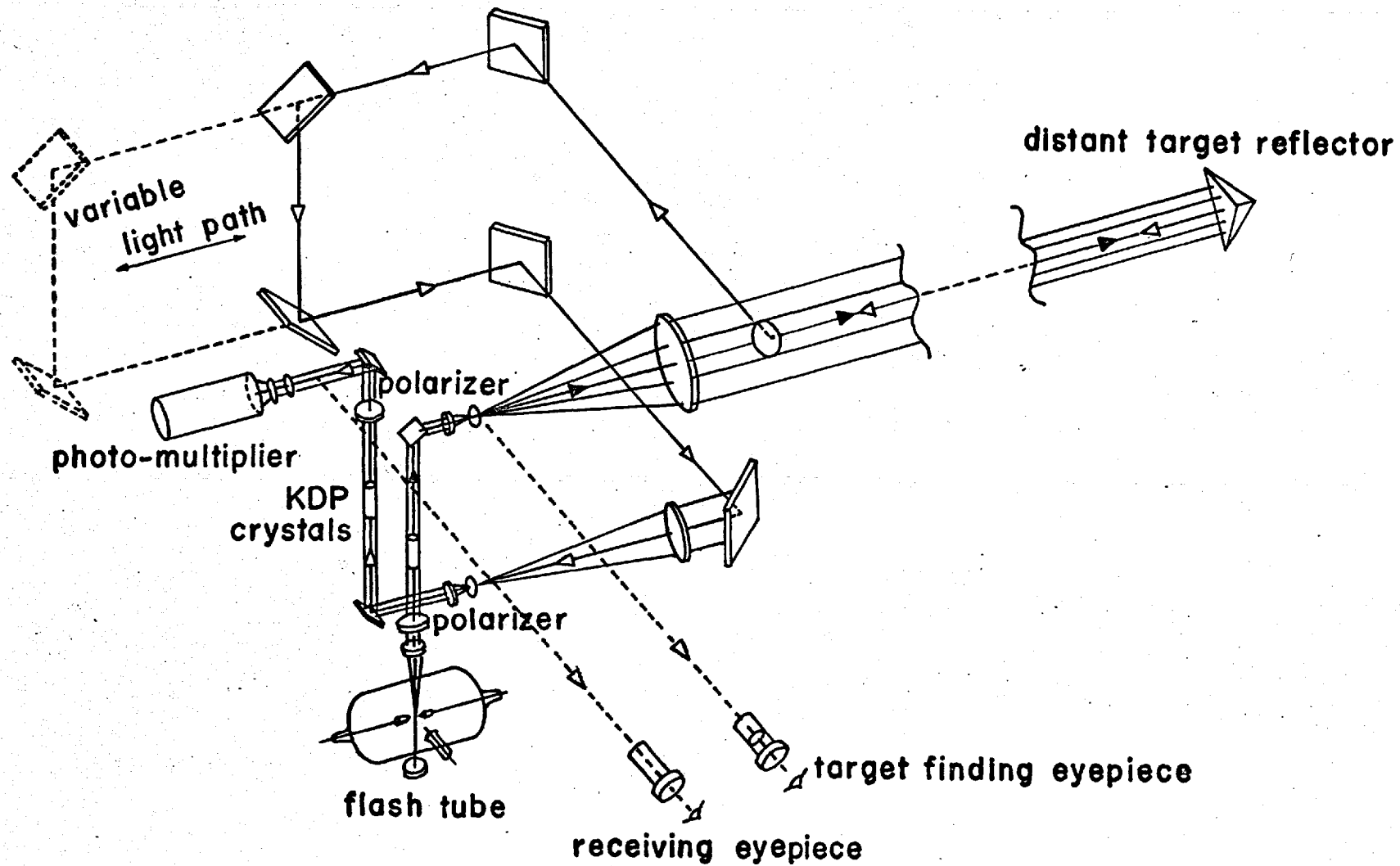
If the light is now passed through a second polariser crossed relative to the first the resultant intensity can be shown to be

$$I = I_0 \sin^2\left(\frac{\theta}{2}\right)$$

Intensity



Distance (modulation wavelengths)



MEKOMETER OPTICAL SYSTEM

The photodetector output is proportional to the time average of this.

$$I = \frac{I_0}{t} \int_0^t \sin^2 \left\{ \frac{\pi V}{V_m} \sin(\omega t + \frac{2\pi\delta}{L}) \cos(\frac{2\pi\delta}{L}) + \frac{e}{2} \right\} dt$$

This reduces to

$$I = \frac{I_0}{2} + \frac{I_0}{2} \text{cose} \left\{ e J_0 \left(2\pi \frac{V}{V_m} \cos \frac{2\pi\delta}{L} \right) \right\}$$

where J_0 is a Bessel function of zero order.

This function is shown plotted for various values of V/V_m and e .

The photodetector output is minimum for

$$\delta = \frac{NL}{2} + \frac{L}{4}$$

where N is an integer.

This shows that the system is an error-free modulator and demodulator. Any change in ellipticity e along the light path weakens the minimum, but does not alter its position. It can also be seen that it is best to use high values of V/V_m , which makes the minima sharp and the maxima broad and double.

2.2 The Optical System.

The light source is a Xenon flash tube. The light is made parallel, plane polarised and modulated. The beam is then imaged down by a short focal length lens at the focus of the transmitting objective. The emitted beam is limited to one milliradian divergence by a stop at the focus of the objective.

The light then passes along the line to be measured and is reflected back by the target, a retro-reflector. The returned light is deflected sideways by a mirror in front of the centre of the transmitting lens onto a trombone-like variable light path made up of plane mirrors. On emerging

from the variable light path the still parallel light is focussed by the receiving objective onto a very fine stop, which limits the diameter of the returned beam and thus cuts down the background light. The light is again rendered parallel, demodulated and plane polarised by a polariser crossed relative to the first. Finally, the beam is spread slightly and passed onto the photomultiplier detector.

Aiming the Mekometer is achieved by using two eyepieces. The first, the target-finding eyepiece looks onto a reflector at the focus of the transmitting objective; this mirror in fact contains the transmitting stop which is seen as a black spot. This system forms a moderately powerful telescope which is used for locating the target.

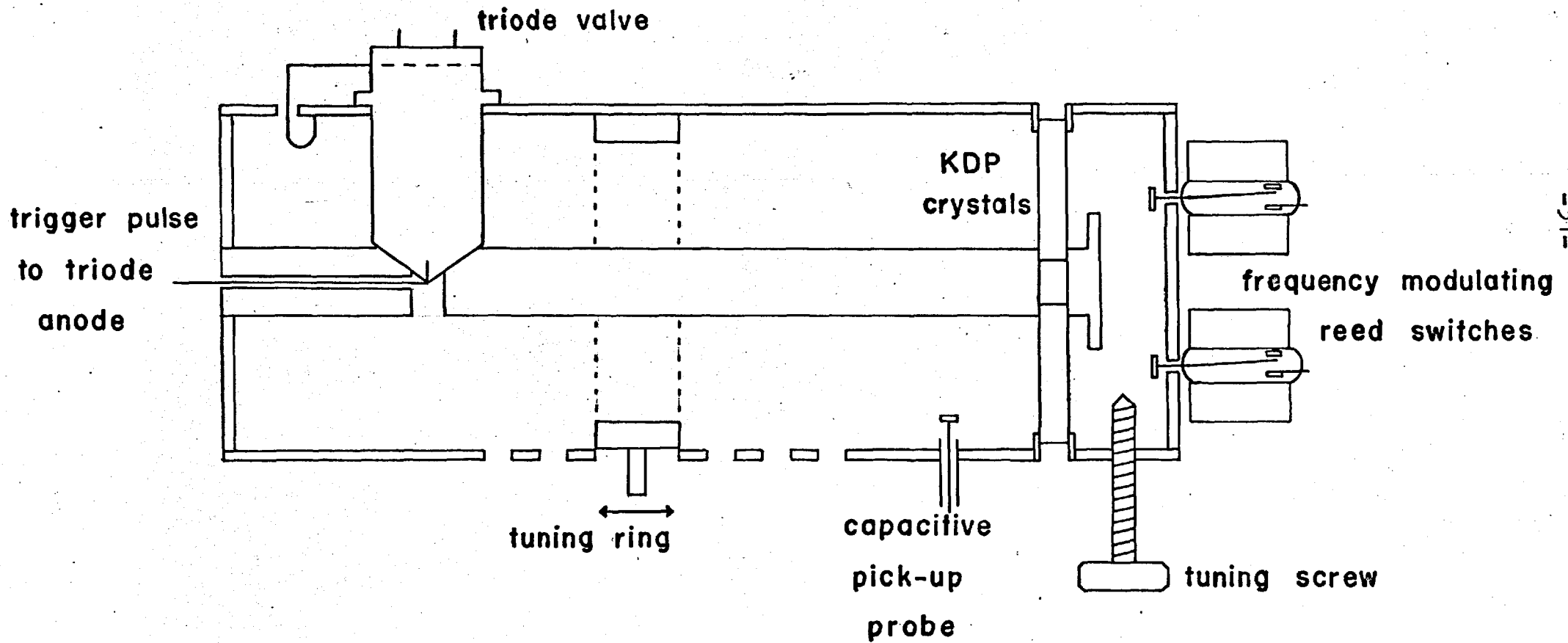
The returned light is seen through the receiving eyepiece, which looks onto a small reflector which can be made to intercept the returned beam just before it reaches the photomultiplier. This system forms a powerful telescope with a very small field of view (1 milliradian) which is used for the final aiming. The practical details of aiming the Mekometer are described in Chapter 4.

2.3 The Electronic System.

The Mekometer is a pulsed instrument and recycles 100 times per second.

Modulation of the light takes place in the modulating cavity, which is a coaxial quarter-wave cavity resonator. This is driven into strong VHF oscillation by pulsing a ceramic discseal triode valve producing about 100 W peak power. The

MODULATING CAVITY



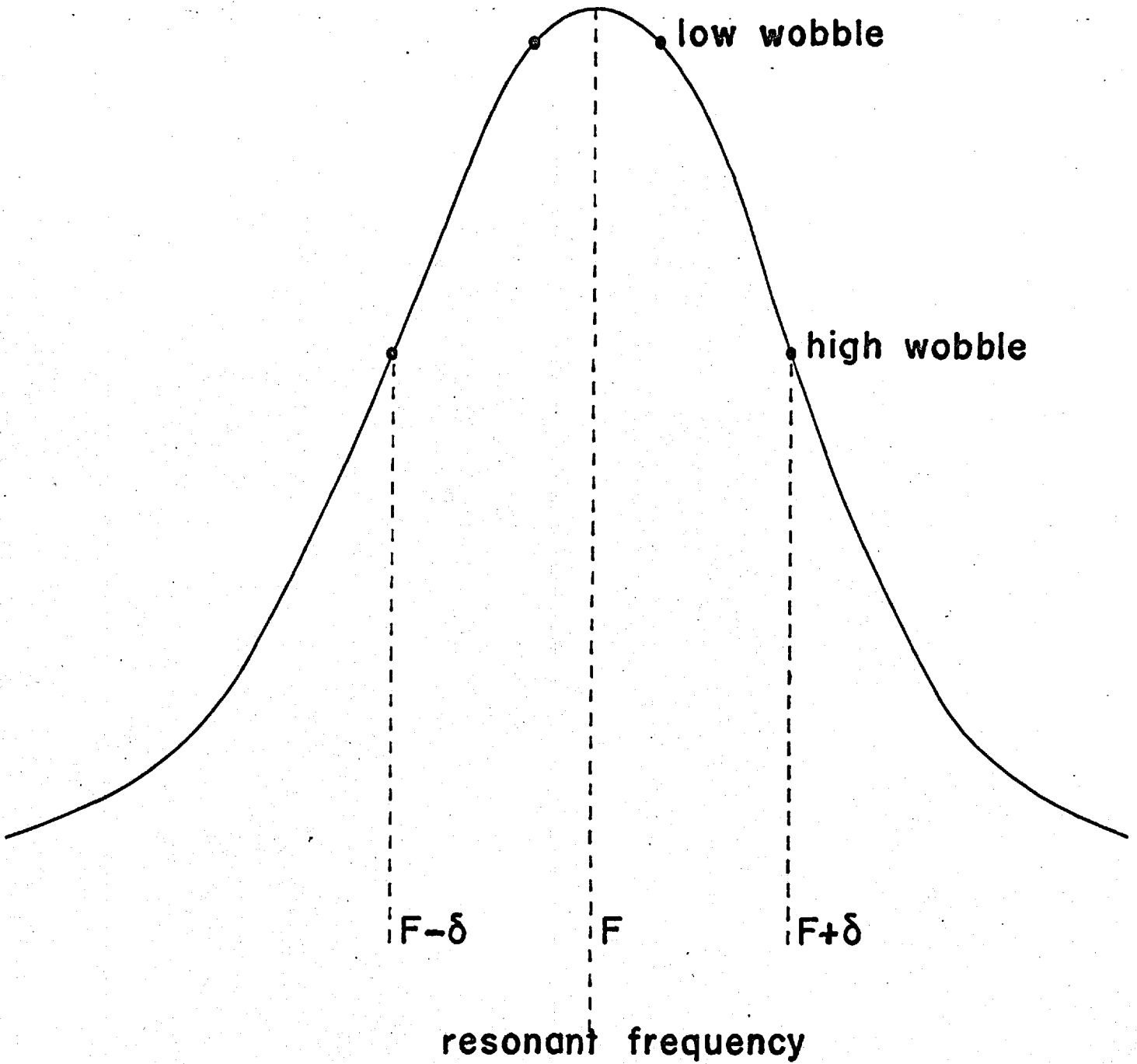
anode is impedance matched near the short-circuit end of the cavity. A low-Q tuned loop dips into the magnetic field at the high current end and feed UHF energy to the cathode of the valve. The cavity is in oscillation for $40\mu s$.

The KDP crystals are situated at the high impedance end of the cavity with their Z axes parallel to the electric field.

The frequency of the cavity is controlable by a tuning ring which slides inside it. This is used for the gross frequency changes required in resolving the number of feet in a given distance. There is also a small screw plunger which is used for fine adjustment of the modulating frequency.

The frequency is referred to a standard cavity, which is the frequency standard of the instrument. The standard cavity is an accurately made high-Q half-wave coaxial-line resonator. It is constructed of fused quartz, silver plated to produce conducting surfaces and mounted in an aluminium casing. It has a resonant frequency of nine times the fundamental modulating frequency. The modulation frequency is sampled by a small capacitive pick-up in the modulating cavity. This is fed across a step-recovery diode producing rich harmonics and loosely coupled by a small loop to the standard cavity. The resonance is then picked up by another small loop, detected and amplified. This gives a D.C. voltage which is displayed on the cavity meter. This may be set to a maximum value by tuning the modulating cavity. The setting is quite precise, as the standard cavity has a Q of 3,500.

RESONANCE CURVE OF STANDARD CAVITY



δ = frequency wobble

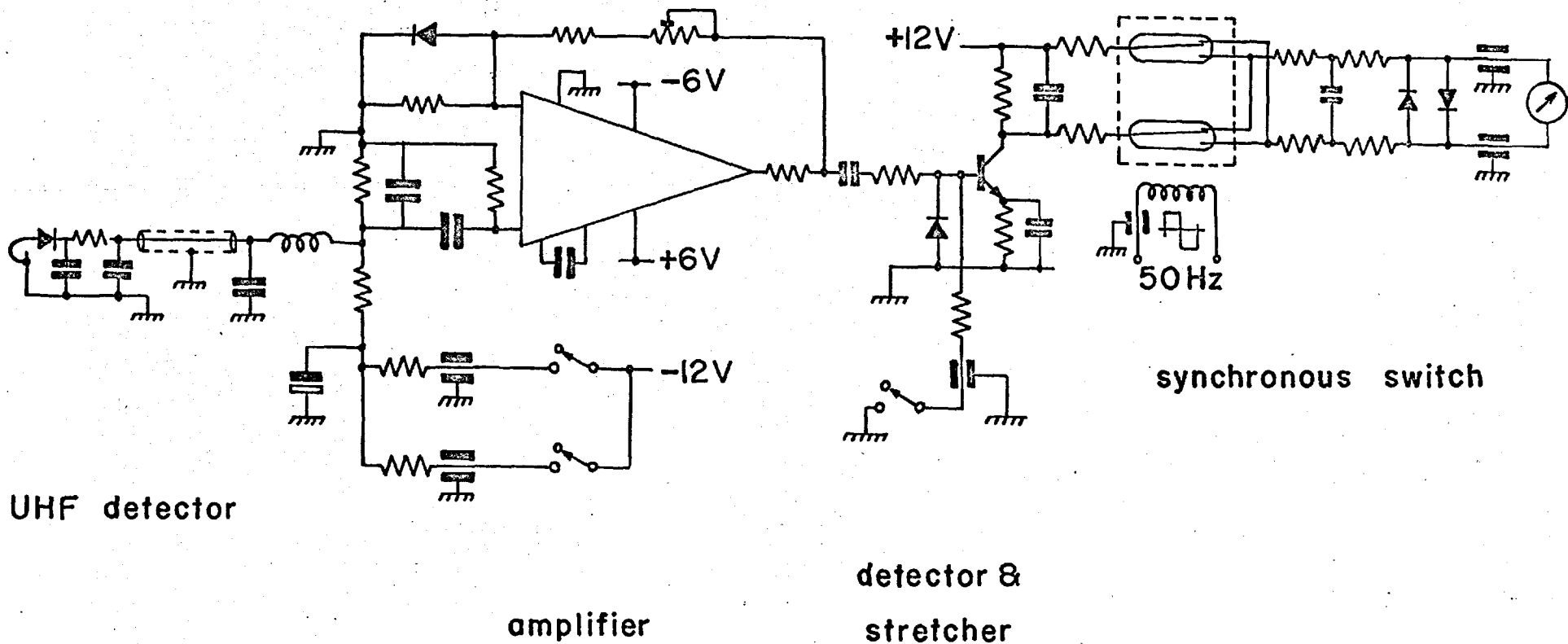
The frequency setting is much enhanced however by an ingenious frequency wobble method. By making alternate pulses of the modulating cavity slightly above and slightly below the nominal frequency and reversing the sign of alternate D.C. voltages to the meter a null setting is obtained which effectively compares the voltages on either side of the resonance curve. If these voltages are on the steep sides of the curve the setting can obviously be made very precisely. When the modulating cavity is on tune the cavity meter will read zero.

This frequency wobble is achieved by switching in and out of the modulating cavity a very small capacity, which is in fact a reed switch operated at 50 Hz. The synchronous switch which reverses the meter on alternate pulses is also a pair of reed switches. The circuit is shown.

With the modulation frequency being wobbled in this fashion the light phase minimum detection is also enhanced in a similar manner. The high tension voltage across the photomultiplier is adjustable by a gain control to allow for the great variation in light intensities to be measured. The fifth dynode of the photomultiplier is pulsed to its operating potential for $40 \mu\text{s}$ which very greatly increases the photomultiplier sensitivity for the duration of the pulse. This effectively gates the photomultiplier on only when there is a signal to be received.

The output from the anode of the photomultiplier sets a tuned circuit ringing as a ringing pulse stretcher. The frequency of this ringing circuit is so arranged that the output due to a square wave input of $40 \mu\text{s}$ duration, as would be the

SYNCHRONOUS RESONANCE DETECTOR



case with uniform background illumination, is very small. The first half of the pulse cancels out the second. So successful is this device that a 60 W light bulb may be held at the front of the Mekometer and the system will not saturate.

The ringing pulse is amplified, detected, and displayed on the phase meter as a D.C. voltage. As with the standard cavity resonance, when frequency wobble is being employed the voltage is reversed to the meter on alternate pulses. There is also a 1,000 μ F capacitor which can be switched in parallel across the meter to provide a time averaged reading when measuring conditions are unsteady.

The amount of frequency wobble which is best for the resonance setting is not necessarily best for determining the photomultiplier minimum. At long distances it is found that the wobble may be such as to take one right off the sharp light intensity minimum. For this reason two degrees of wobble are provided, a high wobble of 1.5 cycles change per pulse, or just under 40 kHz, and a low wobble of about 0.25 cycles per pulse, or just over 6 kHz.

The phase setting system is so good that the phase may be set to about 0.0003 ft (0.1 mm) up to distances of 3,000 ft (1 km), provided that atmospheric conditions are suitable.

The flash tube is triggered by a small ignition coil providing 8 kV. The tube produces a flash about 1 μ s duration with an energy of 0.1 joules. The flash is timed to occur just after the modulating cavity has broken into resonance.

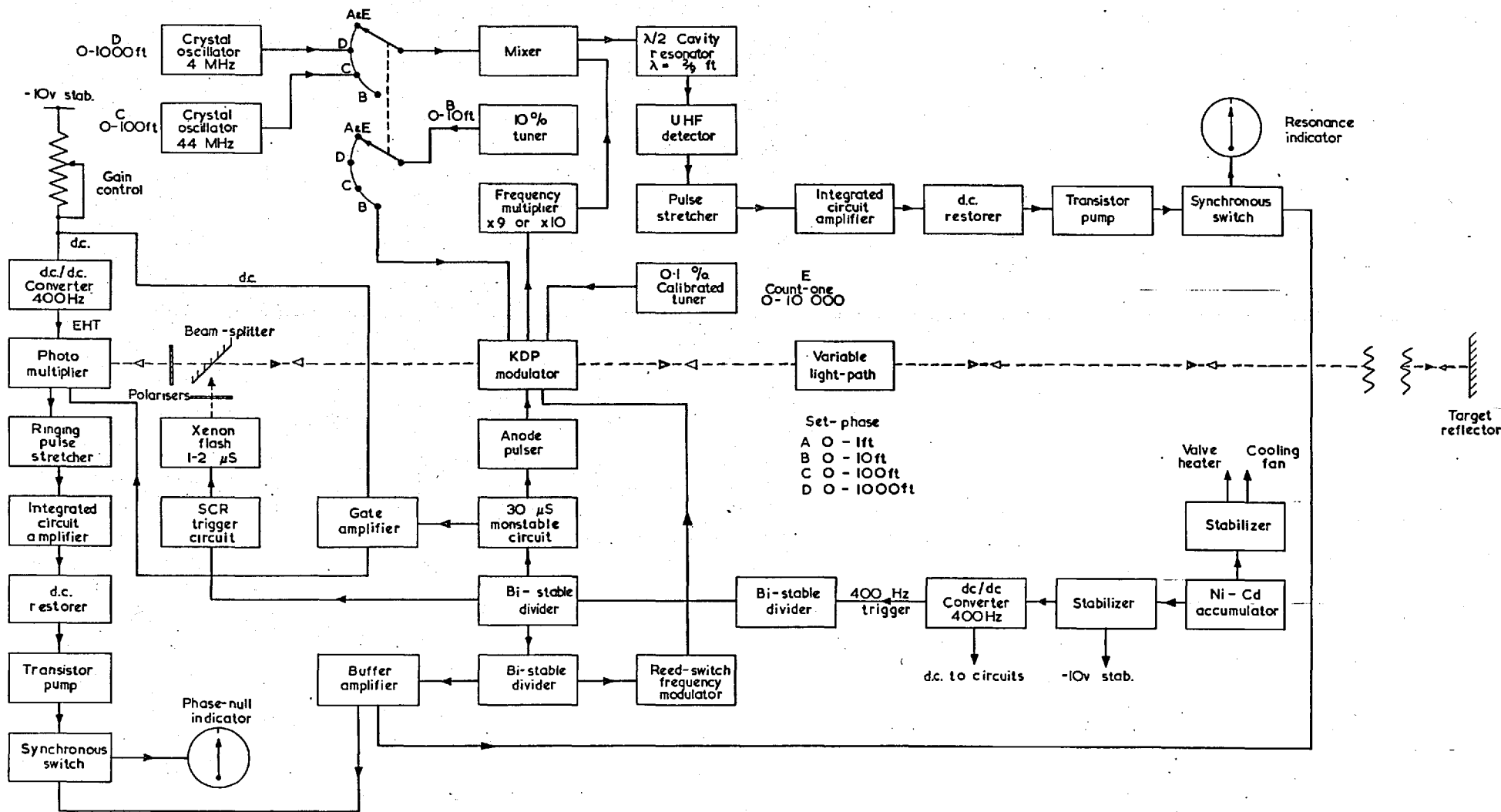
The Mekometer uses a modulation frequency which makes it ideal for operation in feet (a metric model has been made which works in units of 30 cm). The modulation wavelength is two feet exactly. When the instrument is set on a phase minimum there is, in effect, a one foot standing wave pattern between the Mekometer and target. The change that has had to be made in the variable light path to achieve this is the distance above a whole number of feet between the Mekometer and target. This distance may be read from a steel tape which is directly attached to the variable light path.

The frequency is now lowered by 10 per cent so that the modulation wavelength is $2 \times 10/9$ ft, producing another wave pattern. This pattern will be in phase with the first every 10 ft. By now adjusting the variable light path to again set up a standing wave a measure is obtained of the number of feet above a whole number of tens of feet in the distance. The light path will have to be moved $1/9$ ft from the original setting for 1 ft, and $2/9$ ft for 2 ft, and so on. The number of feet is in fact read from a units dial which is correctly geared to the steel tape. The method is the inverse of the Vernier principle.

Similarly, the number of tens of feet is formed by changing the fundamental frequency by one per cent and reading the answer from a dial to two significant figures; this is a check on the units setting. The number of hundreds of feet is found by changing the fundamental frequency by 0.1 per cent and the answer is again read to two significant figures. The number of thousands of feet is read from a map. It could also

NPL MEKOMETER III

ELECTRONIC SYSTEM



be found by counting the number of phase minima passed when tuning from the hundreds frequency to the fundamental. This can be done on the hundreds mode.

These various frequencies are achieved by moving the tuning ring, which slides inside the modulating cavity, to predetermined positions. These positions are selected by a mode switch which is connected by a pulley to the tuning ring. The frequencies are again referred to the standard cavity.

The 10 per cent change is controlled by tuning the 10th harmonic of the modulating cavity to the standard cavity. The one per cent change is monitored by mixing a 44 MHz signal from a crystal oscillator with the signal from the modulating cavity and tuning to the upper sideband. The 0.1 per cent change is determined by mixing 4.4 MHz with the modulating signal.

The pulses, delays and square waves required to operate the various systems are derived from the Mekometer pulse circuits, which divide up the basic 400 Hz supplies from the power unit. These functions are now done mainly by integrated circuits. All the voltages required are derived from the 12 volt batteries by a saturating core D.C./A.C. convertor operating at 400 Hz. The high voltages are transformed up from this and rectified in the normal way. When the power supply is switched on, the valve heater current is immediately supplied and the other supplies delayed by a timing circuit and relay for 20 seconds.

2.4 The Refractive Index Compensation.

So far no mention has been made of one of the main features of the Mekometer which makes it so attractive to the general user as compared with other instruments. The Mekometer standard cavity compensates for changes in temperature and pressure. The cavity is filled with dry air which can take up atmospheric pressure by means of a partially filled soft polythene bag. The cavity is aspirated by a fan so that it takes up the prevailing air temperature. It is so constructed that the capacities between the end aluminium plates and the fused quartz section change in such a manner as to change the resonant frequency by about 1 part in 10^6 per degree Centigrade. It can be made to exactly compensate for changes in the velocity of light arising from changes in air temperature.

This means that the Mekometer can be used to measure a distance in feet directly without the need for correcting for atmospheric temperature and pressure. If it is used on lines which deviate much from the horizontal a small correction due to changing pressure will have to be made. The instrument end correction, which is combined with the reflector end correction, will also have to be subtracted.

Under normal conditions in this country the answer given should be good to ± 0.1 mm ± 3 parts per million. This allows for a mean air temperature along the line differing by up to 3°C from that sampled at the Mekometer, which is usually sufficient. For more accurate results the air temperature will have to be sampled along the light path.

The limiting accuracy of possible measurements is ± 0.1 mm, the setting sensitivity, ± 0.5 parts per million, the limit of the knowledge of the standard cavity frequency, $\pm dt$ parts per million where dt is the deviation of the assumed air temperature from the actual mean air temperature.

2.5 Other Distance Measuring Instruments.

There are other electromagnetic distance measuring devices which are however less accurate for the work considered in this thesis. The two best known will be mentioned briefly.

2.5.1 The AGA Geodimeter, Model 6.

The Geodimeter also uses a modulated light beam. The modulation frequencies are obtained from crystal oscillators and the phase of the modulation of the returned light is compared with the phase of the modulator by means of a variable delay line.

In the Geodimeter the light from a Kerr cell is amplitude modulated and transmitted as a parallel beam to an array of cube corner reflectors. The Geodimeter uses three frequencies 29.970 MHz, 30.045 MHz and 31.469 MHz, derived from ovened crystal oscillators. These frequencies are fed to the Kerr cell and to a photocell via a variable electric delay line.

Four phase adjustments are made to measure a distance. These are made by adjusting the delay line until the modulated photocell records a minimum output. The makers suggest that under perfect conditions the phase setting can be made good to about 0.3 cm. These readings are then converted to length with the aid of a calibration table.

The delay line is calibrated by moving a target known intervals on a short line and computing a smooth calibration curve from the results. The makers say that the delay line errors can give answers differing by up to 1.5 cm for the three fundamental frequencies used for a newly calibrated instrument, and that this difference might increase to 4 or 5 cm with ageing.

The frequencies of the oscillators are claimed to be good to 1 part in 1 million initially, but likely to change by about 1 part in 1 million per year. This need not produce an error if the frequencies are measured.

The makers claim a daylight range of three kilometres and 15 km at night, using their standard lamp. With a high pressure mercury discharge lamp the ranges are 6 km and 25 km. It is of interest to note that the instrument and case weight 30 kg, and that the mercury lamp consumes 300 W supplied by a petrol generator weighing another 16 kg.

2.5.2 The Tellurometer Model MRA-101.

The Tellurometer system depends upon measuring the phase difference of a modulated microwave radio beam before and after travelling the distance to be measured.

The Tellurometer uses a microwave beam modulated at about 10 MHz. The Tellurometer system consists of two similar instruments one at each end of the line to be measured. Observations are made at one station, the master, and the operator at the other, the slave, acts upon instructions. The carrier wave is also used for communication.

Measurement takes place between two parabolic reflectors. The modulated wave is received at the remote

station where it is instantaneously re-radiated back to the master station and the phase shift is measured. Four frequencies and combinations of these are used to resolve the distances.

The Tellurometer will measure up to 50 km. The makers claim that short lines can be measured to within 1.5 cm under favourable conditions and to within 2.5 cm under average conditions. Medium and long lines are also liable to an error of ± 4 parts per million.

One advantage of the Tellurometer over light beam devices is that it is capable of shooting through light vegetation, but with reduced range. A measurement will take at least 20 minutes with experienced operators. The Tellurometer Model MRA-101 weighs about 12 kg per unit, with 12 volt batteries additional as required. The power consumption is 36 W.

The use of a microwave carrier has the advantage of giving a long range. There are, however, drawbacks. The microwave refractive index is much more sensitive to changes in humidity. The biggest drawback however is due to ground swing which is caused by the receivers picking up signals which have undergone reflections off the intermediate ground and any other large objects such as buildings. This can produce large errors in a single reading of up to one metre. This however can be estimated by varying the frequency and observing the apparent change of distance. The transmission and reflection characteristics of microwaves are however a serious weakness.

2.6 Advantages and Disadvantages of the Mekometer over other Systems.

An undoubted disadvantage of the Mekometer at present is its short range. At present the $40\ \mu\text{s}$ gating pulse limits the Mekometer to an absolute range of about 4 km. During the day, light scatter and background light limit the range to about 2.5 km. We have not attempted any distance records but have successfully measured a line 2.4 km long at mid-day with the light path travelling at about 0.5 m above ground level for a considerable portion of the line. If we had known the line was so long it would not have been attempted during daytime.

The superiority of the Mekometer over the other instruments lies in its high sensitivity and accuracy. The sensitivity is due to the high modulation frequency and the sharpness of the interference minima. The accuracy is due to the phase setting system. This is error-free. With the Geodimeter, phase is determined electronically by mixing a delayed signal. This is prone to cyclical errors and varying characteristics with age and circumstances. The mixing system used on the Tellurometer is also prone to cyclical errors but this will be overshadowed by the ground swing. Also, different Tellurometer frequencies have slightly different focus points on their reflectors. Cyclical errors have been looked for in the Mekometer and have been shown to be less than ± 0.05 mm in magnitude.

Other advantages of the Mekometer to the general user are lightness, compactness, low power consumption, quickness and simplicity of use.

2.7 Possible Modifications for Geophysical Use.

The Mekometer system is extremely flexible and may be modified for a number of specialist uses. For the study of small changes in the lengths of lines, as in the present investigations in Iceland, the highest accuracy is required. For preliminary earthquake studies in general, a greater range is desirable, although it seems that the deformation in fact takes place over a very limited area.

2.7.1 Increasing the range.

There is nothing inherent in the Mekometer system which prevents it from attaining a range comparable with the Geodimeter. One obvious step would be the replacement of the single reflector by a cluster of reflectors. At the moment the returned light being deflected away from the receiving mirror seems to be the limiting factor; a cluster of reflectors would increase the range at which this happened. If accuracy was not to suffer, the reflector array would have to be made and aimed so that the reflecting points of the individual reflectors were all the same distance from the Mekometer to within 0.1 mm.

A more powerful light source could also be used, an obvious choice being some sort of laser. With a laser there would be no focusing problems and the whole optical system could be simplified.

With increased range the pulse length of the modulator would also have to be increased. The problem here is that if the pulse length is increased the crystals will start to heat. ADP, in particular, has a dielectric constant that varies considerably with temperature. This varying dielectric constant

inside the modulating cavity would produce frequency variations. KDP is less temperature sensitive but does not display the electro-optic effect so strongly. Another crystal, Lithium Niobate, is very promising, but as yet rather expensive. Possible solutions to the problem are larger crystals and a lower modulation level, some form of temperature compensation, or on very long distances a double pulse.

With longer lines the modulation frequency would have to be lowered because atmospheric shimmer would tend to make it difficult to stay locked to a particular minimum.

2.7.2 Making the frequency more certain.

For the highest accuracy the prevailing atmospheric conditions are measured, together with the cavity temperature to determine its frequency, so that the benefits of a compensating cavity are lost. In fact the compensating standard is a disadvantage for this work because there are uncertainties in the frequency while the cavity temperature is changing, especially when the Mekometer is first switched on.

For geophysical work, the frequency would be better derived from a constant frequency source. This could either be an ovened crystal or a sealed ovened cavity. The crystal oscillator would not be of a high enough frequency but could be multiplied. Instead of comparing the modulation frequency with this standard, as is done at present, the standard could be used to drive the modulator. The modulator would then no longer be an oscillator but a highly tuned amplifier. At present on long lines when the modulating cavity temperature is unsteady the cavity setting does introduce errors, although small and random

With the amplifier arrangement the operator could concentrate entirely upon the phase setting; automatic recording of the phase error would also be possible.

2.7.3 Atmospheric refractive index determination.

Even at present, however, a limit is set by uncertainties about atmospheric conditions; increasing the range is only likely to make this uncertainty even greater. There is a method whereby this difficulty might be overcome.

If the instrument could measure the distance with light of two different wavelengths the average temperature along the line could be estimated, provided the pressure and humidity were known. With a third wavelength, or a Tellurometer measurement, the average humidity could also be resolved.

This method has its limitations however. It can at best only yield a distance with an accuracy 1/10th of the accuracy of either of the individual optical path lengths. For example, if the optical path lengths in blue and red light were both determined to 1 part in 10 million the average air temperature could be determined to the nearest degree yielding a corrected distance good to 1 part in a million.

On long lines this would be a considerable improvement over merely measuring atmospheric conditions at the terminals. The high sensitivity of the Mekometer makes it particularly favourable for this kind of study.

The method would produce no benefit on a fairly uniform line where there was atmospheric turbulence or shimmer; the average temperature would be better determined with a thermometer. It would give great benefit however when shooting across water or across varying terrain under a stable atmosphere.

A feasible method for doing this would be by converting the Mekometer to laser operation. The use of conventional light sources would involve focusing difficulties. With lasers, however, reflecting optics could be used almost throughout. The transmitted beam would need no focusing. The variable light path could be in the transmitting system, be more folded, and use smaller reflectors. The received light would be collected by a parabolic reflector and focused before a small lens for demodulation.

This instrument would require two lasers or one laser and a frequency doubler. It could be made to operate over long distances. Even without dual wavelength facilities a long range Mekometer could produce useful results on a horizontal line over water, for example, from one island to another. Away from continental influence the air should be highly uniform and would only need sampling at one point; the middle would be the best.

CHAPTER 3

THE CORRECTIONS

To determine the distance between two points there are two independent types of correction which have to be applied to the Mekometer readings, firstly those like the refractive index arising from the prevailing conditions at the time of measurement and secondly the geometry of a particular line.

The Mekometer has a sensitivity of about 1 part in 10^7 or 0.1 mm, whichever is the greater. Over long distances 1 in 10^7 is the bound, and over short distances 0.1 mm. We set out to make our atmospheric and geometric corrections better than or equal to these limits.

3.1 The Theory of the Atmospheric Corrections.

The Mekometer transmits modulation at a frequency F on a light beam which has an effective wavelength λ . Using this value of λ the group velocity V of the modulation for the prevailing atmospheric conditions may be calculated. We can read from the Mekometer the number N , of cycles or wavelengths of modulation between the transmitted and returned beams. The modulation wavelength is arranged to be two feet. The measured distance is then one half N divided by F multiplied by the

modulation velocity V , i.e. one half N times the average modulation wavelength.

$$D = \frac{NV}{2F}$$

The Mekometer thus reads distances in feet.

3.1.1 The effective wavelength.

The Xenon flash tube light source in the Mekometer emits not one single frequency but several. The photomultiplier does not respond equally to light of all wavelengths. The effective wavelength λ of the Mekometer light was estimated by determining with a spectrometer the power distribution of the light going through the instrument as a whole just before falling on the photomultiplier. This was done using the light viewed through the receiving eyepiece after travelling through the instrument and reflector. This method was used because the effective wavelength will probably vary with the focusing and absorption of the various lenses, reflectors, polarisers and crystals.

The photomultiplier has a known frequency response and by combining these responses the effective wavelength was calculated.

3.1.2 The dispersion of the atmosphere.

Air is dispersive and so the modulation velocity will differ from the phase velocity. The refractive index n_s for dry air at normal pressure and 15°C is given by (Bengt Edlen, 1953)

$$(n_s - 1) 10^8 = 27259.9 + 153.58/\lambda^2 + 1.318/\lambda^4 \quad (1)$$

where λ is the wavelength in μm .

The variation of refractive index with atmospheric conditions is given by (Barrel, 1951)

$$(n_{tph} - 1) = (n_s - 1) \frac{p(1 + \beta_t p)(1 + 15\alpha) - (0.0624 - 0.000680/l^2)h \cdot 10^{-6}}{760(1 + 760\beta_{15})(1 + \alpha t)} \quad (2)$$

where t = air temperature $^{\circ}\text{C}$

p = pressure mm Hg

h = water vapour pressure mm Hg

$\alpha = 0.003661$

$\beta_t = (1.049 - 0.015) \cdot 10^{-6}$

$\beta_{15} = 0.813 \times 10^{-6}$.

In a given atmosphere the Mekometer light beam may be considered as a group ψ of waves each with its own wavelength l , amplitude q_l , phase, and phase velocity v_l given by the dispersion equation (1).

$$\psi = \sum_l q_l e^{\frac{2\pi i}{l}(v_l t - x)}$$

The condition for modulation to be propagated at a certain velocity V will be stationary phase for different phase velocities, and hence stationary phase for different wavelengths, since the phase velocity depends only upon wavelength for a given atmosphere.

$$\frac{\partial}{\partial l} \left(\frac{v_l t - x}{l} \right) = \frac{t}{l} \frac{\partial v_l}{\partial l} - \frac{v_l t}{l^2} + \frac{x}{l^2} = 0$$

$$\frac{x}{t} = v_l - l \frac{\partial v_l}{\partial l}$$

i.e. modulation travels at a velocity

$$V = v_l - l \frac{\partial v_l}{\partial l}$$

This is the standard expression for the group velocity of a

packet of waves in a dispersive medium. The phase velocity V_p is given by

$$V_p = \frac{c}{n}$$

c = velocity of light in vacuo

Therefore

$$V = \frac{c}{n} + \frac{c\lambda}{n^2} \frac{dn}{d\lambda}$$

We calculate n and $dn/d\lambda$ from the expressions above. The effective wavelength λ has been found by direct measurement to be $0.486 \mu\text{m}$. An error of $0.002 \mu\text{m}$ in λ will give an error in n_s of 1 in 10^7 . Substituting in (1) we have

$$(n_s - 1) = 0.00027933748$$

From (2)

$$n_{tph} = 1 + 0.00027933748x - \frac{0.0000000595h}{1 + 0.003661t}$$

where

$$x = \frac{P(1 + (1.049 - 0.015t)P10^{-6})(0.001387188)}{(1 + 0.003661t)}$$

$$\begin{aligned} \left[\frac{dn_{tph}}{d\lambda} \right] &= \left[\frac{-2(153.58)}{\lambda^2} - 4 \frac{(1.318)}{\lambda^3} \right] x 10^{-8} + \frac{(-2 \times 0.000680)h 10^{-6}}{\lambda^2 (1 + 0.003661t)} \\ &= -0.0000139494507x - \frac{0.00000000567h}{(1 + 0.003661t)} \end{aligned}$$

The corrected distance D is then

$$D = \frac{N}{2F} \left(\frac{c}{n_{tph}} + \frac{c\lambda}{n_{tph}^2} \frac{dn}{d\lambda} \right)$$

The value of c used is that determined by Froome (1958).

3.2 The Frequency Measurement of the Mekometer.

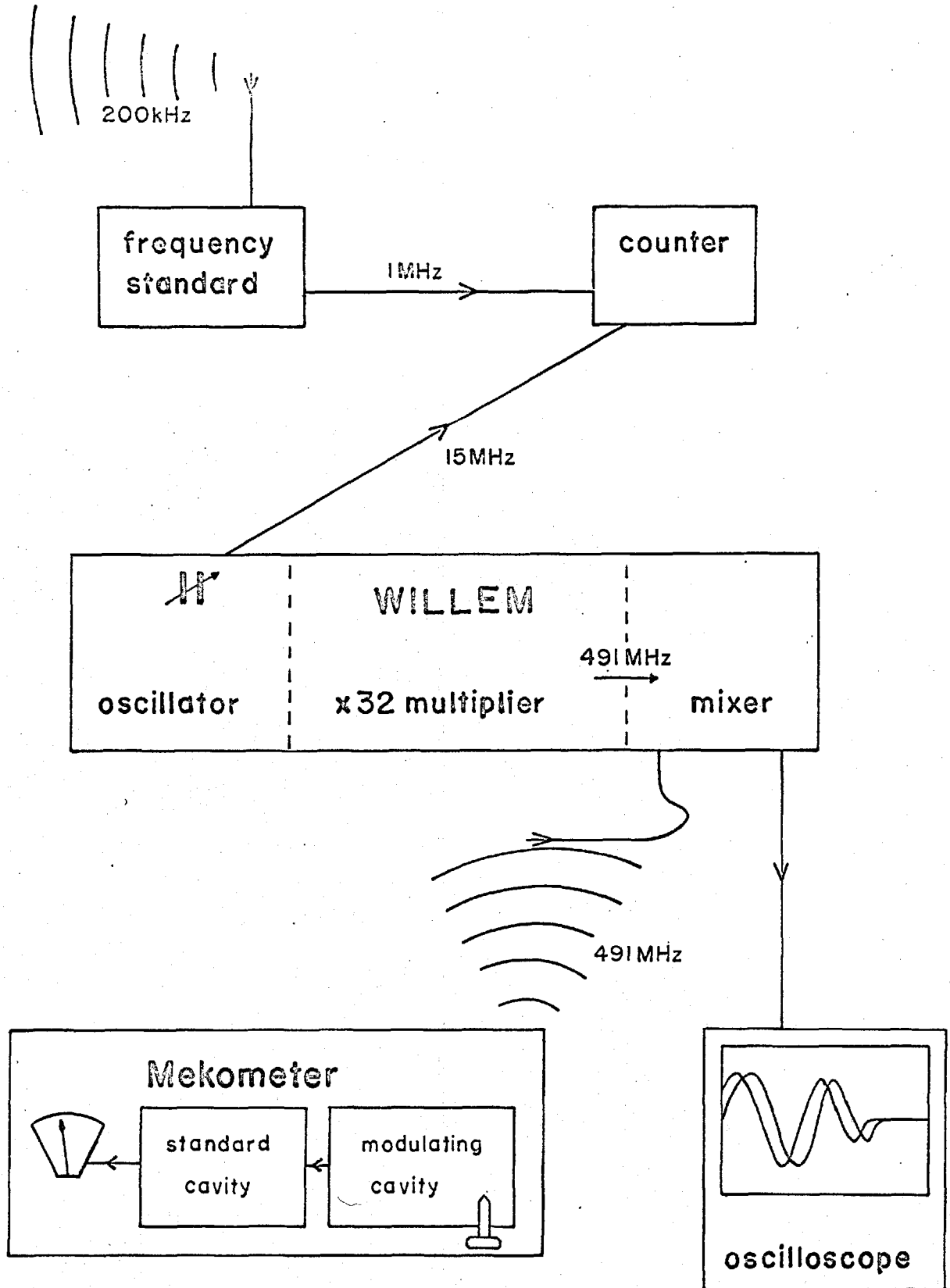
The modulation frequency F of the Mekometer depends upon the temperature of the standard cavity and the pressure of the dry air inside it.

During the first Icelandic field season the frequency was measured in the field simultaneously with the distance measurements. During subsequent seasons the behaviour of the cavity frequency with temperature and pressure was so well known that the cavity temperature and atmospheric pressure were measured and the frequency found from a temperature-frequency calibration curve, which was checked at frequent intervals under laboratory conditions.

The modulation of the Mekometer consists of 500 MHz bursts of $40\mu\text{s}$ duration at a 100 Hz repetition rate. When the Mekometer is in the "high wobble" mode successive pulses have frequencies approximately 1 part in 10,000 above and below the nominal value. The modulating cavity is trimmed by a screw plunger until it is exactly the right frequency to resonate the standard cavity. The standard cavity is a precise high Q (3,500) passive resonator). In fact it resonates at 10 times the modulating frequency. In the "high wobble" mode the two modulation frequencies are respectively above and below nominal, and resonance is determined by balancing the responses of the two frequencies. When this condition is satisfied, as shown by a null on the cavity meter, the two frequencies are symmetrically disposed about the standard cavity resonance peak. The adjustment of this setting is clearly much more sensitive than setting on the peak itself.

Frequency measurements are done in the high wobble mode, since in this mode the cavity meter is most sensitive. Measuring the frequency of these pulses is not easy and is done by using a device which has come to be called WILLEM (Wavelength Investigator of Light Modulation).

MEKOMETER FREQUENCY MEASUREMENT



WILLEM consists of a controllable crystal oscillator of 15.363 MHz, a times-32 multiplier and UHF mixer. The principle of operation is that a continuous-wave oscillator operating at a submultiple frequency of the Mekometer is measured accurately as described below. This submultiple frequency is then multiplied up to the Mekometer frequency. The Mekometer frequency is sampled by holding a quarter wave aerial near the modulating cavity. There is enough radiation from the modulating cavity to pick up and mix with the continuous wave generated by WILLEM. The beat is observed on an oscilloscope.

Two traces can be seen, one for each modulation frequency. When the phases of the pulses are correct and WILLEM is generating a frequency half-way between the two modulation frequencies the two traces can be superimposed. The phases are adjusted by the positioning of the quarter wave aerial and other nearby bodies. The frequency of WILLEM is controlled by a variable capacitor in the tuned circuit of the crystal oscillator. The frequency of this oscillator is measured by a counter which is referred to a frequency standard.

To make a measurement of the Mekometer frequency the modulating cavity is tuned by the screw tuning plunger until the two oscilloscope traces are superimposed. WILLEM's frequency is then adjusted until this condition coincides with a null on the cavity meter. The counter reading multiplied by 32 is then the modulation frequency F of the Mekometer. Under good conditions the frequency may be determined to within about 3 cycles/sec in 15 million or 2 parts in 10^7 .

The standard cavity is working in the microwave region and its frequency is thus very dependent upon water vapour present inside the cavity. To obtain reproducible results the air must be completely dry. In the prototype cavity there are slight air leaks at the various input and output terminals, so a silica gel dessicator is provided in the cavity enclosure and this must be changed regularly. A noticeable drop in frequency occurs before the silica crystals turn pink, so daily frequency checks are the best method of ensuring that all is well.

This also guards against any frequency change due to accidental shocks. It has been found that the standard cavity is not prone to disturbance by normal use and required its silica gel to be changed about every fortnight.

In Britain the frequency measurements are referred to the B.B.C. Radio 2 Droitwich 200 kHz transmitter. The frequency accuracy of the Droitwich carrier is better than 5 parts in 10^9 . This carrier is received and used to phase-lock a 1 MHz crystal oscillator. The crystal oscillator acts as a flywheel during periods of very high modulation. The output of this oscillator is used as the time-base of the counter.

A commercially available oscillator unit, the Advance O.F.S.I. Off Air Frequency Standard was used during the third season, but was found to be very unreliable with weak signal owing to a very wide-band front end which will pick up nearby stations. It could only be used after midnight when the local radio station had shut down. It was then used to check the counter's internal time-base, which proved to be very stable.

During the first two field seasons the N.P.L. off-air standard incorporating an Air-Mek front end was used. This was more selective but in Iceland receptive difficulties arose.

During the fourth field season an accurate ovened crystal oscillator was used, which was checked against Droitwich at the beginning and end of the expedition. This oscillator was used to check the counter whenever frequency checks were made.

3.2.1 Description of WILLEM.

WILLEM was designed by N.P.L. specifically for Mekometer measurements, although the principle is applicable to all UHF pulses. The N.P.L. apparatus is integrated into one box, with a counter and frequency standard. As we needed our counter for other field measurements all our units were kept separate.

The first stage is a 15.363 MHz crystal controlled Clapp oscillator. This is made tunable by having variable capacity in the crystal feed-back loop. The output is fed to a common emitter buffer amplifier. The frequency is then multiplied by a series of class-C doublers. After the third doubler the signal is amplified back to a working level and two more doublers follow before the output amplifier. The last two stages have trough-line tuned circuits. The output is then mixed with the radiation signal from the Mekometer and the beat observed on an oscilloscope

The circuits are all screened from one another in separate compartments of a long brass box, except the mixer stage, which is in a cigar box.

3.3 Obtaining the Atmospheric Corrections.

The effect of pressure on the standard cavity is known, so all frequencies can be reduced corrected to 760 mm of Hg. By plotting frequency against cavity temperature, the variation of F with cavity temperature is determined. In the field, cavity temperature is noted as a parameter determining F. The variation of F with pressure is the inverse of refractive index and in frequency checks is taken to be -5.82 Hz per mm of Hg.

For the general user the frequency temperature coefficient of the standard cavity has been adjusted to be very nearly the inverse of the refractive index of air. The standard cavity has air drawn over it by a fan so that its temperature should follow that of the external air. Thus, in a uniform atmosphere with the standard cavity at air temperature the Mekometer will read correct distances. However to obtain the highest accuracy from the instrument it cannot be assumed that these conditions are met.

The refractive index of air decreases by about 1.1 parts per million per degree Centigrade, increases by 0.4 ppm per mm of Hg, and decreases by 0.05 ppm per mm of Hg of water vapour pressure. To obtain corrections which are good to 1 part in 10 million air and cavity temperatures must be measured to the nearest 0.1°C, pressure differences along the line to the nearest 0.2 mm of Hg and the humidity to the nearest 2 mm of Hg.

3.3.1 Pressure.

Pressure was measured using an accurate aneroid barometer capable of resolving 0.1 mm of Hg. The pressure difference between end stations on a line was calculated from

the length of the line and the angle of elevation of one station from the other, as measured by theodolite. These pressure differences are accurate to about 0.02 mm of Hg, which is well within the required accuracy.

3.3.2 Humidity.

Humidity was measured using a wet and dry bulb whirling hygrometer.

3.3.3 Air temperature.

Air temperature proved to be very difficult to measure. At a given instant the average temperature along the light path is required to within 0.1°C. Except during very favourable atmospheric conditions this could not be obtained.

The air temperature was measured using mercury-in-glass thermometers, and, on some occasions, temperature probes. Temperature probes were light-weight sensors designed to be carried by hydrogen balloons or kites, and are described in detail in section 3.3.3.1.

During the first two field seasons air temperature was measured by mercury-in-glass thermometers held in shade by the observer and read at various points along the line. These temperatures were taken as near to the height of the light path as possible. This method proved very unsatisfactory in summer as the observer was usually below the line of sight, where the air was warmer. There was also the difficulty of preventing the reading being influenced by heat from the observer.

During the second field season in the Spring of 1968, the weather was too cold for using the new temperature probes but the temperatures were very constant as the ground was snow covered.

During the third field season temperatures probes were used on some lines. These probes are electronic temperature sensors which transmit the temperature back to a receiver. The air was always sampled at both ends of the line. By the nature of things the end-points were usually on high ground so that the air sampled at either end was more likely to be typical of the light path than air sampled half-way at the wrong elevation. The end points were measured by mercury-in-glass thermometers which were held in stands so that they were shielded from the sun. These were quickly read when required and were not heated by the observer. Operators at the two ends of the line were in communication by portable radio.

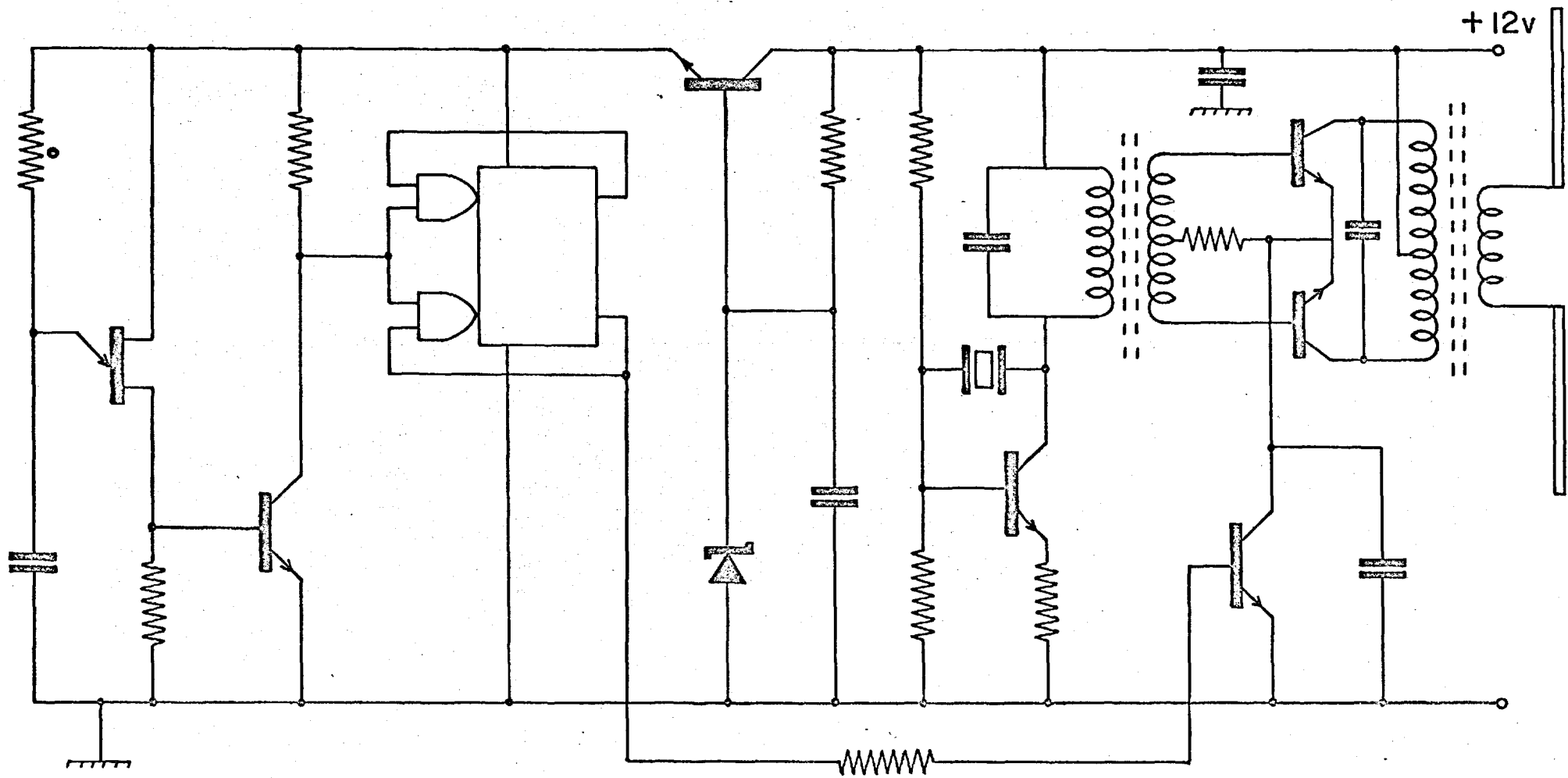
3.3.3.1 Description of temperature probes.

For field use these devices had to be strong and yet light enough to be flown on a balloon or kite. They would thus be able to measure the air temperature wherever required.

Many possible transducers were investigated, but a thermistor was finally chosen because it was small, light, sensitive and fairly cheap. The next most favourable transducer would have been fine platinum wire but this would have been bulky and rather fragile.

The thermistor was used in a unijunction relaxation oscillator. This was chosen because it contains few components and is inherently voltage-independent.

TEMPERATURE PROBE CIRCUIT DIAGRAM



relaxation
oscillator

amplifier

divider

stabiliser

crystal
oscillator

modulated power
amplifier

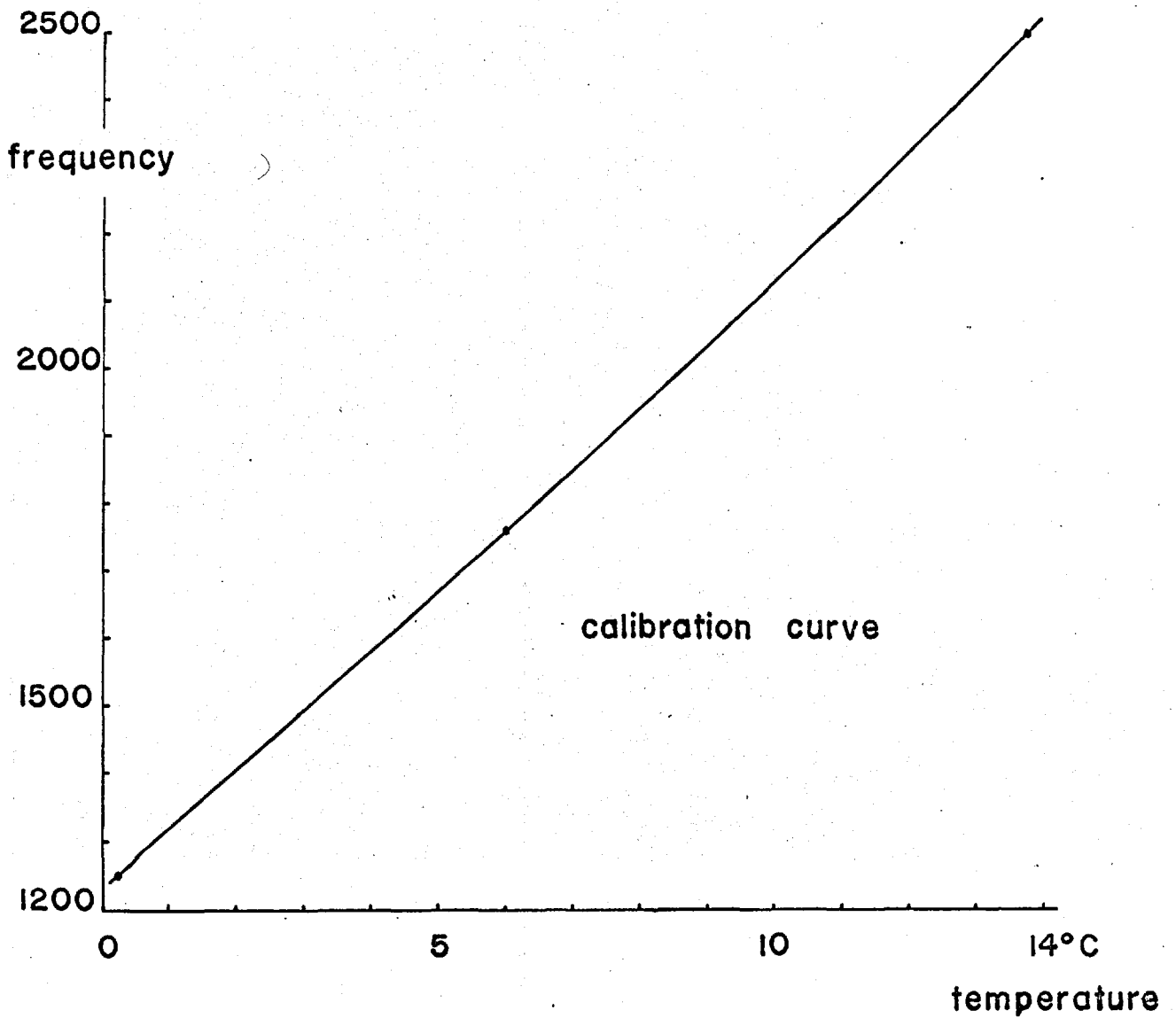
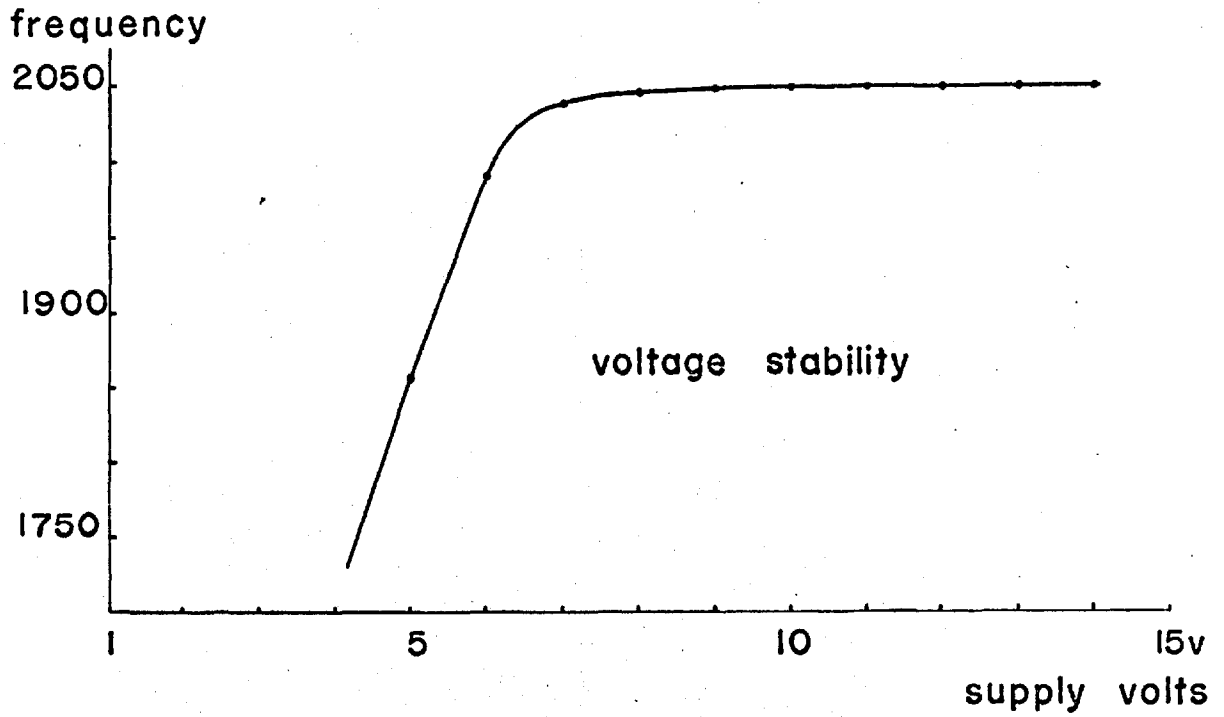
The thermistor resistance decreases by about four per cent per degree Centigrade at 20°C. A capacitor is charged through the thermistor until the unijunction peak point is reached. Then the emitter diode junction is forward biased and a sharp pulse occurs, discharging the capacitor. The frequency of discharge will increase with temperature. Values were chosen so that the frequency changed 100 Hz per degree Centigrade.

The pulse from the unijunction is amplified and fed to a DTL integrated circuit flip-flop. This divides by two and gives out a square wave which is amplified and used for modulating a 27 MHz transmitter.

It was decided to transmit on 27 MHz because of the cheapness and availability of crystals used on this, the model radio-control band. The transmitter consists of a free-running crystal oscillator which is coupled to a tuned push-pull power amplifier modulated by the square wave. This is coupled to a resonant dipole aerial.

The probe is powered by eight pen cells, giving 12 volts. As these quickly polarise in continuous use, the supply to the front end was stabilised by a single transistor zener stabiliser. The zener diode was placed in the base circuit of a transistor, as the breakdown voltage of a zener diode is slightly dependent upon current. In this arrangement power is not wasted by resistive dissipation. The voltage dependence of the probe was tested. It was found that the probe reading did not register an error until battery volts had dropped below eight volts, as shown in the graph. There is no more than 3 Hz difference in 2,000 Hz between the reading at eight volts and that at 12 volts; this corresponds to a temperature error of less than 0.03°C.

TEMPERATURE PROBE CHARACTERISTICS



As a fast response was required from the probe a small thermistor bead was chosen, mounted upon a thin black metal disc. A great danger in this type of instrument is self-heating of the thermistor. A thermistor was chosen having a high dissipation constant of $1 \text{ mW}/^{\circ}\text{C}$, i.e. 1 mW is required to raise the thermistor 1°C above ambient in still air. The thermistor was run at about 0.05 mW . No temperature rise could be detected from self-heating, except when the bead was placed in a small insulated enclosure. When a fan was turned on the bead it was warmed slightly by the fan rather than being cooled.

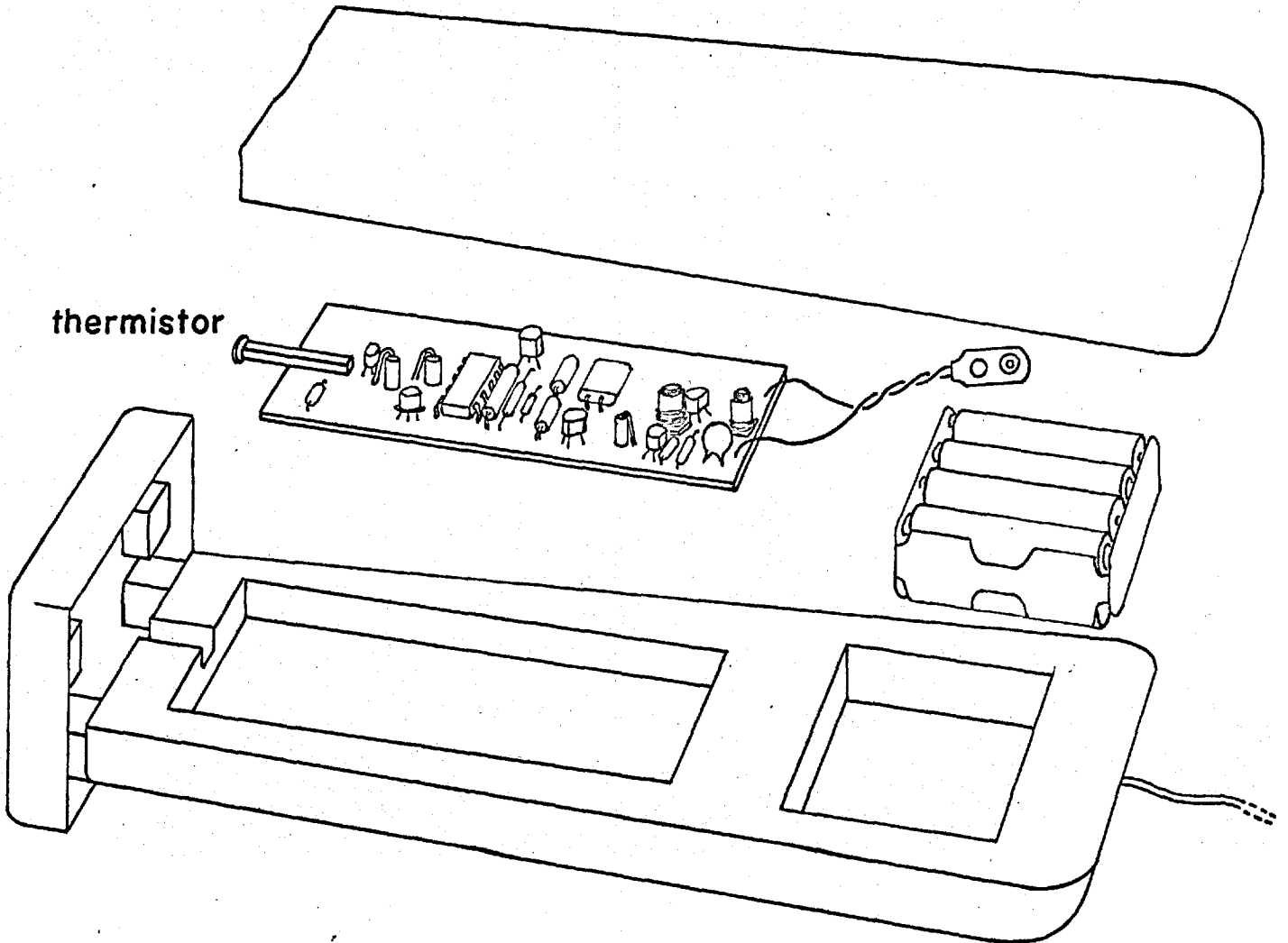
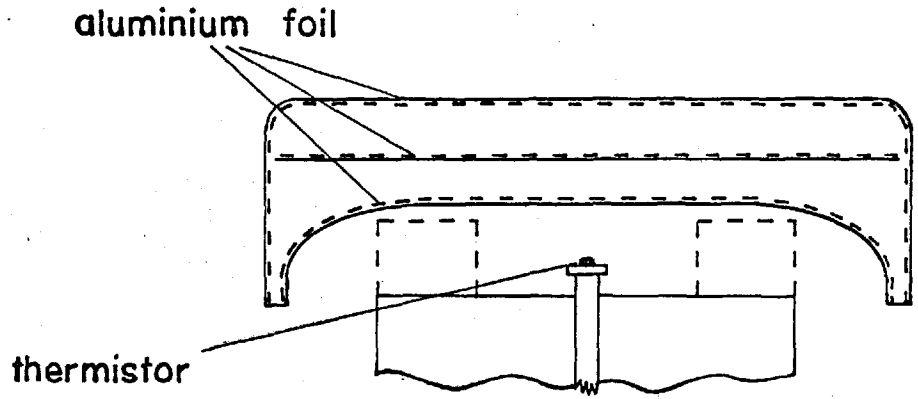
While investigating the probe it was found that air temperatures are very variable. This variation increases with sampling rate and clearly it will never be possible to measure the air temperature continuously all along a line to 0.1°C .

A calibration curve was plotted by dipping the thermistor covered by a polythene bag, into stirred water of various temperatures. The water temperature calibration agreed with air temperatures as well as could be measured.

The probe was radiation-sensitive and could detect a person or a cup of tea from several feet away. For this reason the thermistor bead was shielded by several layers of aluminium foil separated by insulating foam polystyrene in the form of a cap, which protected the bead from direct radiation but allowed a free flow of air.

The prototype probe was built of balsa wood and its first flying test was done from a tethered hydrogen balloon on a windy day. It was found that tethered balloons were unsuited to windy conditions and that balsa wood probes were incapable of withstanding crash landings.

TEMPERATURE PROBE LAYOUT

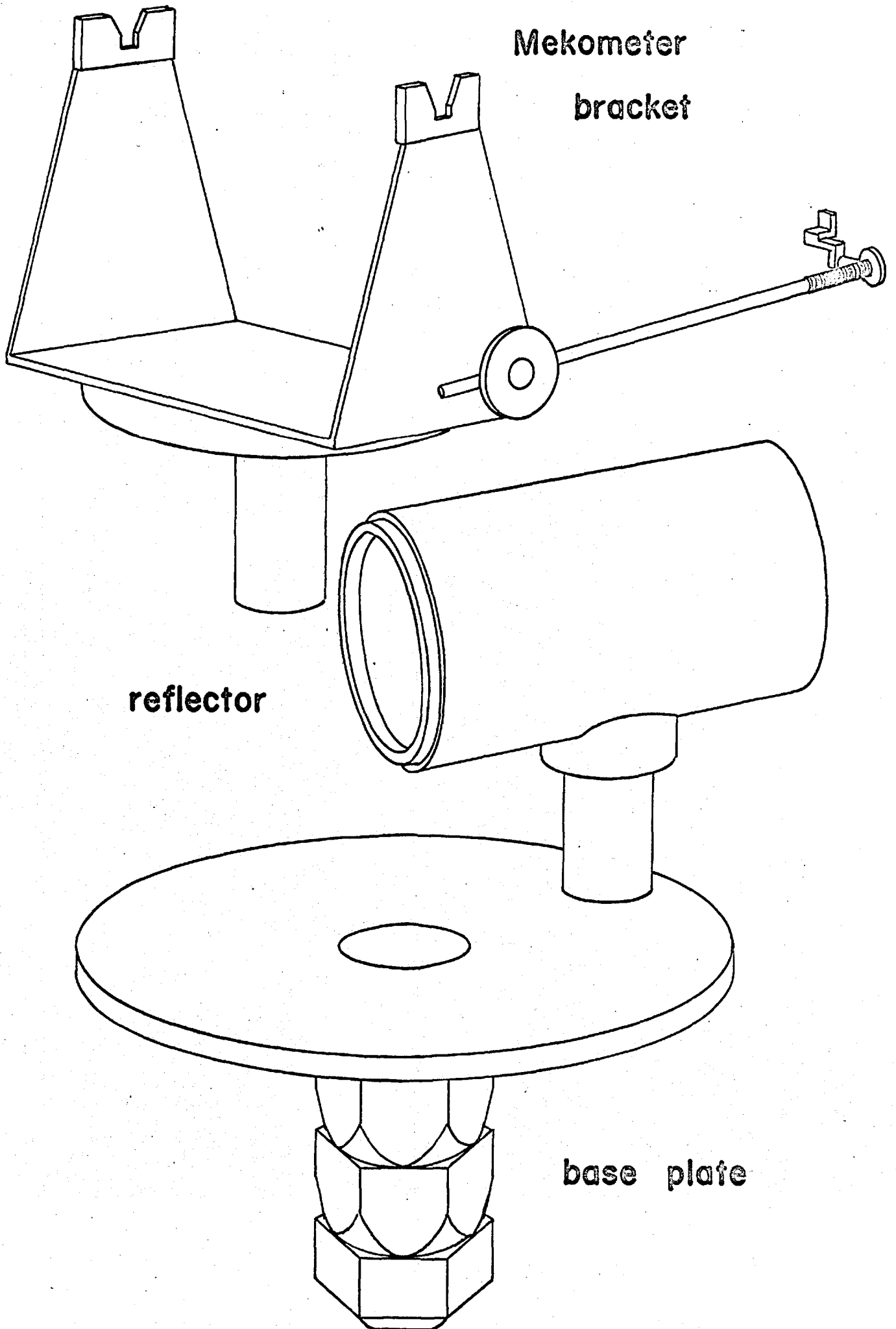


Past experience had shown that Iceland was a windy place, so tests were carried out using kites. An improved probe was built, mounted on a balsa wood circuit board and enclosed in solid expanded polystyrene, which could be opened for battery access. The batteries were contained in a plastic battery holder, held in a separate compartment from the circuit board. This design has proved extremely strong and weighs about 270 grams. The weight could be reduced, but probably at the expense of strength.

Four such probes have been constructed operating at frequencies separated by about 100 kHz.

The signals from these probes were picked up using a modified Heathkit 'Mohican' communication receiver. This is a super heterodyne receiver using transfilters in the i.f. stages. These have a 2 kHz pass bandwidth, making the receiver extremely selective. To avoid time consuming tuning in the field the i.f. oscillator was modified using four crystals separated in frequency by 455 kHz (the i.f.) from corresponding probe crystals. These crystals are switched into the feed-back loop of the i.f. oscillator as required. The main tuning control of the receiver can be left in a compromise position and the probe signals received by switching to the four crystals in turn. This allows the four probes to be sampled in about seven seconds, allowing a one second counter display for each.

The output to the loudspeaker was amplified so that with all but very weak signals the amplifier ran into saturation, producing a squared output and noise immunity for the counter. The counter signal was taken from a headphone jack.



The range of transmission depends upon the receiver antenna but no difficulty was encountered up to about one kilometer range. The batteries last for up to six hours continuous use, and longer with intermittent use.

Thermistors are notorious for drift, and to guard against errors, frequent calibration checks were made. Each time a probe was used its reading was compared with a thermometer in air. All these checks were recorded to see whether there was any noticeable drift. No drift was detected during the few weeks of field work, but nine months later three of them had slightly different calibration curves.

3.4 The Geometrical End Corrections.

In addition to the corrections necessary for atmospheric factors certain geometrical end corrections have to be made, to reduce the measured distance to the distance between the centres of the holes in the surveying plates. The plates are cemented into the tops of the pillars with their tops approximately level. In the centre of each plate is an accurately reamed one inch diameter locating hole. These holes are about four inches deep. The Mekometer mounting bracket sits on this plate, located by a three inch long spigot making a good fit in the locating hole. The cube corner reflector mounts also have spigots which fit these holes.

3.4.1 The reflector calibration.

There are six cube corner reflectors and one Mekometer mounting bracket. In none of these does the reference axis and the effective plane of reflection, or transmission,

coincide. The discrepancy has to be determined and applied as a correction. The end correction for each of the reflectors was measured on the N.P.L. 50 m standard tape bench, whose length is accurately known to the nearest 0.01 mm.

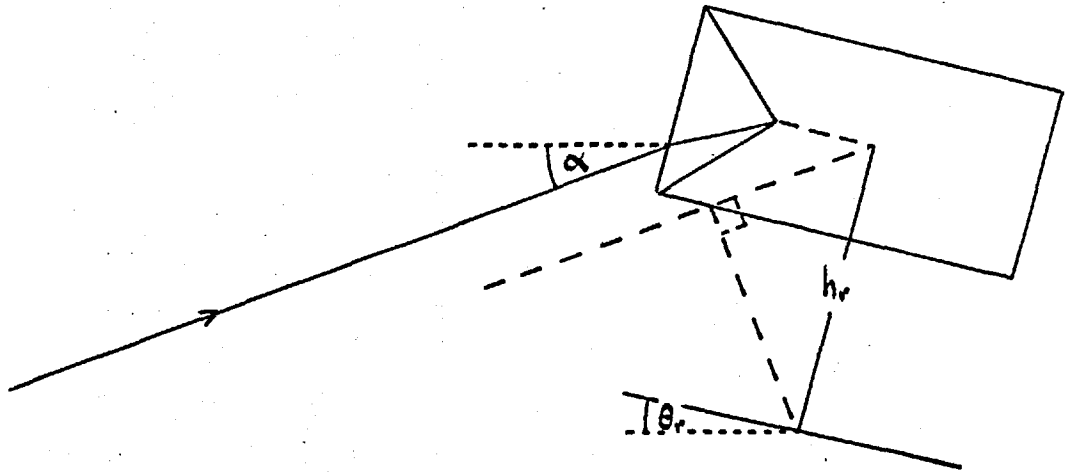
Two of the mounting plates with their holes drilled right through were mounted vertically on carriages above the tape-bench marks. The plates were levelled with an accurate bubble. A one foot long tube was made which was a good fit in the plate holes. This had two, close, parallel hairs stuck across one end. With two lenses and a paper tube it was made into a microscope which could be used to position the plates accurately over the tape bench marks. These positions were checked before and after each Mekometer measurement.

The tape bench room at N.P.L. is thermostatically controlled and thus has a relatively uniform atmosphere. Mekometer measurements were made to each of the reflectors. A small cosine correction was applied to allow for the fact that the Mekometer was further above the bench than the reflector.

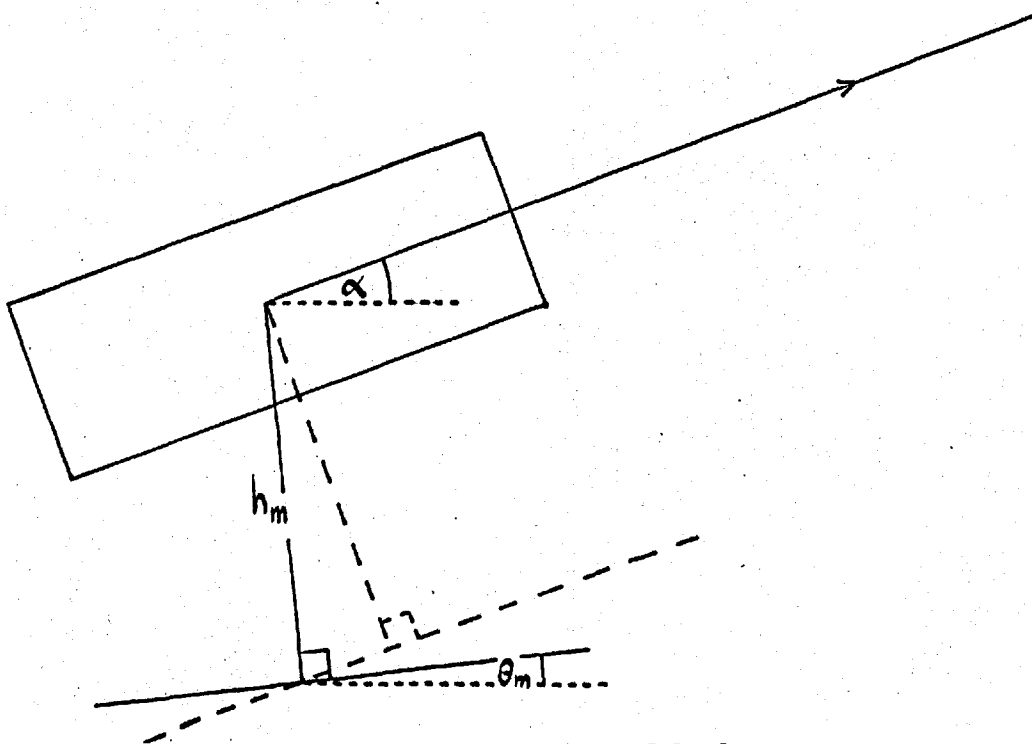
The differences between these readings and the bench length are the corrections to be applied in measuring from the trunion axis of the Mekometer to the intersections of the principle axes of the cube corner reflectors with their rotation axes. The azimuth rotation axis of the Mekometer intersects the trunion axis. These corrections are about 1.7ft and are always subtracted from Mekometer readings. This high value arises from nearly two feet of light path inside the Mekometer.

The corrections necessary to convert distances measured to distances between plate centres may be divided into separate corrections for the Mekometer and reflector.

END CORRECTIONS GEOMETRY



reflector



Mekometer

3.4.2 Geometrical corrections at the Mekometer end.

If the mounting plate has a tilt θ_m in the direction of the target and the elevation of the light path, measured from the Mekometer, is α then a correction $h_m \sin(\alpha - \theta_m)$ must be added, where h_m is the perpendicular height of the Mekometer trunion axis above the plate. There is no angular error produced by the Mekometer as the line of sight goes through the trunion axis within a millimetre. For 1 mm off-set of the line of sight from the trunion axis a vertical angle of 6° will produce a 0.1 mm error.

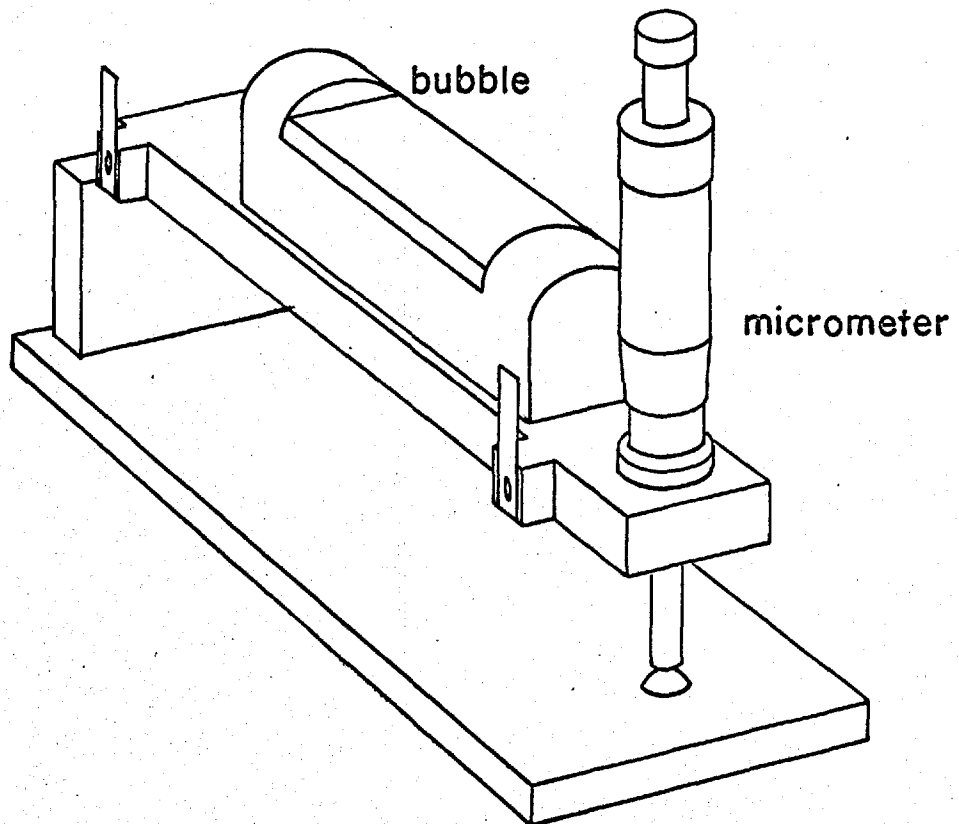
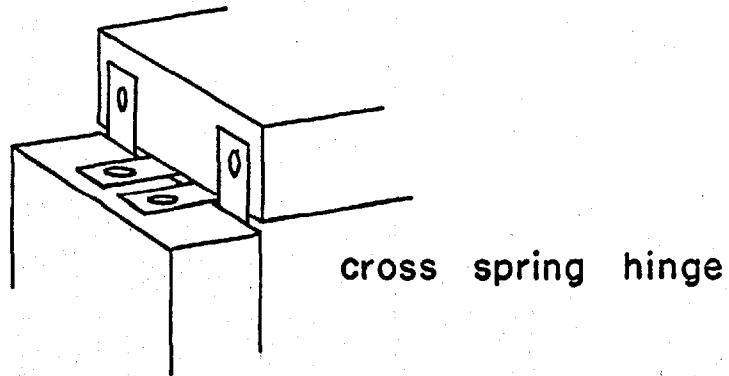
The vertical angle α was estimated from a theodolite survey and is corrected for the height differences of the Mekometer, reflector and theodolite above the surveying plates. Since $h_m = 17.3$ cm, α must be known to within two minutes of arc. α was measured using a Watts Microptic No. 1 theodolite, which is capable of resolving vertical angles to within 20 seconds of arc.

3.4.2.1 The tiltmeter.

The plate tilt θ_m was measured using a tiltmeter especially designed for the purpose. It has three feet which rest on the plate, and a bubble mounted upon a hinged bar. The bubble is levelled by raising one end of the bar on which it is mounted by means of a micrometer screw. The micrometer reading is a measure of the plate tilt.

The two branches of the tiltmeter are joined by a cross spring hinge made of phosphor bronze. This is a perfect error-free hinge for small angles of rotation as are involved here.

THE TILTMETER



The bubble used has a sensitivity of six seconds per division. There are crude gun-sights on it so that it can be oriented to measure the tilt in a particular direction.

The tiltmeter has been calibrated on a tilting table at N.P.L. It was dropped during the 1968 summer season but only the zero changed, and this was noted. The zero may be checked at any time on a flat surface by finding the direction in which the tiltmeter reading does not change when rotated through 180 degrees.

The plate tilts are measured each time a pillar is used, as a check against the pillar having moved.

3.4.3 Geometrical corrections at the reflector end.

The reflector correction is more complex because the optical path length depends upon the angle of entry of the light beam into the cube corner.

To compute this variation requires analysis of the paths of light through a cube corner reflector.

Consider the cube corner shown, with cube sides of length a and refractive index n .

(i) The front face is the plane $x+y+z=a$

Consider a ray incident at $P_0(x_0, y_0, z_0)$ with direction cosines $-\alpha, -\beta, -\gamma$.

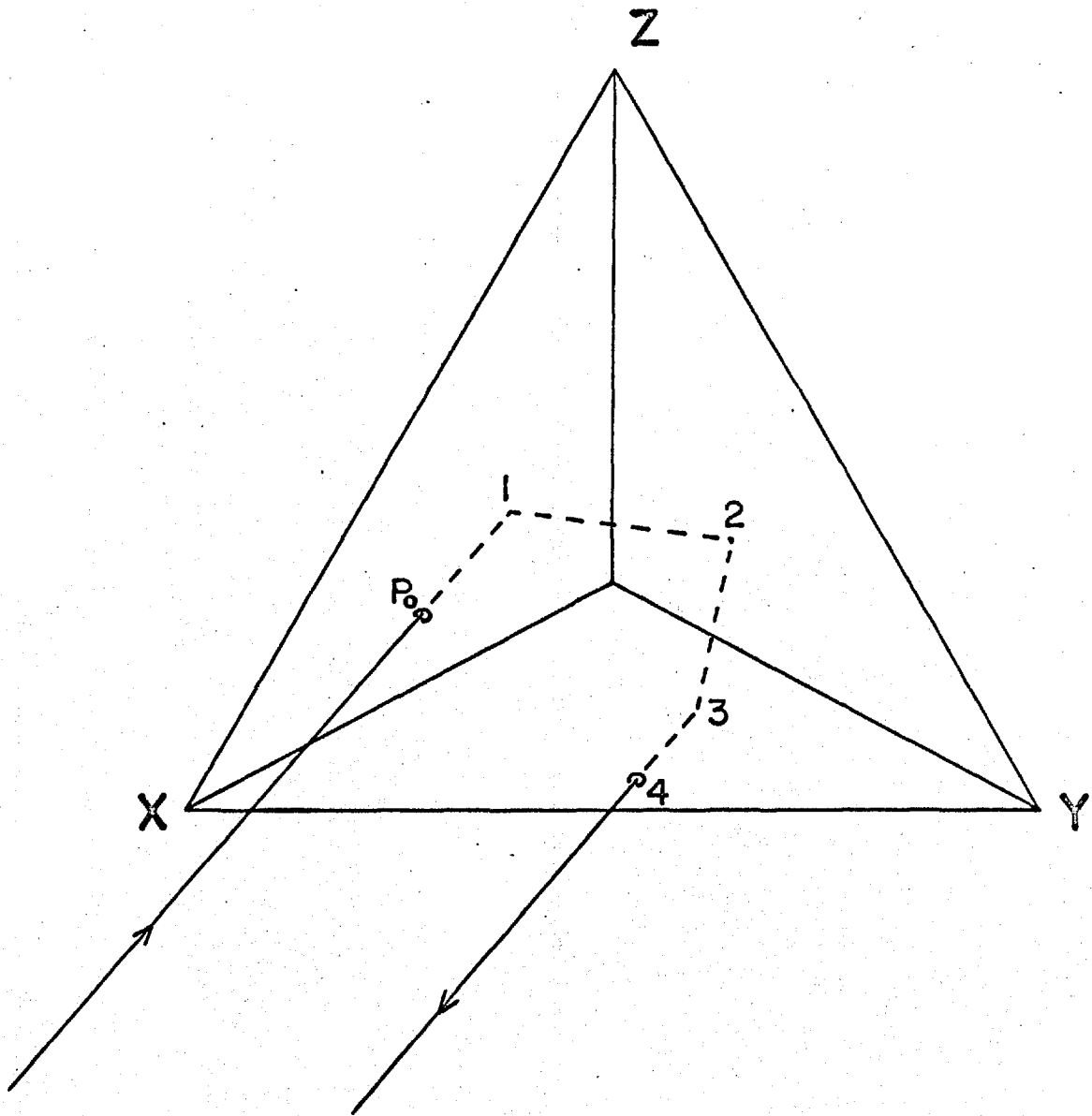
The distance d_1 to point 1 on the first face, say $y=0$, is given by

$$x_1 = x_0 - \alpha d_1, \quad y_1 = y_0 - \beta d_1 = 0, \quad z_1 = z_0 - \gamma d_1,$$

(ii)

$$d_1 = \frac{y_0}{\beta}$$

The direction cosines of the ray are now $-\alpha, \beta, -\gamma$.



Path of light ray through cube-corner reflector

The distance d_2 to point 2 on the second face, say $x=0$ is given by

$$x_2 = x_0 - \alpha d_1 - \alpha d_2 = 0 \quad y_2 = \beta d_2 \quad z_2 = z_0 - \gamma d_1 - \gamma d_2$$

(iii)

$$d_2 = \frac{x_0}{\alpha} - d_1$$

The direction cosines of the ray are now $\alpha, \beta, -\gamma$.

Similarly

$$x_3 = \alpha d_3 \quad y_3 = \beta d_2 + \beta d_3 \quad z_3 = z_0 - \gamma d_1 - \gamma d_2 - \gamma d_3 = 0$$

(iv)

$$d_3 = \frac{z_0}{\gamma} - d_1 - d_2$$

The new direction cosines are α, β, γ .

(a) The ray returns parallel to its original path.

The distance d_4 to the cube corner front face is given

by

$$x_4 = \alpha d_3 + \alpha d_4 \quad y_4 = \beta d_2 + \beta d_3 + \beta d_4 \quad z_4 = \gamma d_4$$

by (i)

(v)

$$x_4 + y_4 + z_4 = a$$

substituting we get

$$d_4 = \frac{a - \alpha d_3 - \beta d_2 - \gamma d_3}{\alpha + \beta + \gamma}$$

from (ii), (iii), (iv) (v) we get

$$d_1 + d_2 + d_3 + d_4 = \frac{2a}{\alpha + \beta + \gamma}$$

This means

(b) The distance a ray travels in a cube corner depends only upon the direction of entry.

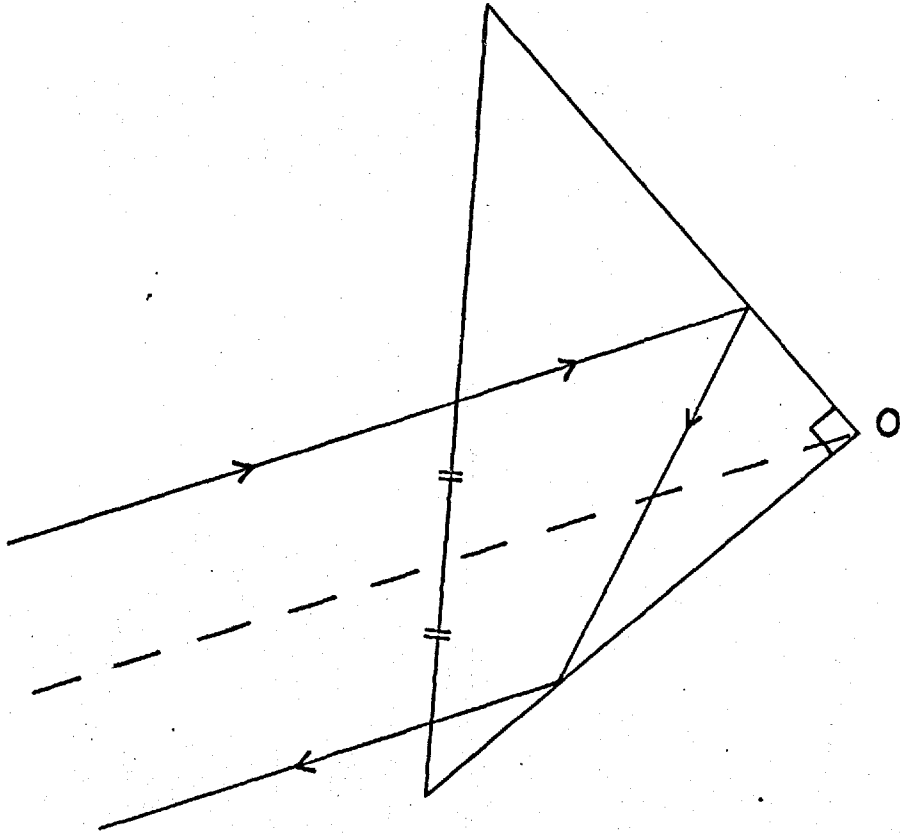
$$z_4 = \gamma d_4 = \gamma \left(\frac{a - \frac{\alpha z_0}{\gamma} + x_0 + y_0 - \frac{\beta z_0}{\gamma}}{\alpha + \beta + \gamma} \right)$$

$$= \frac{2a\gamma}{\alpha + \beta + \gamma} - z_0$$

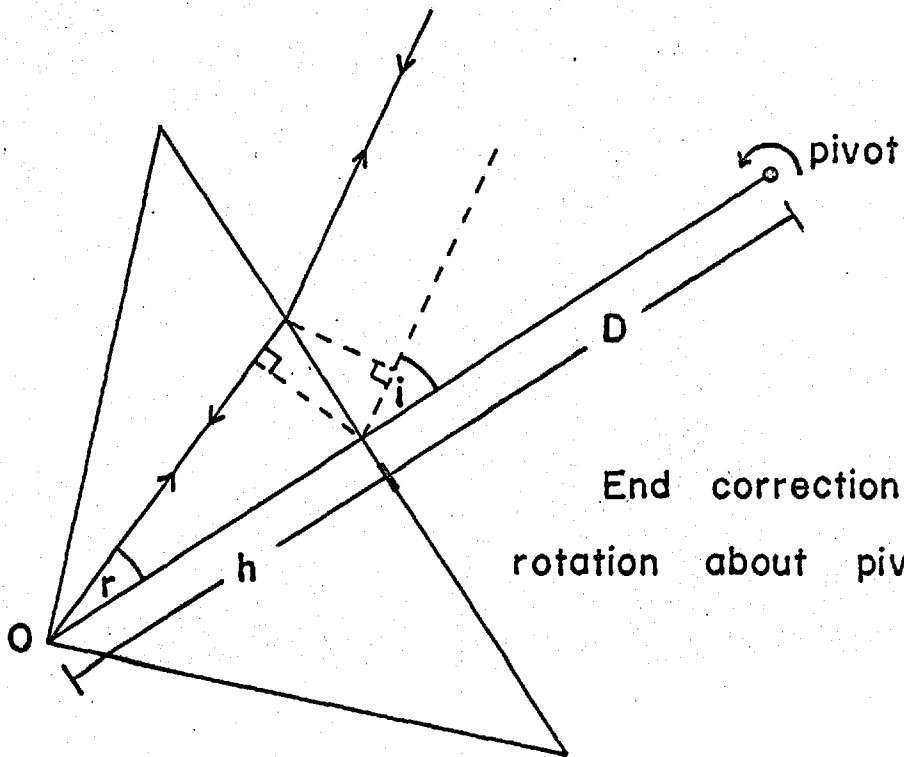
a line from 0 with direction cosines α, β, γ cuts the front face

at a point with $z = \frac{\gamma a}{\alpha + \beta + \gamma}$

$$z_4 = \frac{\gamma a}{\alpha + \beta + \gamma} + \left(\frac{\gamma a}{\alpha + \beta + \gamma} - z_0 \right)$$



result(c) The incident and reflected rays are symmetrical about a parallel line though O



End correction for rotation about pivot axis

This shows

(c) The incident and emergent rays are reflected in a parallel line going to the apex O. (see diagram).

Consider a ray travelling to the apex at an angle r . r is the angle of refraction at the front face. The optical distance the ray travels in the cube corner is $2nh/\cos r$, where h is the height of the cube corner.

By result (b) all rays parallel to this ray also travel a distance $2nh/\cos r$. Result (d), the optical distance a ray travels in a cube corner reflector is $2nh/\cos r$.

We may now consider the actual case of a reflector mounted for rotation about an axis distance D in front of the front face. From result (c) we see that for an inclined reflector not all the front face is used. Considering measurement to the pivot point, the correction C is

$$c = D \cos i + nh \cos r$$

and varies with i (see diagram).

It is of interest to note the best position for pivoting the reflectors. By differentiating we find that $\partial c / \partial i$ is minimum for $D = -h/n$. This result is to be expected since an air-filled cube corner should obviously be pivoted about its apex. For a glass-filled cube corner the apparent apex is $-h/n$ in front of the face.

The reflectors have all been calibrated for normal incidence. The angular correction E of measured distances is given by

$$E = D(1 - \cos i) + nh \left(1 - \sqrt{1 - \left(\frac{\sin i}{n} \right)^2} \right)$$

For the reflectors used the correction is as shown in the table.

0°	1°	2°	3°	4°	5°	6°
0 mm	-.008	-.019	-.045	-.075	-.120	-.175

Compare with $D = -h/n$

0°	5°	10°	20°
0 mm	.000	-.002	-.030

These corrections will not be significant for horizontal rotations because the reflectors were aimed by eye to within about $\pm 2^\circ$. The vertical correction may be significant in some cases. In our case therefore $i = \alpha + \theta_r$, where θ_r is the tilt of the reflector plate.

If the reflector plate has a tilt θ_r and the light is coming up-hill with an angle of elevation α then a correction $-h_r \sin(\alpha + \theta_r)$ must be added, where h_r is the height of the cube corner apex above the plate.

The total geometrical reflector correction is thus

$$-h_r \sin(\alpha + \theta_r) + D(1 - \cos(\alpha + \theta_r)) + nh_r \left(1 - \sqrt{1 - \left(\frac{\sin(\alpha + \theta_r)}{n} \right)^2} \right)$$

The primary use of these geometrical corrections in the present case is to be able to compare distances measured from A to B with distances measured from B to A. It should be pointed out, however, that if the reflector apex was arranged to be the same height above the reflector plate as the Mekometer trunion axis above the Mekometer plate then the distances A to B and B to A could be compared without correction.

By making these corrections, other workers can compare measurements of the same lines with different

instruments. The plate tilts should be measured in any case, as a precaution against post movements. The angles of elevation must be measured to determine the pressure corrections. It is also best to mount the Mekometer and the reflectors as low as possible to reduce any errors due to accidental tilt in the plates.

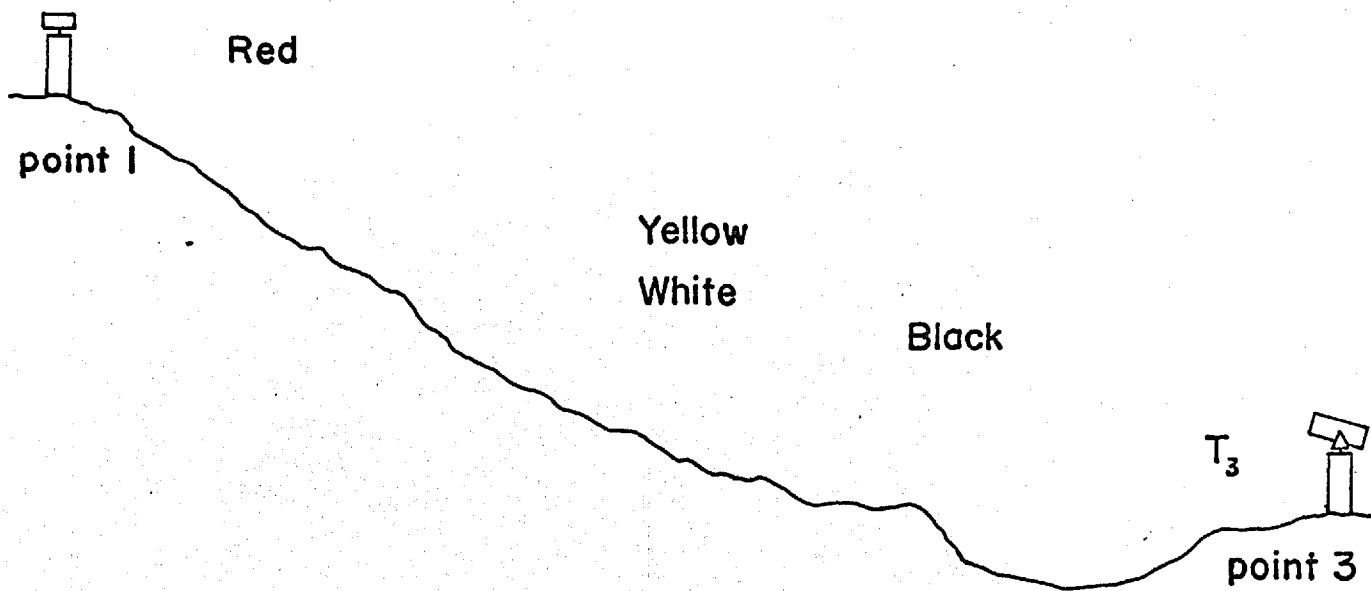
Where lines have been measured in both directions, no significant differences have been found between the two measurements after the appropriate corrections have been applied. The latter range up to 1 cm.

3.5 The 48 Hour Watch as a Check on the Atmospheric Corrections.

As a check on the various atmospheric corrections a single line was measured for 48 hours with readings taken at 10 to 15 minute intervals. The line chosen was 3-1 at Reykjanes, which is in the thermally active area. This was thought to provide a good test because of the large temperature variation in time and space.

The line was sampled by three temperature probes, approximately on line, hung from poles, and one mercury thermometer. Recorded air temperatures ranged from 15°C to 3°C. Fortunately, the conditions were extremely variable during the 48 hours, ranging from still air with sunshine to cloud, high wind and low temperature.

A tent was erected around the Mekometer pillar so that measurements could continue through rain, if necessary. This had the effect of raising the cavity temperature further above air temperature than normal. On the first day which was



PROFILE OF 48 HOUR
WATCH

still and sunny, the cavity temperature was up to 9°C above air temperature. On the second day, with intermittent cloud and more wind, the cavity was only two to three degrees above air temperature. For three hours while the wind was trying to blow the tent down the cavity temperature was within 0.5 degrees of air temperature.

All the distance readings were corrected for atmospheric conditions, as described. A mean air temperature was used which was the unweighted arithmetic mean of three probe values and a mercury thermometer reading.

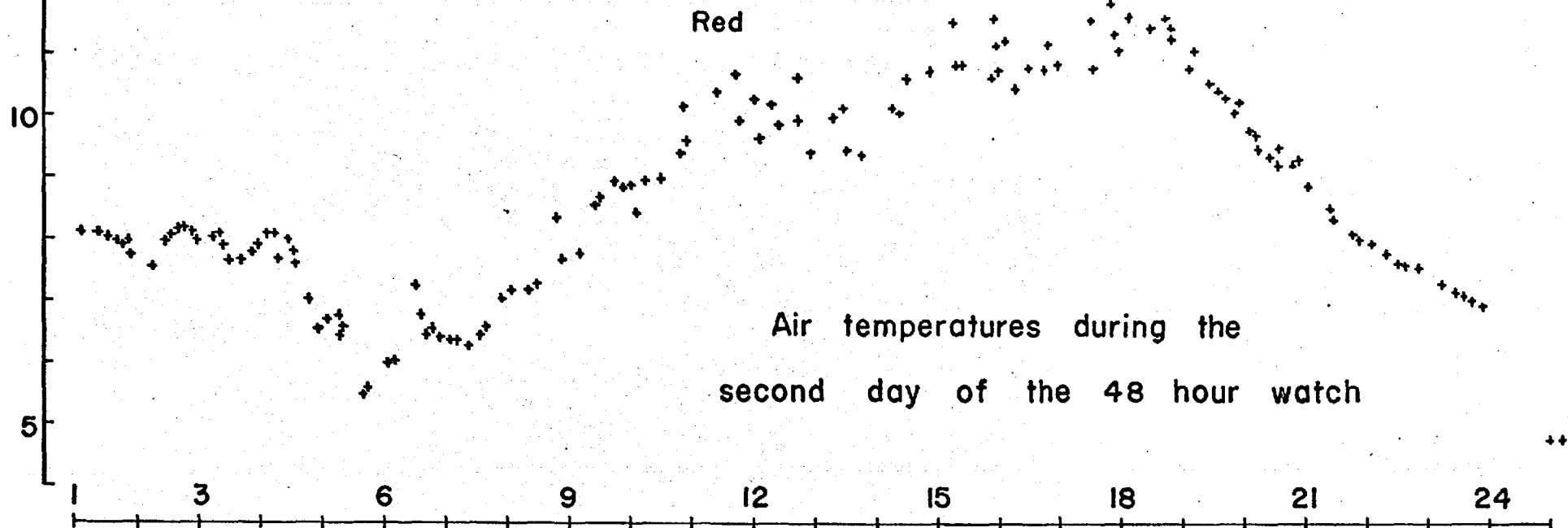
As expected, the readings had a high scatter. They followed a normal distribution with the uncorrected measurements having a standard deviation of 0.0048 ft and the corrected measurements a standard deviation of 0.0040 ft.

To test various interdependences a computer program was written which would give the linear correlation coefficients between various parameters.

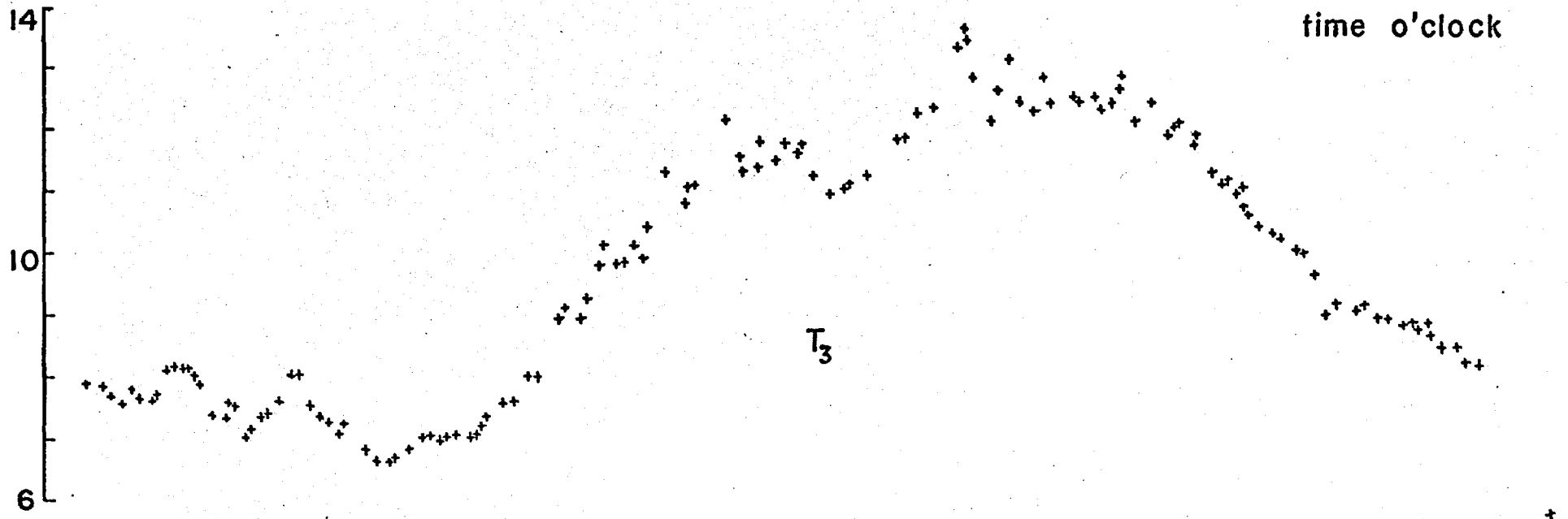
The results are shown in the table.

Quantities	Correlation Coeff.	Significance Level
distance-cavity temp.	-0.1342	80%
Mekometer-cavity temp.	0.5337	100
red-red	1.0000	100
red-black	0.9187	100
red-thermometer	0.9357	100
red-cavity temp.	0.8856	100
black-thermometer	0.9255	100
Mekometer-red	0.3538	99.9
distance-red	-0.1141	50
Mekometer-black	0.3950	99.9
distance-black	-0.1314	80
Mekometer-thermometer	0.4491	100
distance-thermometer	-0.0657	60
distance-tide	0.0973	75
red-tide	-0.5037	100

13 temperature °C



Air temperatures during the second day of the 48 hour watch



It was found that there was very high correlation between various air temperatures measured. There was very high, but slightly less, correlation between the air temperatures and the cavity temperatures. There was high correlation, 0.53, between the uncorrected Mekometer readings and the cavity temperatures, as might be expected. The correlation between corrected distance and cavity temperatures was -0.13. For random figures the probability of a correlation less than this is about 80 per cent. This is not very significant, but coupled with the behaviour of the air temperatures warrants investigation.

The correlations of the air temperatures with the uncorrected Mekometer readings were 0.4991, 0.3950 and 0.3538 in order of their increasing distance from the Mekometer and also increasing height above the Mekometer. The correlations with the corrected readings were -0.0657, -0.1314 and -0.1141 respectively. The similar behaviour of the effect of atmospheric corrections on the correlations of distance with air and with cavity temperatures is a product of the high correlation between air and cavity temperatures and cannot be used to argue about the corrections themselves.

To test what magnitude of systematic errors could be concealed within these results the cavity frequency/temperature coefficient was adjusted by an iterative process to obtain zero correlation between cavity temperatures and corrected distances. The adjustment required to do this was only 0.0844 parts per million per degree. Using this new value of cavity coefficient it was found that the small correlations between air temperatures and distance also nearly vanished, being 0.0639, -0.0071, 0.0033.

This means that the same result could also have been obtained by adjusting the air temperatures or cavity temperatures by 0.08°C per degree. It is indeed likely that the air temperatures are in error by this amount. The sense is such that the air temperatures should vary more than they did. One of the probes was at point 1 on the top of a hill so this point might have heated up less during the day than the line as a whole. As the effect is not significant, no definite answer can be found. The result is looked upon as a tribute to hours of careful frequency measurement of the Mekometer and probes alike.

Even though the measurements were not of a high quality an investigation was carried out to see if there was any detectable effect due to earth tides. Gravity values were computed for each of the measurement times and these were correlated with the corrected distance. The correlation was 0.0638, which is not significant, especially when it is realised that the correlation of tide with air temperature was -0.5037 ; as they both are diurnal effects this is not surprising. When the temperature dependence was removed from the readings the tidal correlation was 0.0473, which is not significant above the 50 per cent level.

An attempt was made to make use of the different characters of the two days. The first day was warm and sunny and the second day cold and windy. On the first day the correlation between distance and cavity temperature was -0.17 (90%) and on the second day $+0.10$ (75%). Because on the first day the cavity temperature was varying more with respect to air temperature than on the second, it is tempting to think that this is evidence for the cavity coefficient being in error,

rather than the air temperatures, if either. However, because the first day was warm and sunny without much wind, any air temperature bias is also likely to be larger. From the nature of the terrain there was little choice as to where the probes were to be situated, if they were to be at the correct height. This effect of an unrepresentational sampling of the air temperature is going to produce an error which cannot readily be estimated. It will vary from line to line and day to day. The effect is discussed more fully in Chapter 5.

It was interesting to note that while the standard deviation of the readings was 0.004 ft for the two days, the standard deviation of the readings taken from sunset until 1.00 a.m. was 0.002 ft. This confirmed what had been noticed previously, that these are the hours when the air is most steady. During this time the temperature is dropping steadily.

Dawn was not so good. The physical explanation of this is that when the sun is above the horizon, the rocky ground heats up very quickly and the air warms from the bottom up. The warm air rises and mixes with the cooler air, causing turbulence and erratic air temperatures.

The temperature variations during the day showed up very well. At 1.00 a.m. the scatter was $\pm 0.2^{\circ}\text{C}$ from a smooth curve, and this lasted until sun rise at 5.00 a.m., when the scatter increased until noon, when it was $\pm 1.0^{\circ}\text{C}$. During the afternoon the scatter remained constant at about $\pm 1.0^{\circ}\text{C}$ until sunset, when it suddenly dropped to $\pm 0.1^{\circ}\text{C}$ and remained at this level until 1.00 a.m.

The reasoning used in working out the above correlation figures is as follows. The best estimator of the correlation coefficient between two variables x_i and y_i is

$$\hat{r} = \frac{\sum (x_i - \bar{x})(y_i - \bar{y})}{\sqrt{\sum (x_i - \bar{x})^2 \sum (y_i - \bar{y})^2}}$$

The significances quoted are probabilities that there is in fact some correlation as opposed to no correlation. In other words, for a correlation coefficient estimated as 0.5 there is a 99.9 per cent chance that there is some correlation, i.e. that when x increases, so also does y . The significance is not a measure of how well x_i and y_i follow each other. The correlation coefficient is itself a measure of how good a straight line can be put through the points x_i, y_i .

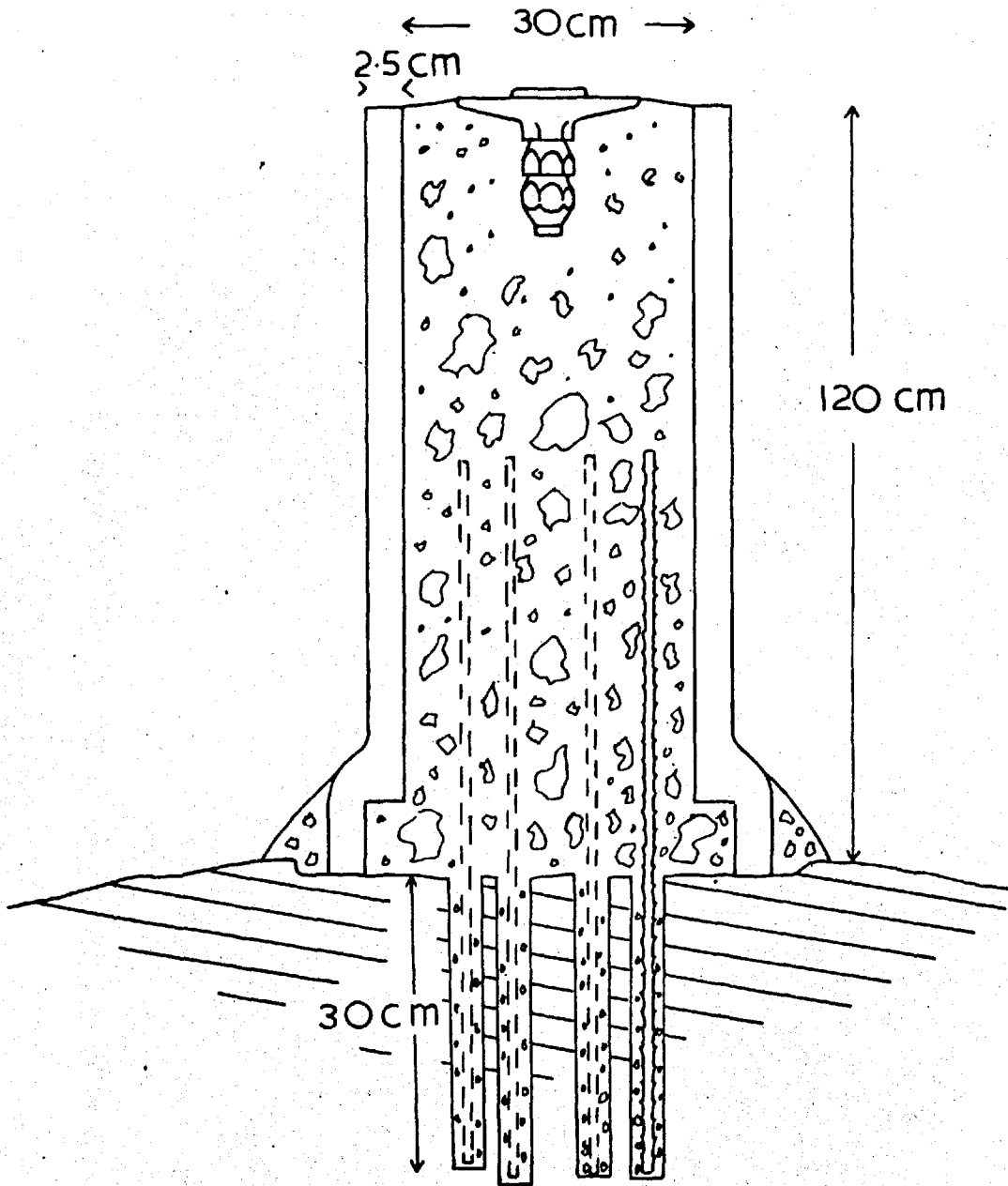
CHAPTER 4

PRACTICAL CONSIDERATIONS

Work was started in Iceland during the summer of 1967. Thingvellir was chosen as a site for one of the networks on the recommendation of Dr. G.P.L. Walker, a geologist from Imperial College. This recommendation was based on Thingvellir having some of the best formed and most dramatic open tectonic fissures in Iceland. Thingvellir is also served by a good road from Reykjavik. The appeal of Thingvellir for geodetic investigations was demonstrated by the number of other teams working there in 1967. They included Professor R.L. Decker (1968), Professor K. Gerke from Brunswick, who measured some lines by Geodimeter and Tellurometer respectively, and Professor Eysteinn Trygvasson (1968) who very precisely levelled across the active zone.

After the Thingvellir network had been built the SW tip of Iceland, Reykjanes, was rocked by an earthquake swarm. This took place during the first few days of October 1967 and consisted of 16 shocks, the four largest being poorly located events of magnitude 4.3 to 4.4 on the Richter scale. New cracks were reported on the ground, and the Reykjanes lighthouse, the oldest in Iceland, was cracked. Although it is a long established

A GEODETIC PILLAR



thermal area steam was now coming up in new places. There was fear of an eruption and the possibility of further earthquakes, so it seemed an obvious area for geodetic investigation. Accordingly, a network of posts was quickly constructed, limited because of shortage of time to eight posts. It was planned and almost completely built in a day.

4.1 Description of the Pillars.

As the aim was to keep the corrections to within 0.1 mm the Mekometer had to be relocatable to within this limit. Some experiments were tried using tripods and optical plumbs. It was not felt that these would be suitable for the highest precision in the field. It is a lengthy procedure setting an optical plumb to better than 0.5 mm, as the reference point has to be placed in the centre of a circle of error. There is also a chance in using a tripod that it will be accidentally disturbed by the wind or other factors.

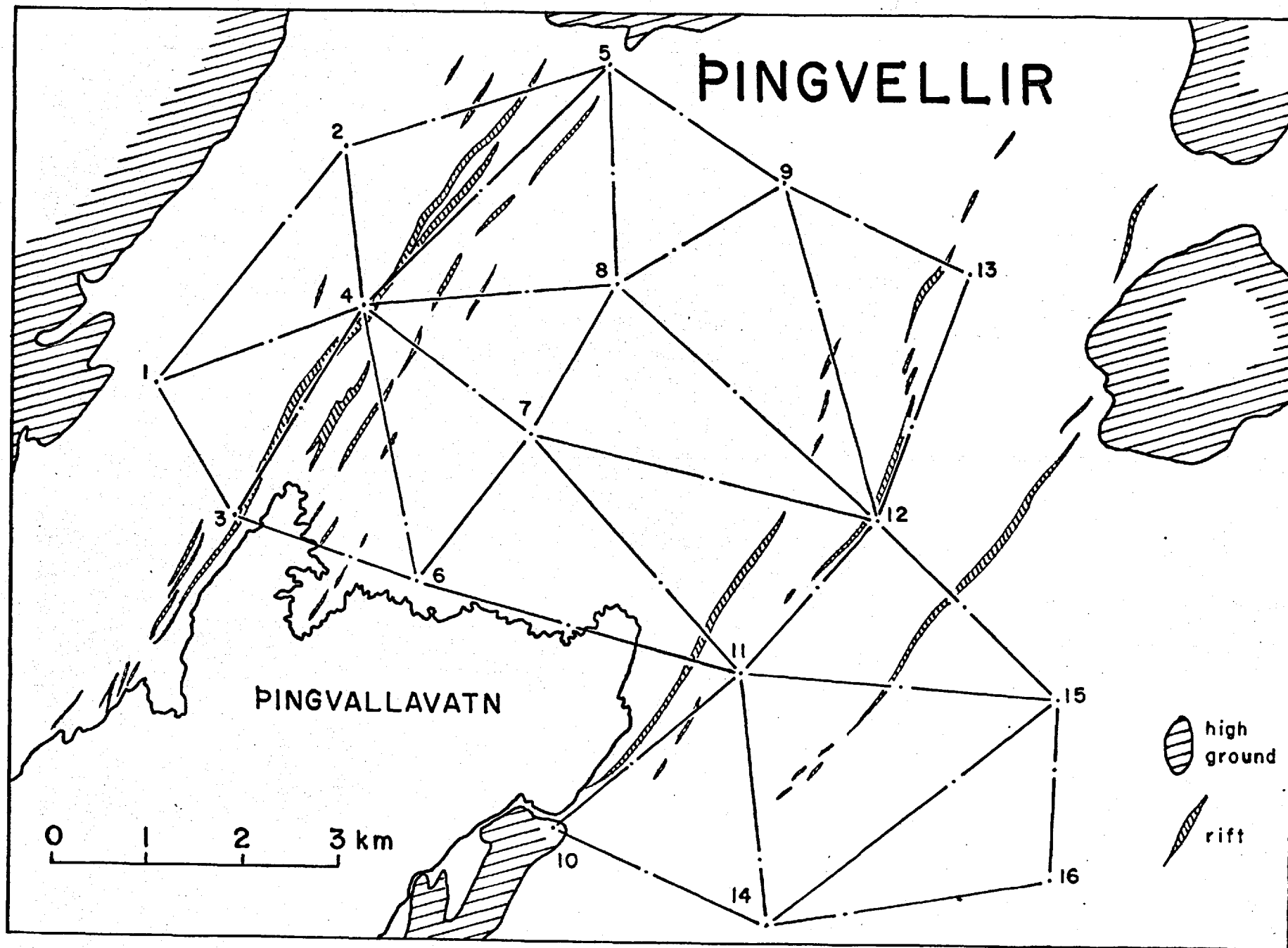
Geodetic pillars seemed to be the answer. On consultation with Landmaelingar Islands, the Icelandic Geodetic Survey, it was decided to build pillars based upon concrete pipes. These pipes were filled with concrete and anchored to the rocks by knurled steel stressing rods grouted into holes drilled in the bedrock, as shown. The pillars are 1.3 m high to set the instrument at a convenient height for use and to eliminate the worst ground shimmer. They are of two types. At Thingvellir the lines are each divided by an intermediate pillar enabling the lines to be measured in two halves. The vertices of the triangular network at Thingvellir have pillars

35 cm in diameter while the intermediate points have pillars 25 cm in diameter. At Reykjanes all our pillars are 25 cm in diameter.

The pillars were built on solid rock, which, as far as could be judged, was continuous to depth. In regions of pahoehoe or ropey lava and palagonite tuff this can be done with fair confidence. Regions of aa or blocky lava were avoided where possible. Where this was not possible, the posts were built on the least blocky and most stable looking area, usually away from the edge of the flow.

The pillar sites were prepared by knocking away the mossy or weathered surface with a pick. This work gave a good indication as to the goodness of the rock being built on. Holes were drilled 3 cm in diameter for the stressing rods. Four stressing rods were used for the larger pipes and one or occasionally two for the smaller pipes. When the foundation was basalt we drilled about 30 cm and on palagonite tuff about 75 cm. Most of the holes at Thingvellir were drilled with a large two-stroke percussion drill lent to us by the Icelandic Telephone Company. The remainder were drilled with a core sampling drill developed for palaeomagnetic work.

At Thingvellir the cement was mixed at a local hotel and carried in oil barrels to the site. Sand was obtained from the shore of the lake. At Reykjanes we mixed the cement on site and used sand from the desert. A rich mixture of three parts sand to one part cement was used to make the concrete water and frost proof. Stones were built into the pillars to economise on cement.



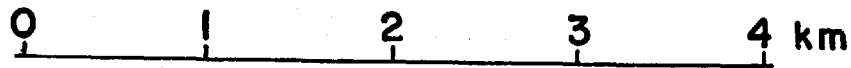
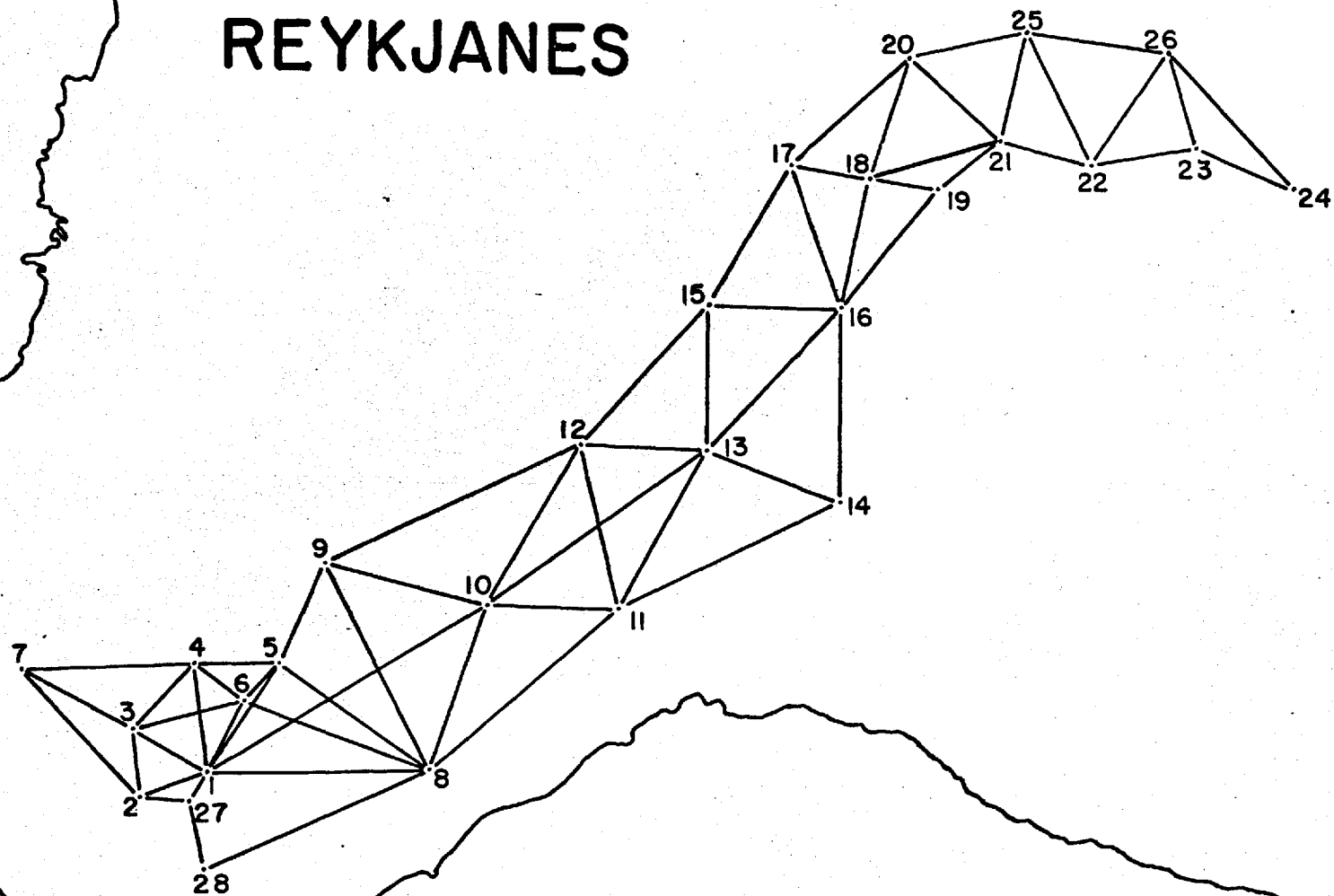
The plates for the top of the pillars are required to position the Mekometer mounting bracket and reflectors uniquely. They are flat plates with an accurately reamed hole 1 ± 0.0003 inches in diameter and 4 inches deep, into which a well-fitting spigot will fit and may rotate. The Mekometer bracket and reflectors are mounted on these spigots. The plates, together with the Mekometer bracket and reflector mounts were made of gunmetal bronze. The holes were protected by a cap.

4.2 The Laying out of the Networks.

When the work was first started there was some doubt as to the optimum length of the lines. The Mekometer has an absolute range of 3-4 km and an effective range depending upon local conditions. The network at Thingvellir was set up with the aim of covering the area as efficiently as possible with pillars not more than 2 km apart.

A triangular network of points was laid out with sides 3-4 km long which would be measured in two halves. The mid-points of these sides, the smaller pillars, were situated as nearly on a line between the end points as possible, and always close enough so that the cosine of the deviation could be determined by theodolite to better than 1 in 10^7 . Thus if one of the small pillars were knocked or fell down, it would still be possible to determine the distance between the end points. The end points themselves were also made inter-visible so that a longer range instrument, or even the present Mekometer could measure the whole length, if expedient. The vertical misalignment of the mid-points was made as small as

REYKJANES



possible and were chosen to bisect the line fairly closely on solid rock. These requirements are stringent and would have been impossible to satisfy in some terrains.

In the Reykjanes network, shorter lines were used, and mid-points were not necessary. Three pillars were placed on each side of what looked like the active zone so that as many lines as possible could be shot across the zone to evaluate both side-slip and extension. Additional pillars were placed on each side away from the active zone to act as reference points and to enable the lateral extent of the disturbed zone to be evaluated.

In the summer of 1968, on the basis of preliminary measurements on the early posts the network was extended with the object of investigating the extent and direction of the disturbed zone.

It has been found that the Mekometer is most sensitive at a range of one kilometre. Since this is also the distance at which the Mekometer has the greatest theoretical accuracy, this would appear to be the optimum length for measurement.

4.3 Field Procedure for Measurement.

This section is meant as a users guide to the Mekometer and field measurements.

The minimum practical number of personnel in a Mekometer party is four when using temperature probes and three when not. With extra people there would be some redundancy some of the time. With fewer than these numbers there would be waiting, with sacrifice of speed and probably accuracy. Speed

is an important economic factor because, with the poor weather encountered in Iceland, it was found that in two six week periods of measurement on both occasions about half the measurements were made in 10 days.

One man operates the Mekometer full time during a line measurement, another acts as meteorologist and book-keeper at the Mekometer station, while the third takes the reflector to the target pillars. The last is in communication with the book-keeper by radio and gives the air temperatures at the target end when asked. The fourth man would be responsible for setting out the probes along the line and operating their receiving system.

With the present probes it is essential to be able to drive close to the Mekometer pillar. This is because the radio receiving system for the probes requires a battery and inverter to run the counter and receiver. As every line can be shot in two directions, this is generally possible with a Land Rover and perseverance.

The first operation on reaching the Mekometer pillar is to unpack the Mekometer, place it on the pillar and then connect the power supply and switch it on. This is to allow the maximum possible time for the standard and modulating cavities to reach equilibrium. Tests carried out by frequency measurement under such conditions have shown that this will take up to 20 minutes. Until the modulating cavity has reached equilibrium the tuning screw has to be continually adjusted, this makes measurement difficult and increases the scatter of the readings. A thermometer is placed in contact with the

A TYPICAL RECORD

Date	March 30 th	Pressure	999.5 mb.
Time	20.30	Wet bulb temp.	5.2
Line	4-5	Dry bulb temp.	5.6
Reflector	E	Wind strength	Light. Force 1.
Tilt-meter	.2822	Wind direction	E.
		Shimmer	None.
Weather	Cloud all around. Very wet to the north.		
Comments	Nearly full moon. Calm. Steady measuring conditions.		

Mekometer Reading			Temperatures				
H	T	U	Fractions	Point 4	Probe	Point 5	Cavity
7.4	4.3	2	.2240	2.95	996	2.28	5.8
			.2215	2.95	991	2.28	5.7
			.2200	2.97	986	1.68	4.7
			.2210	2.76	986	1.88	4.7
			.2215	2.95	984	2.18	4.5
			.2215	2.95	983	1.68	4.4
			.2230	2.93	983	2.18	4.3
			.2215	2.97	979	1.88	4.2
			.2220	2.96	980	1.90	4.2
			.2215	2.97	978	1.89	4.2
			.2215	2.95	979	1.89	4.2
			.2218	2.94	978	1.88	4.1

standard cavity and when this approaches a steady reading measurements can begin.

During this period a temperature station is set up, which consists of a thermometer held in a stand shielded from the sun. This is placed up wind of the observers in an exposed position. The pressure and humidity are measured. The time, day, line name and general weather conditions are also noted together with any comments which may be useful in interpretation. A typical record is shown.

The reflector man aims the reflector at the Mekometer by eye. With our reflector mounts this can be done with sufficient accuracy. He also sets his thermometer up in a suitable place. Usually it can be strapped to the reflector mount. The reflector mounts have shields which keep rain off the surface of the reflector and also act as sun shields. If the front of the reflector does become wet it must be dried because water droplets on the front face produce random phase and effectively reduce the return signal.

The probe man should set out the probes along the line. If the wind is strong enough then kites are used. These have proved compact and very convenient. The probe batteries should be checked and replaced when below 10.5 volts. The kite is let up to about 80 m say and then a probe attached to the string. Having the kite well above the probe gives a more stable probe height. The probe is positioned on instructions by simple semaphore from the Mekometer operator.

Balloons are used in still air or light wind. One small pilot balloon produces enough lift. They have practical

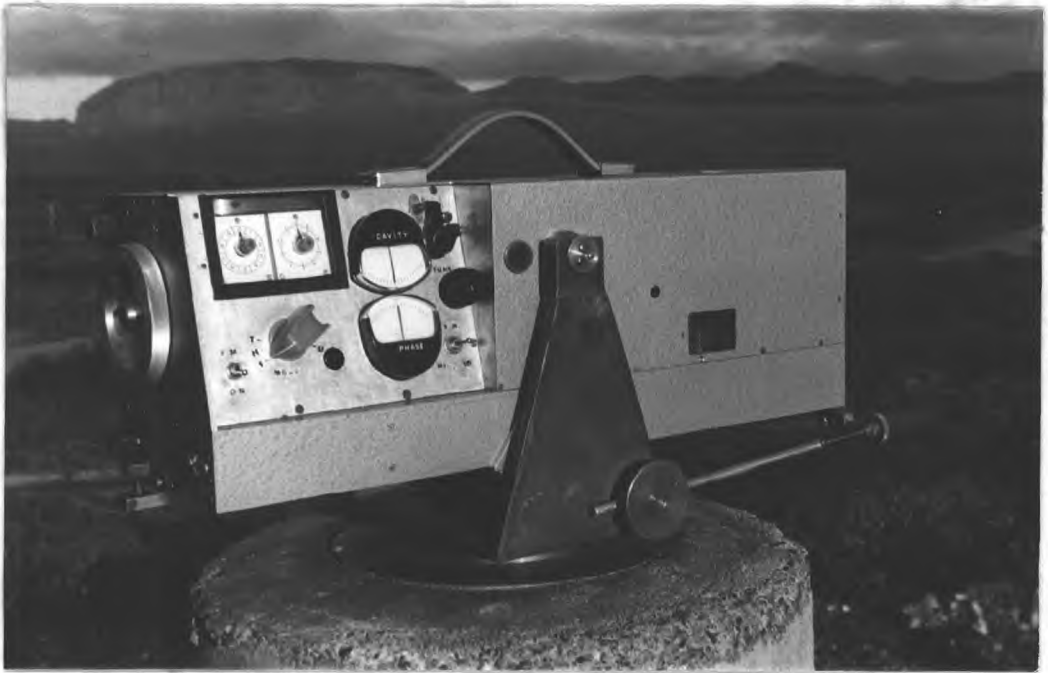
drawbacks however, Hydrogen cylinders are big, awkwardly shaped and possibly dangerous things to drive about with in a short wheel-based Land Rover, and should probably be towed in a trailer. When the balloon is inflated it cannot be moved around above 5 m.p.h. With erratic weather conditions the balloons could not be left tethered over night and had to be placed inside a large tent. It has been found that quite a large hydrogen bank is needed if much balloon work is to be done. It seems likely that a hovering device powered by a model diesel engine would be more suitable.

With the probes in place the receiving system is set up. The counter is powered by a lead-acid accumulator via an inverter; the receiver has its own dry cells. It was found that a screened lead from the receiver to the counter had to be used to prevent pick-up from the inverter. The receiver is tuned and the probes selected by a switch which crystal controls the i.f. oscillator to the required frequencies.

The probe temperatures are displayed on the counter as frequencies in the region 1-2 kHz. These are read whenever a distance measurement is made.

4.3.1 Mekometer operation.

The Mekometer is first aimed at the reflector. This is done by means of two eyepieces. The first looks through the transmitting system and is equivalent to a normal telescope. This field of view has a black spot on it which is in fact a stop for the transmitted light. The elevation of the Mekometer is adjusted by a screw on the Mekometer bracket, and the azimuth by rotating the bracket in the mounting plate until the black dot is over the reflector. The reflector is now receiving light from the Mekometer.



The Mekometer in operation at Thingvellir.



The field laboratory installed at Reykjanes.

The other eyepiece looks through the receiving system. It is sampled by pulling a little reflector into the light path just before the photomultiplier. The image here is highly magnified and only subtends one milliradian. Since no eyepiece lens has been inserted the observer has to focus his eye at infinity. He should then see the reflector and the reflected light somewhere inside a circular field of view. The elevation and azimuth are slightly adjusted until the returned light is in the centre of this field of view. The little reflector should then be pushed back and the eyepiece closed. The Mekometer is then correctly aimed.

The mode switch marked F, H, T, U for fractions, hundreds, tens, units is switched to F. The FM switch should be switched on and the high or low wobble selected by switching to HI or LO. High wobble should be used for short distances up to say 300 m and low wobble used on longer distances.

The cavity tuning screw should be adjusted in search of the resonance position. On cold days the screw will have to be screwed out and on hot days, in. The resonance position is close when the needle on the cavity meter starts to deflect. As the tuning is continued the needle will go full scale and then sharply back through the zero and full scale the other way. Wind back to the zero and the modulating cavity is at the correct frequency.

The distance measurement can now be made by setting the variable light path to its correct position as shown by the phase meter. This is done by turning the large knurled wheel at the end of the Mekometer. All the phase controls are on the

end panel. Typically the phase meter will be deflected at this stage. If it is not then either the Mekometer is set on a broad maximum of interference or the photomultiplier gain is too low. Wind the wheel until some deflection is seen on the phase meter. If this cannot be done increase the photomultiplier gain by turning the gain knob clockwise; if it can, turn the gain knob until the deflection is greatest. This sets the photomultiplier gain to optimum, i.e. just before saturation by returned light. If the phase meter deflection is to the left turn the wheel clockwise. Unless the light path is very nearly in the correct position the meter needle will deflect to the right, and then very sharply back through zero, and then deflect to the left. As with the cavity setting wind back to the zero. If the phase meter needle is to the right of zero turn the wheel anti-clockwise. This then is the position of the interference minimum required. If all is well a slight movement of the cavity tuning screw will send both meter needles the same way. If they move in opposite directions the Mekometer is set on a maximum.

With both meters set on zero the fraction of a foot, above a whole number of feet, in the line being measured may be read from a tape at the top of the front panel, graduated in thousandths of a foot. Usually the phase meter cannot be held steadily on zero because of variations in refractive index along the light path. In this case the phase is adjusted until the deflections are symmetrical about the zero. This requires estimation, so for very accurate work several settings should be made. If the deflections are rather large and wild the time

constant switch should be switched to high. This should not be used except at the final setting because it makes the meter deflections very sluggish. This effectively integrates the meter deflections over a few seconds and presents a time averaged deflection.

When the fraction has been obtained the hundreds, tens and units of feet can be measured. While the tape is in the fraction setting, the pointers on the two rounding dials should be set on zero by turning them; they are friction driven. Now turn the mode switch to hundreds and trim the cavity. The cavity tuning screw should not have to be turned very much. If it is the wrong resonance will be found. The resonance position is determined as before. The phase is also adjusted as before only this time the answer is read from the hundreds and tens dial to two significant figures, e.g. 3.7 hundreds.

The mode switch is now moved to the tens position and the process repeated to give, say 6.5 tens. The mode switch is finally moved to the units position, the meters set to zero, and the units read from the units dial. The pointer will unambiguously be pointing at some number, say 4. In the example given then, the distance would be the appropriate number of thousands of feet plus 364 plus the originally determined fraction of a foot.

The hundreds setting should give an estimate of the tens, e.g. 6.5 tens agrees with an estimate of 3.7 hundreds. If one of the settings is obviously out then it can be checked, if they are all in disagreement then the fraction should be

rechecked. It is good practice to return to fractions to do another setting as it can be used to check that the rounding dials return to zero, prevents time being wasted by doing the next fraction setting on the units mode, and gives another fraction estimate.

This procedure is quickly learned. All the switches, knobs and meters work in the expected and natural directions so that nearly anyone can operate the Mekometer successfully first time.

4.3.2 Problems likely to be met with in the field.

Each extreme weather condition produces characteristic measurement problems. In Iceland nearly all conditions except intense heat have been experienced. Most of the effects are readily explained and some can be reduced by simple measures.

4.3.2.1 Wind.

Light wind in general improves measuring conditions since it reduces the temperature gradients. During long periods of constant sunshine the wind should be as high as force 4.

If the wind increases to strong it is nearly always gusting. This produces two undesirable effects. Firstly, the standard cavity pressure becomes erratic and secondly the modulating cavity temperature becomes unsteady.

The standard cavity in the Mekometer is arranged to be at atmospheric pressure. When a strong gust blows on the Mekometer the pressure is instantaneously increased, producing a frequency change in the standard cavity. This is observed as a sharp deflection of the cavity meter needle with the arrival of a gust. The effect is greatest when the Mekometer is pointing

directly into the wind because the Mekometer is open at the front.

When the wind is gusting it also produces temperature fluctuations of the modulating cavity, which normally has an operating temperature a few degrees above ambient. This is also seen as irregularities on the cavity meter. These two causes combine to make the frequency setting more difficult and less accurate.

4.3.2.2 Rain.

Light rain does not completely inhibit operation. The main problem is keeping the Mekometer dry; being a prototype instrument it is not water-proof.

For protection, an umbrella on a pole with guys was used like a parasol with some success. Since rain is usually associated with some wind the best form of protection was found to be a polythene sheet cover, in the form of a box, which could be strapped onto the Mekometer. The portion over the side panel was liftable so that the operator could work underneath it.

If the rain becomes at all heavy work is stopped by poor visibility. After working in rain the Mekometer frequency must be checked at frequent intervals in case the standard cavity has become damp.

4.3.2.3 Intense cold.

Intense cold produces tuning difficulties. The Mekometer at present cannot be tuned when the standard cavity temperature drops below -4.0°C . At this temperature the tuning screw must be taken fully out. Below this temperature the Mekometer has to be artificially heated. Since intense cold is

usually associated with clear skies the greenhouse principle works well. A double thickness of polythene over a dexion frame was used.

4.3.2.4 Background light.

The Mekometer has to pick out its own signal from the background light around the reflector. If there is, for instance, bright snow behind the reflector, the signal to noise ratio is decreased. This can often be restored by the reflector man standing behind the reflector, although on long lines he will not be big enough. Severe noise is introduced by a background of sunlight on a lake and work must be timed to avoid this.

4.3.2.5 Prolonged sunshine.

The worst effect of prolonged sunshine is the high temperature variation produced in the atmosphere. This effect is discussed in Chapter 5.

During dry spells in Iceland it was found that the atmosphere became very dusty, particularly in the desert regions. This caused many moving parts of the instruments to become stiff. Dust also entered the modulating cavity and caused arcing. The dust had to be removed using compressed air.

In general it is best to avoid adverse conditions rather than fight them because only under favourable circumstances can the best measurements be made. When the weather is sunny it is best to work during the evening and at night.

Working at night has obvious drawbacks however. Aiming at reflectors is more difficult. A good method for

locating reflectors at night was found to be for someone at the Mekometer end to shine a torch in the general direction of the reflector. The reflector can then be seen as a spot of light. At night it has also been found that the Mekometer operator and book-keeper both need torches strapped to their heads to be able to perform their manual tasks.

CHAPTER 5

THE RESULTS AND THEIR ERRORS

5.1 The Computing of the Results.

As outlined in Chapter 3 the Mekometer readings have to be corrected for the atmospheric parameters, pressure, temperature and humidity. This was done using the University of London Atlas computer. The pressure correction requires a knowledge of the pressure difference between the two ends of the line; to determine this was the object of the first program. Finally a third program corrected for geometrical factors to give the distances between mounting plate centres.

In the first place the pressure differences between the ends of each line were calculated. The pressure exerted by 1 cm of air at standard pressure and 8°C at a latitude of 64° is 1.232×10^{-3} mb. This value was assumed to hold for all the air throughout our work. This assumption at the most could introduce a two per cent error in the pressure correction which is negligible. A simple program was written to calculate the pressure differences. The data used was:

1. The circle right theodolite reading for the vertical angle.
2. The circle left theodolite reading for the vertical angle.

3. The uncorrected Mekometer reading.
4. The line name.

There was a bubble error in the theodolite used so that angles given by the two theodolite readings were systematically different. The vertical angle was computed together with the random difference between the theodolite readings, having taken into account the bubble error. The difference was used to show up gross errors. Using the slope length of the line, the height difference between the ends and the corresponding pressure difference were computed. The theodolite readings generally differed by about 0.00005 radians or 10 seconds of arc. The vertical angles however are not this good as will be discussed later.

Atmospheric corrections were then made to the Mekometer readings. To do this a computer program was written using the following data.

1. The atmospheric pressure measured at the Mekometer station.
2. The pressure difference between end stations (previously computed from the surveying results).
3. The humidity as measured at the Mekometer station.
4. The particular reflector being used, i.e. A, B, C, D, E or F.
5. The air temperature as measured by thermometers at the Mekometer station.
6. The temperature-probe readings when the probes were being used.
7. The air temperature as measured at the reflector station.

8. The Mekometer reading.
9. The temperature of the standard cavity.
10. The name of the line and the date when it was measured.

The program corrected the Mekometer reading for atmospheric conditions by using the estimated mean pressure on the line, the mean of the air temperatures, and the humidity, which was assumed to be constant along the line. The distance was also corrected for the Mekometer frequency via the cavity temperature. Finally the appropriate reflector correction was applied to give a line length between the Mekometer trunion axis and the reflector rotation axis. The program had sub-routines which computed the Mekometer frequency from the cavity temperature and the air temperature from the various probe readings.

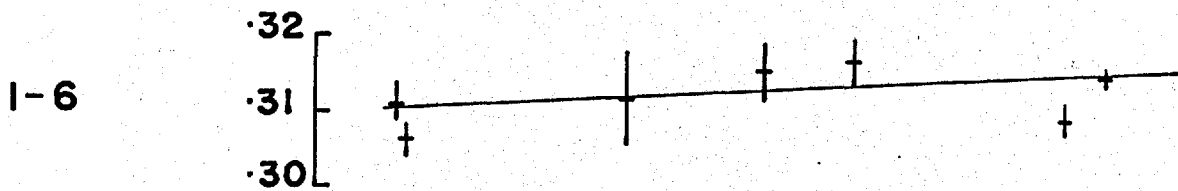
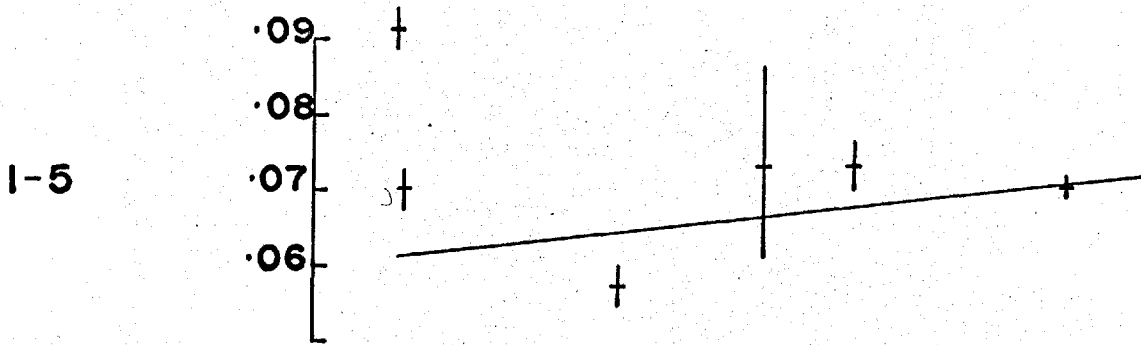
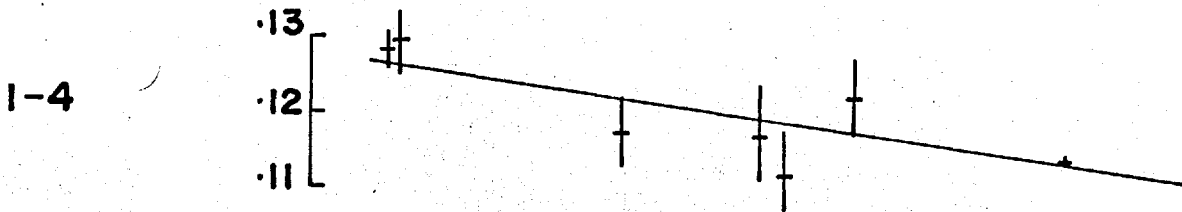
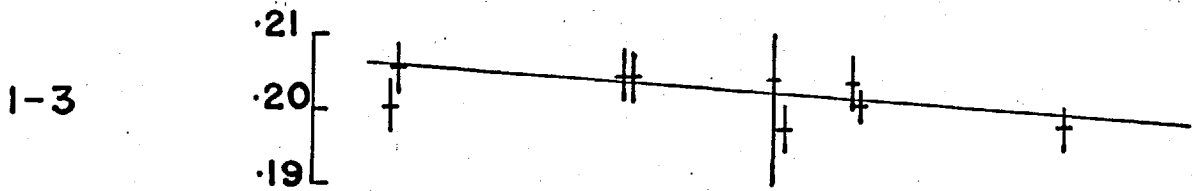
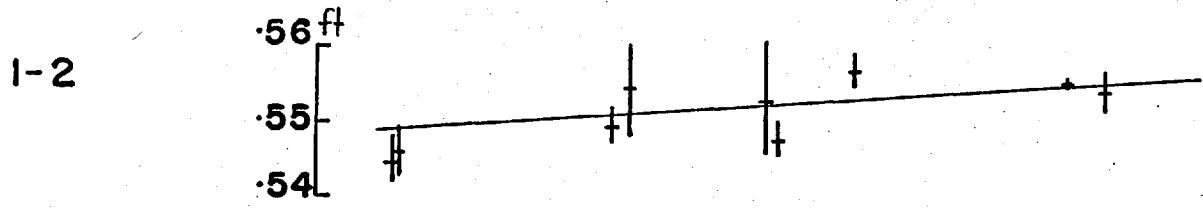
These results were printed out, together with their mean and the estimate of the standard deviation of this mean, assuming that the results were normally distributed.

These means were then used in another program which computed the geometrical corrections. The data for this program was as follows:

1. The tiltmeter reading for the mounting plate at the Mekometer station.
2. The tiltmeter reading for the mounting plate at the reflector station.
3. The height difference between the plate centres as computed from the surveying results.
4. The atmospherically corrected Mekometer results.
5. The line name and date of measurement.

Reykjanes.

O N D J F M A M J J A S O N D J F M A May 1969



The program converted the tiltmeter readings into angles and then computed the correction to be applied to convert the results to distances between plate centres as outlined in Chapter 3. This correction was output together with the corrected distance and the horizontal distance. In no case has a significant error been found due to this geometrical correction, i.e. measuring from A to B gives the same answer as measuring from B to A.

The results were as follows.

5.2 The Line Lengths.

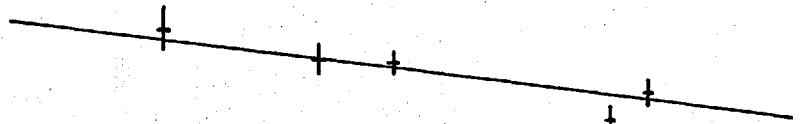
At Reykjanes

Line	Distance (ft)	Estimated error (ft)	Date measured
1-2	1404.54490	.0050	5 Oct 67
	.54610	.0050	9 Oct 67
	.54940	.0050	30 Mar 68
	.55310	.0050	2 Apr 68
	.55290	.0075	31 Jul 68
	.55670	.0020	6 Oct 68
	.55512	.0006	27 Mar 69
2-1	.55481	.0050	2 Apr 68
	.54751	.0020	3 Aug 68
	.55397	.0026	29 Apr 69
1-3	1684.20046	.0030	5 Oct 67
	.20566	.0030	9 Oct 67
	.20456	.0030	2 Apr 68
	.21726	.0686	31 Jul 68
	.20366	.0036	6 Oct 68
	.19787	.0024	27 Mar 69
3-1	.20455	.0030	3 Apr 68
	.20015	.0098	2 Aug 68
	.19735	.0134	13 Aug 68
	.20035	.0005	6 Oct 68
1-4	2180.12823	.0050	5 Oct 67
	.12973	.0050	9 Oct 67
	.11723	.0050	2 Apr 68
	.11683	.0060	31 Jul 68
	.12193	.0050	5 Oct 68
	.11354	.0016	30 Mar 69

O N D J F M A M J J A S O N D J F M A M

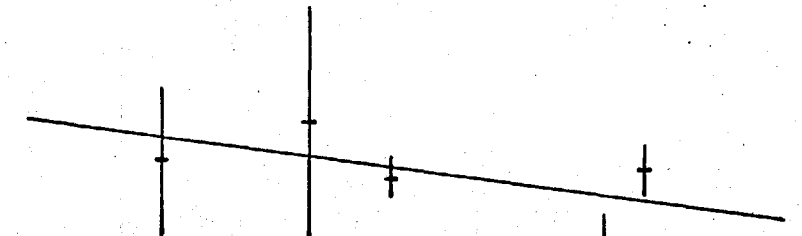
2-3

.74
[
.73
[
.72



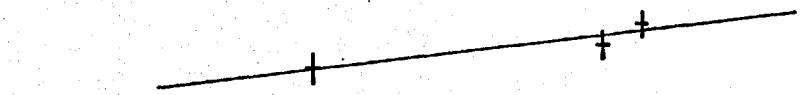
2-7

.00
[
.99
[
.98



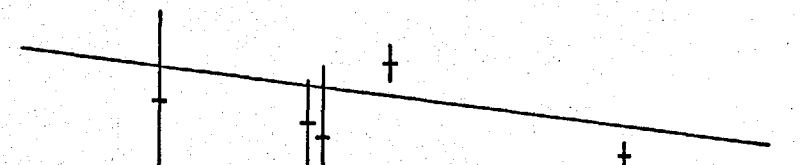
2-27

.73
[
.72



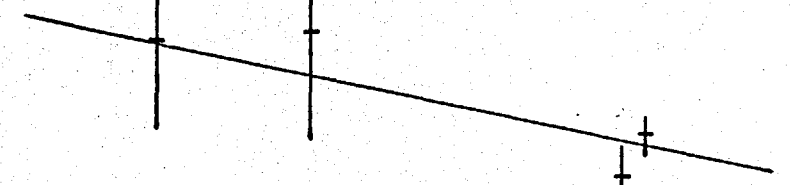
3-4

.43
[
.42



3-6

.50
[
.49
[
.48



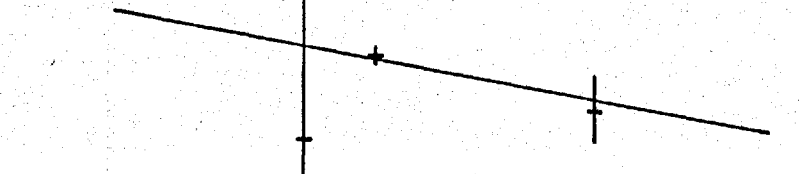
3-7

.96
[
.95
[
.94



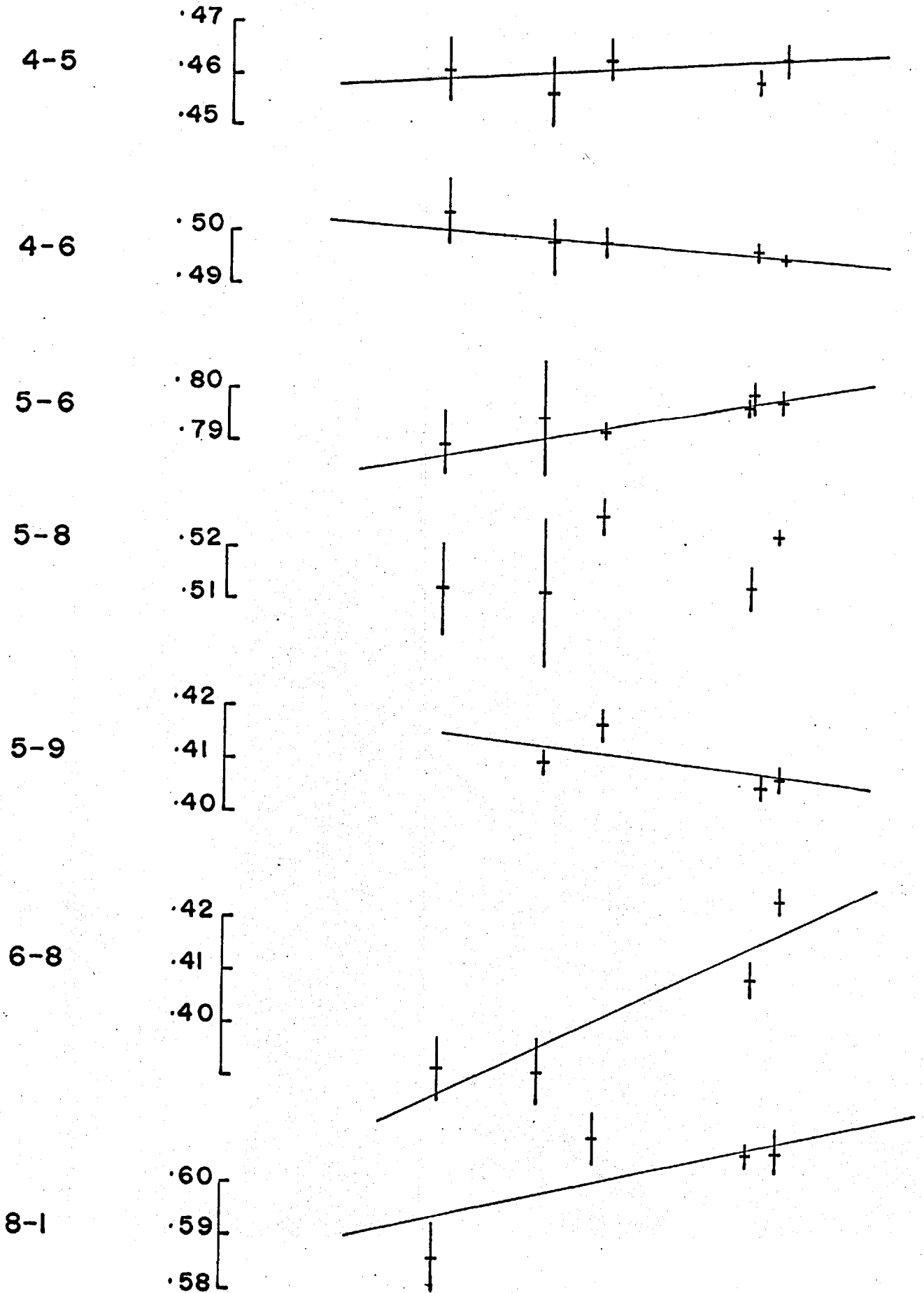
3-27

.95
[
.94



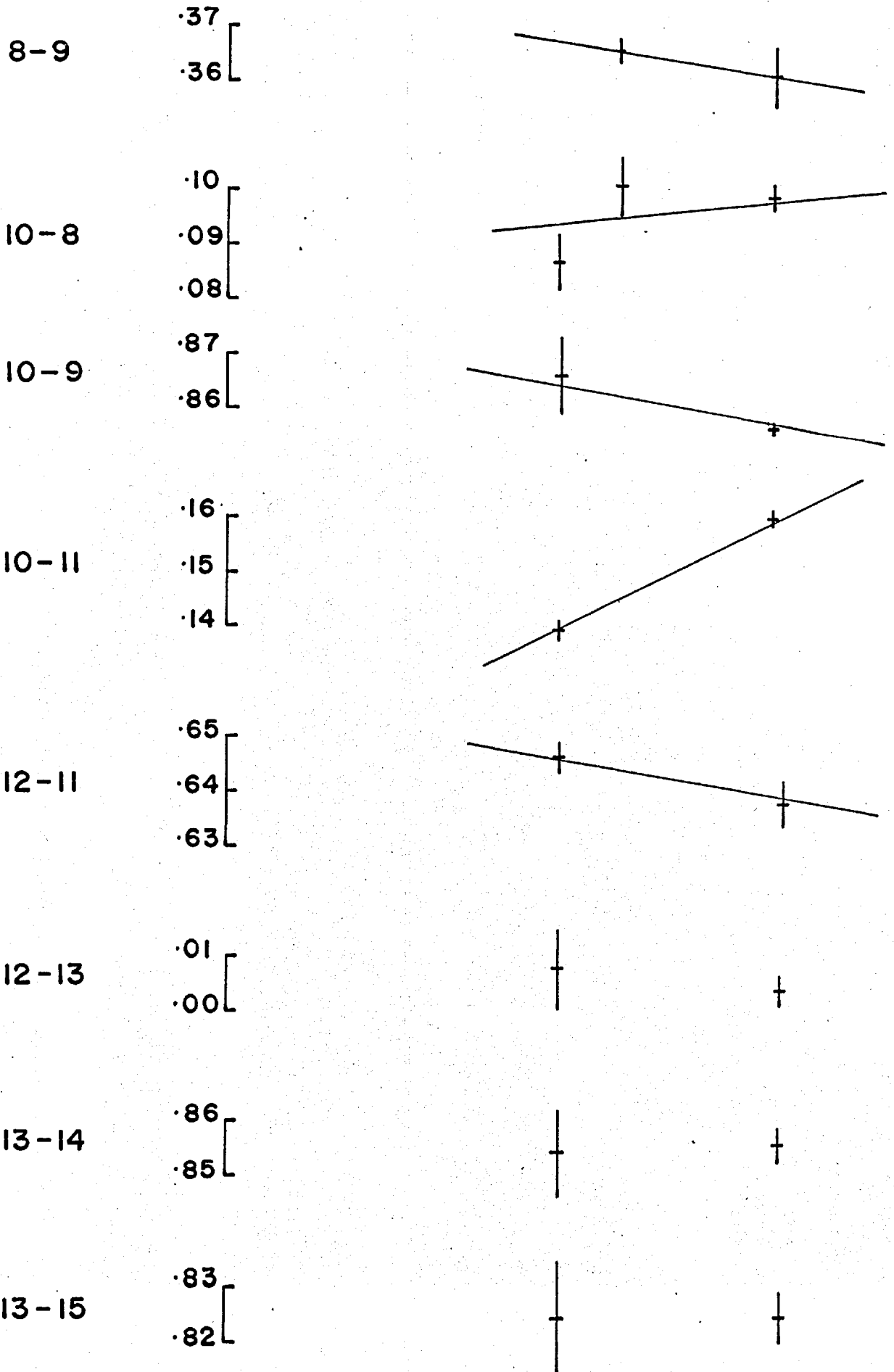
Line	Distance (ft)	Estimated error (ft)	Date measured
1-5	2606.09155	.0050	5 Oct 67
	.07025	.0050	9 Oct 67
	.05745	.0050	2 Apr 68
	.07355	.0131	31 Jul 68
	.07375	.0034	5 Oct 68
	.07031	.0010	27 Mar 69
1-6	1684.31106	.0030	5 Oct 67
	.30646	.0030	9 Oct 67
	.31176	.0057	2 Apr 68
	.31516	.0035	31 Jul 68
	.31566	.0029	5 Oct 68
	.30874	.0020	27 Mar 69
	.31431	.0009	29 Apr 69
1-27	592.58068	.0005	31 Jul 68
	.58327	.0019	27 Mar 69
	.58342	.0016	29 Apr 69
2-3	1331.73516	.0010	6 Oct 68
	.72793	.0015	29 Mar 69
	.73113	.0011	29 Apr 69
3-2	.73949	.0022	3 Apr 68
	.73519	.0014	2 Aug 68
2-7	3366.99565	.0099	3 Apr 68
	3367.00435	.0145	3 Aug 68
	3366.99415	.0016	6 Oct 68
	.98439	.0036	29 Mar 69
	.99429	.0027	27 Apr 69
2-27	1138.72223	.0021	3 Aug 68
	.72556	.0015	29 Mar 69
	.72856	.0016	29 Apr 69
3-4	1829.42713	.0109	3 Apr 68
	.42443	.0048	2 Aug 68
	.43223	.0015	6 Oct 68
	.42003	.0094	7 Apr 69
4-3	.42249	.0014	3 Aug 68
3-6	2303.49858	.0113	3 Apr 68
	.49988	.0141	2 Aug 68
	.48054	.0039	7 Apr 69
	.48634	.0024	29 Apr 69
3-7	2453.94866	.0109	3 Apr 68
	.94646	.0024	2 Aug 68
	.95596	.0027	6 Oct 68
	.94450	.0029	29 Mar 69
	.94780	.0022	29 Apr 69

O N D J F M A M J J A S O N D J F M A M J J A



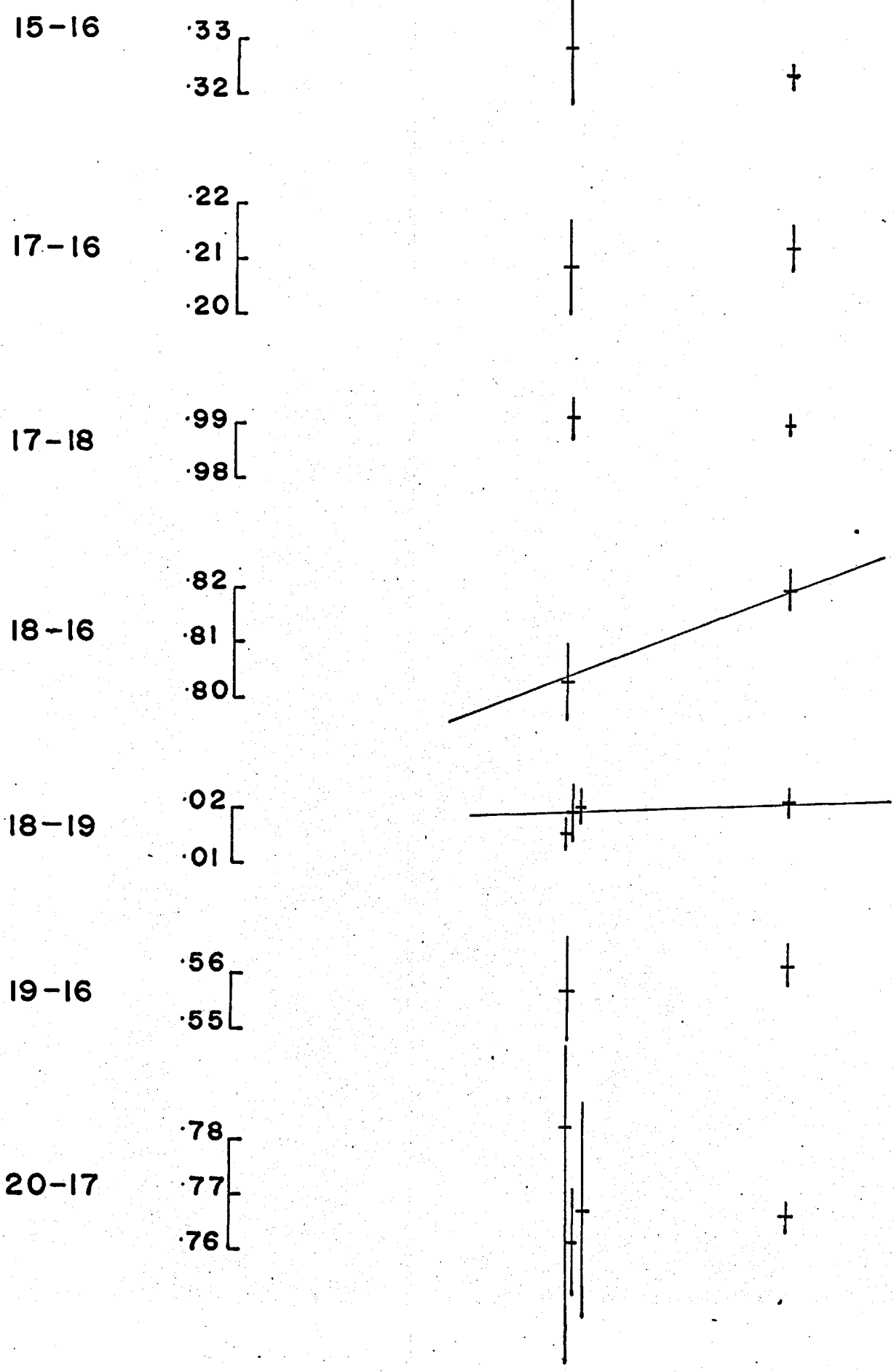
Line	Distance (ft)	Estimated error (ft)	Date measured
3-27	1821.94312	.0265	2 Aug 68
	.95432	.0004	6 Oct 68
	.94677	.0039	29 Mar 69
4-5	1740.46084	.0057	3 Apr 68
	.46294	.0037	7 Oct 68
	.45855	.0020	30 Mar 69
5-4	.45611	.0055	1 Aug 68
	.46411	.0011	29 Apr 69
4-6	1155.50383	.0057	3 Apr 68
	.49513	.0070	3 Aug 68
	.49813	.0026	7 Oct 68
6-4	.49630	.0014	30 Mar 69
	.49490	.0005	29 Apr 69
5-6	989.78957	.0057	4 Apr 68
	.79117	.0015	7 Oct 68
	.79645	.0013	29 Mar 69
6-5	.79755	.0021	29 Apr 69
	.79448	.0109	31 Jul 68
	.79968	.0024	30 Mar 69
5-8	3364.51204	.0087	4 Apr 68
	.51134	.0141	1 Aug 68
	.52594	.0029	7 Oct 68
	.51232	.0040	29 Mar 69
	.52222	.0010	29 Apr 69
5-9	2153.41674	.0029	7 Oct 68
	.40954	.0015	1 Aug 68
	.40497	.0021	4 Apr 69
	.40637	.0025	29 Apr 69
6-8	3809.39160	.0050	4 Apr 68
	.39100	.0057	31 Jul 68
	.40865	.0031	30 Mar 69
	.42375	.0022	29 Apr 69
8-1	4344.60882	.0047	5 Oct 68
	.60551	.0055	30 Mar 69
	.60581	.0036	29 Apr 69
1-8	.58588	.0057	4 Apr 68
8-9	4364.36532	.0022	5 Oct 68
	.36075	.0051	30 Mar 69
10-8	3389.08637	.0043	1 Aug 68
	.10207	.0051	7 Oct 68
	.09808	.0025	31 Mar 69
10-9	3259.86587	.0162	1 Aug 68
	.85598	.0015	31 Mar 69

O N D J F M A M J J A S O N D J F M A M



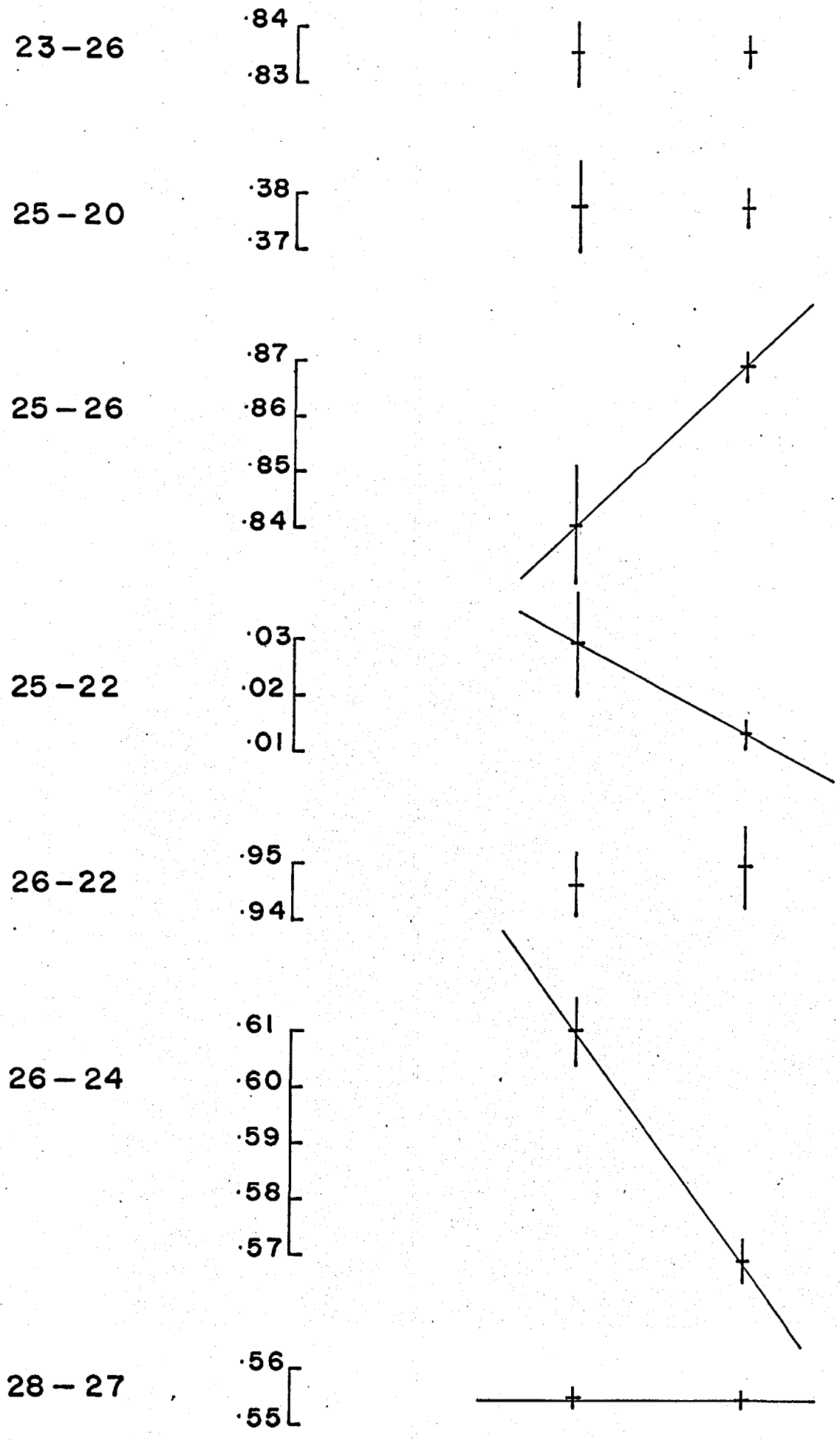
Line	Distance (ft)	Estimated error (ft)	Date measured
10-11	2564.13906 .15951	.0010 .0030	1 Aug 68 31 Mar 69
11-8	4773.78015 .80309 .30220 .31840	gross gross .0020 .0029	1 Aug 68 2 Aug 68 31 Mar 69 5 Apr 69
11-13	3408.16069 .13201	.0423 .0078	4 Aug 68 5 Apr 69
11-14	4532.27596 .26044 .76193	gross gross .0070	2 Aug 68 5 Aug 68 5 Apr 69
12-9	5311.96905 .45841	gross .0043	5 Aug 68 7 Apr 69
12-10	3141.66125 .64242	.0236 .0035	5 Aug 68 5 Apr 69
12-11	2899.64617 .63760	.0021 .0031	5 Oct 68 5 Apr 69
12-13	2356.00680 .00353	.0069 .0020	4 Aug 68 5 Apr 69
12-15	4041.97250 .90296	.0890 .0091	5 Aug 68 7 Apr 69
13-14	2482.85405 .85503	.0077 .0026	4 Aug 68 4 Apr 69
13-15	2983.82423 .82432	.0102 .0047	4 Aug 68 4 Apr 69
13-16	3845.32660 .33589 .29902	.0691 .0294 .0052	5 Aug 68 4 Aug 68 4 Apr 69
14-16	3862.88265 .82362	.0385 .0039	5 Aug 68 7 Apr 69
15-16	2187.32859 .32361	.0098 .0010	5 Aug 68 7 Apr 69
17-15	3674.67492 .65569	.0208 .0019	7 Aug 68 9 Apr 69
17-16	2891.20859 .21212	.0084 .0037	7 Aug 68 12 Apr 69

O N D J F M A M J J A S O N D J F M A M



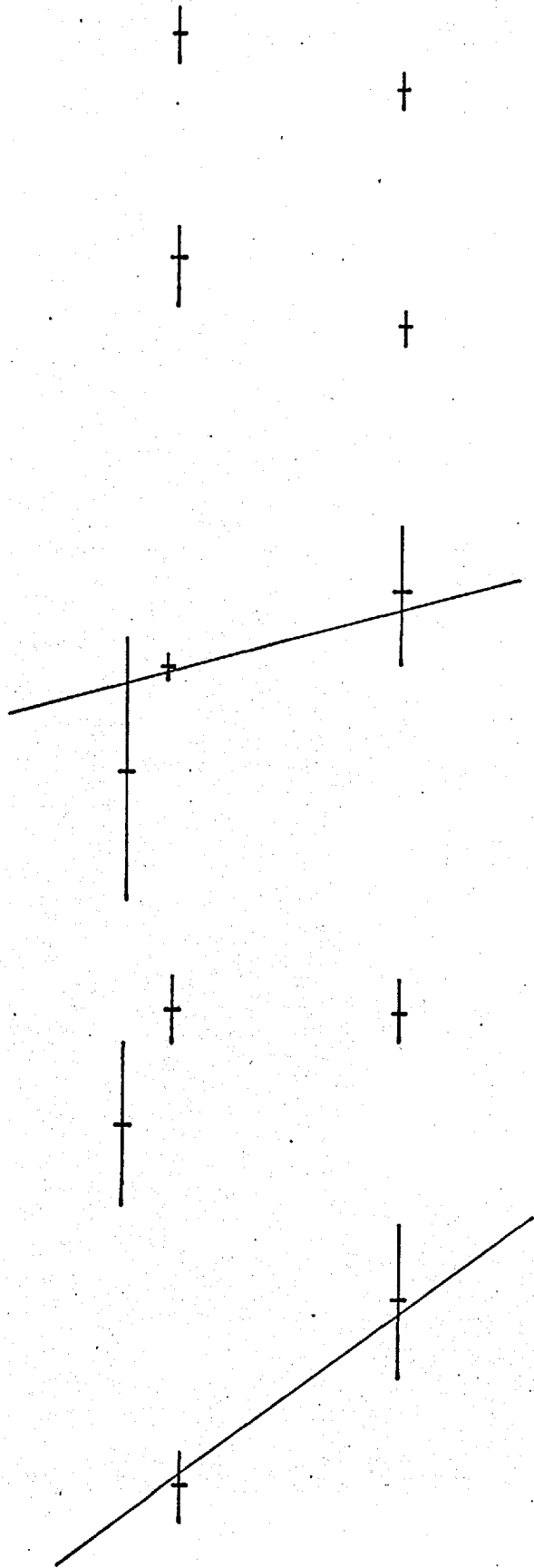
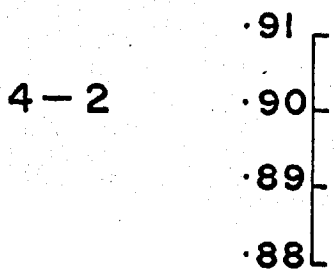
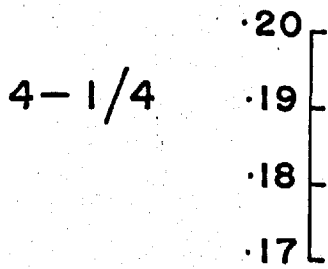
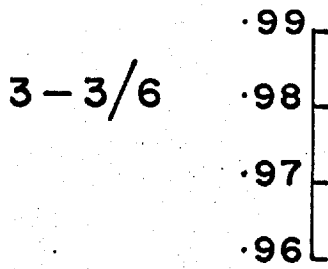
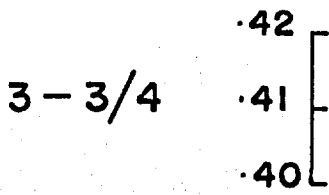
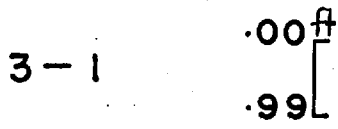
Line	Distance (ft)	Estimated error (ft)	Date measured
17-18	1263.99120	.0031	7 Aug 68
	.98989	.0010	9 Apr 69
18-16	2825.80298	.0068	7 Aug 68
	.81967	.0036	9 Apr 69
18-19	1440.01522	.0021	7 Aug 68
	.02116	.0016	9 Apr 69
19-18	.01955	.0047	9 Aug 68
	.02025	.0026	10 Aug 68
19-16	2989.55713	.0100	10 Aug 68
	.56199	.0030	10 Apr 69
20-17	3225.78242	.0402	10 Aug 68
	.76122	.0100	11 Aug 68
	.76702	.0287	12 Aug 68
	.76665	.0025	10 Apr 69
20-18	2849.99692	.0113	10 Aug 68
	.98322	.0120	10 Aug 68
	.98952	.0107	11 Aug 68
	.98042	.0084	12 Aug 68
	.99077	.0024	10 Apr 69
21-20	2404.30818	.0066	10 Aug 68
	.30612	.0047	10 Apr 68
21-18	2426.55935	.0074	10 Aug 68
	.55587	.0031	10 Apr 69
21-19	1833.80016	.0052	10 Aug 68
	.79565	.0026	10 Apr 69
21-22	1816.86906	.0048	10 Aug 68
	.86586	.0021	10 Apr 69
21-25	2230.61950	.0042	10 Aug 68
	.61484	.0017	10 Apr 69
23-22	2362.21647	.0044	11 Aug 68
	.21437	.0033	11 Aug 68
	.26771	.0052	12 Aug 68
23-24	2337.09197	.0028	11 Aug 68
	.09323	.0050	12 Apr 69
23-26	1795.83569	.0053	11 Aug 68
	.83550	.0026	12 Apr 69
25-20	2028.37775	.0086	11 Aug 68
	.37735	.0030	12 Apr 69

D J F M A M J J A S O N D J F M A M

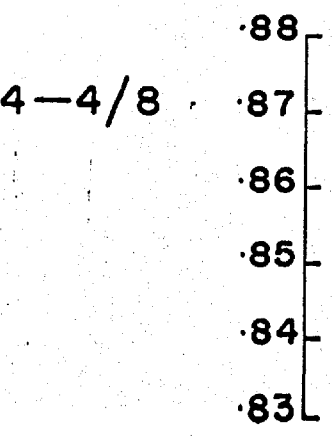
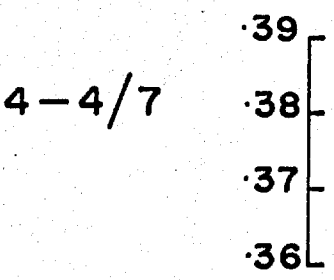
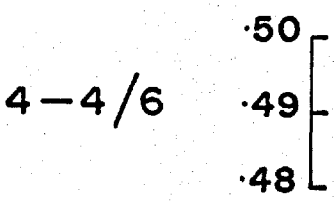
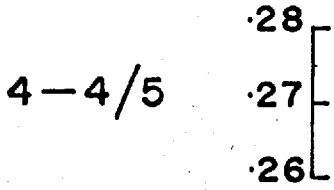
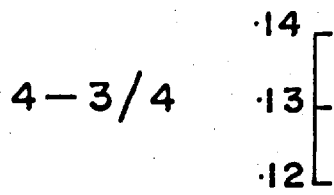


Thingvellir.

O N D J F M A M J J A S O N D J F M A M



D J F M A M J J A S O N D J F M A M



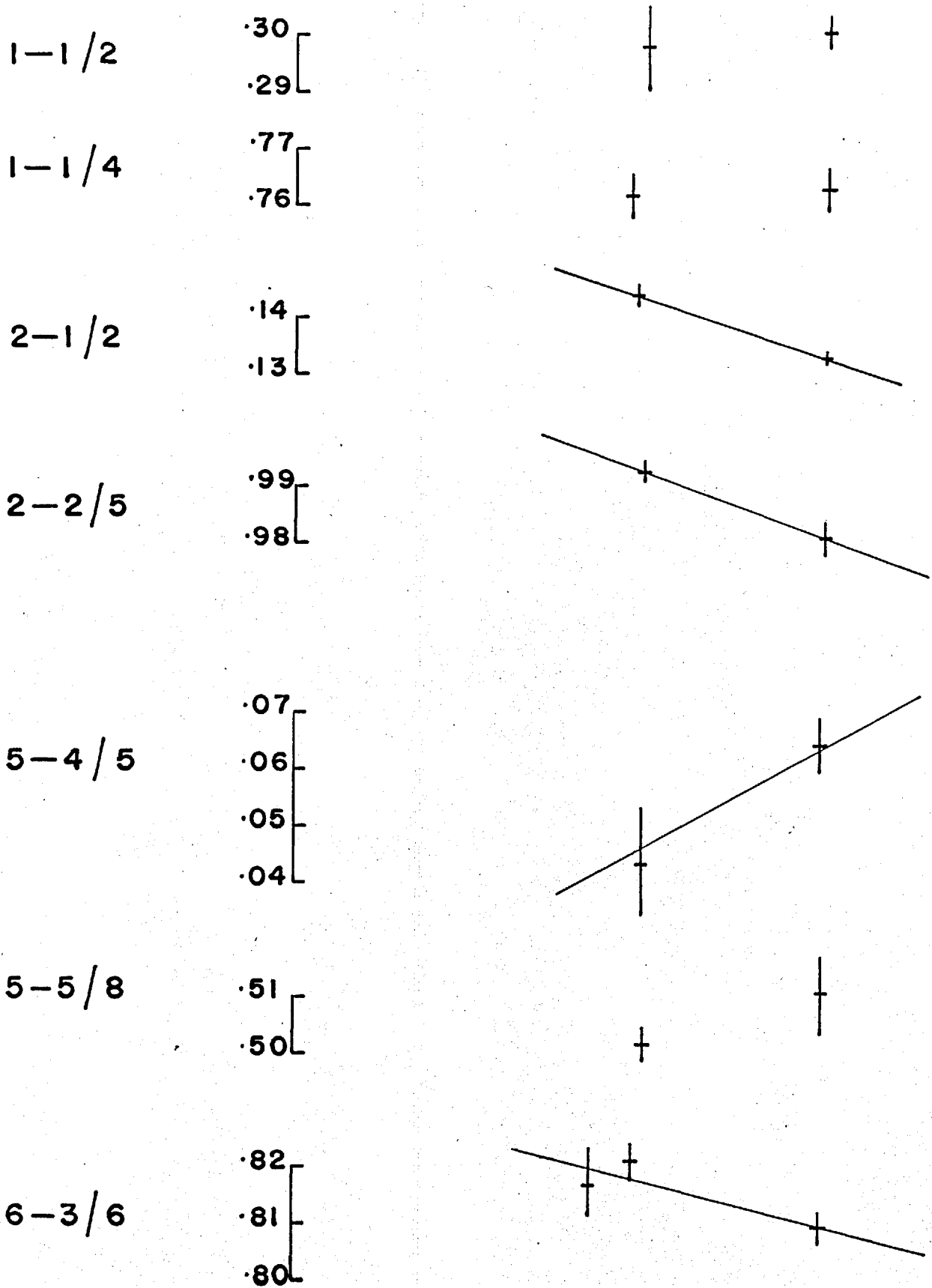
Line	Distance (ft)	Estimated error (ft)	Date measured
25-26	2933.88443	.0386	11 Aug 68
	.84020	.0102	12 Aug 68
	.86900	.0026	12 Apr 69
25-22	2799.02914	.0094	11 Aug 68
	.01312	.0020	12 Apr 69
26-22	2743.94627	.0058	11 Aug 68
	.94979	.0073	12 Apr 69
26-24	3720.61026	.0059	11 Aug 68
	.56891	.0034	12 Apr 69
28-27	1001.55503	.0017	4 Aug 68
	.55472	.0015	7 Apr 69
28-8	4001.77315	gross	
	4475.60017	.0030	7 Apr 69

Note. Errors for the 1967 results were estimated from subsequent readings under similar conditions.

At Thingvellir

Line	Distance (ft)	Estimated error (ft)	Date measured
3-1	5318.0004	.0039	25 Sep 68
	5317.9918	.0025	13 Apr 69
3-3/4	4418.3989		4 Oct 67
	.4176	.0038	25 Sep 68
	.4070	.0024	13 Apr 69
3-3/6	6002.9716	.0193	19 Aug 68
	.9873	.0019	25 Sep 68
	.9981	.0105	13 Apr 69
4-1/4	3402.1804	.0118	21 Aug 68
	.1973	.0041	26 Sep 68
	.1970	.0047	15 Apr 69
4-2	5330.8885	.0058	9 Oct 68
	.9155	.0110	15 Apr 69
4-3/4	3997.1050		4 Oct 67
	.1339	.0105	3 Oct 68
	.1292	.0058	15 Apr 69
4-4/5	5563.2623	.0057	9 Oct 68
	.2806	.0090	15 Apr 69

D J F M A M J J A S O N D J F M A M

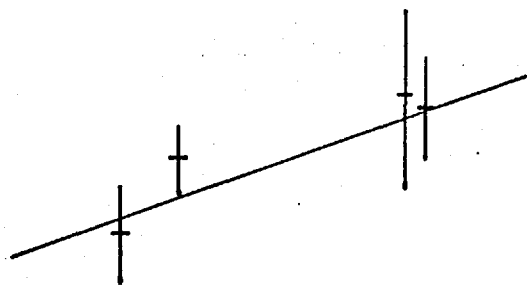


Line	Distance (ft)	Estimated error (ft)	Date measured
4-4/6	7353.4908	.0169	3 Oct 68
	.4876	.0045	16 Apr 69
4-4/7	4332.3651	.0070	23 Aug 68
	.3834	.0098	3 Oct 68
	.3827	.0043	15 Apr 69
4-4/8	5498.8348	.0026	9 Oct 68
	.8754	.0057	15 Apr 69
1-1/2	7379.2979	.0073	10 Oct 68
	.3003	.0026	23 Apr 69
1-1/4	4306.7615	.0035	26 Sep 68
	.7623	.0034	23 Apr 69
2-1/2	3001.1438	.0015	10 Oct 68
	.1326	.0005	20 Apr 69
2-2/5	3175.9925	.0016	10 Oct 68
	.9805	.0022	20 Apr 69
5-2/5	6147.8584	.0436	9 Oct 68
	.8452	.0021	20 Apr 69
5-4/5	5995.0431	.0102	9 Oct 68
	.0638	.0047	20 Apr 69
5-5/8	3593.5015	.0024	9 Oct 68
	.5104	.0059	20 Apr 69
5-5/9	3072.8371	.0007	24 Apr 69
6-3/6	2473.8114		7 Oct 67
	.8165	.0055	19 Aug 68
	.8207	.0029	28 Sep 68
	.8089	.0026	13 Apr 69
6-4/6	2004.5243		7 Oct 67
	.5192	.0054	19 Aug 68
	.5302	.0020	28 Sep 68
	.5233	.0019	13 Apr 69
6-7	6247.2171		7 Oct 67
	.2431	.0050	28 Sep 68
	.2450	.0083	14 Apr 69
6-6/11	5306.8571	.0075	28 Sep 68
	.8501	.0182	14 Apr 69
	.8345	.0021	27 Apr 69

D J F M A M J J A S O N D J F M A M

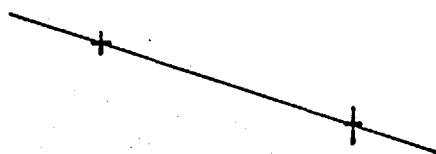
7-7/12

.40
[
.39
[
.38



8-4/8

.40
[
.39
[
.38



8-5/8

.40
[
.39



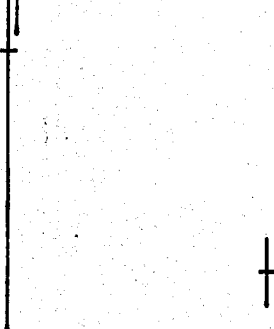
8-8/12

.98
[
.97



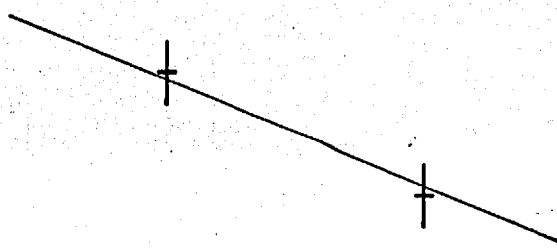
11-6/11

.40
[
.39
[
.38
[
.37

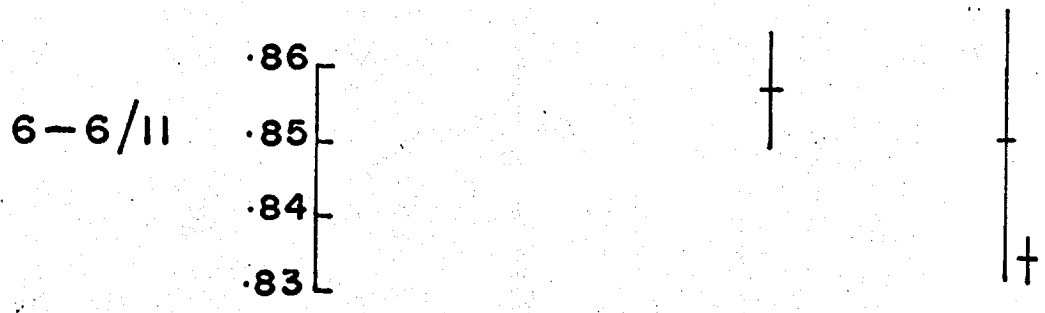


11-7/11

.03
[
.02
[
.01
[
.00

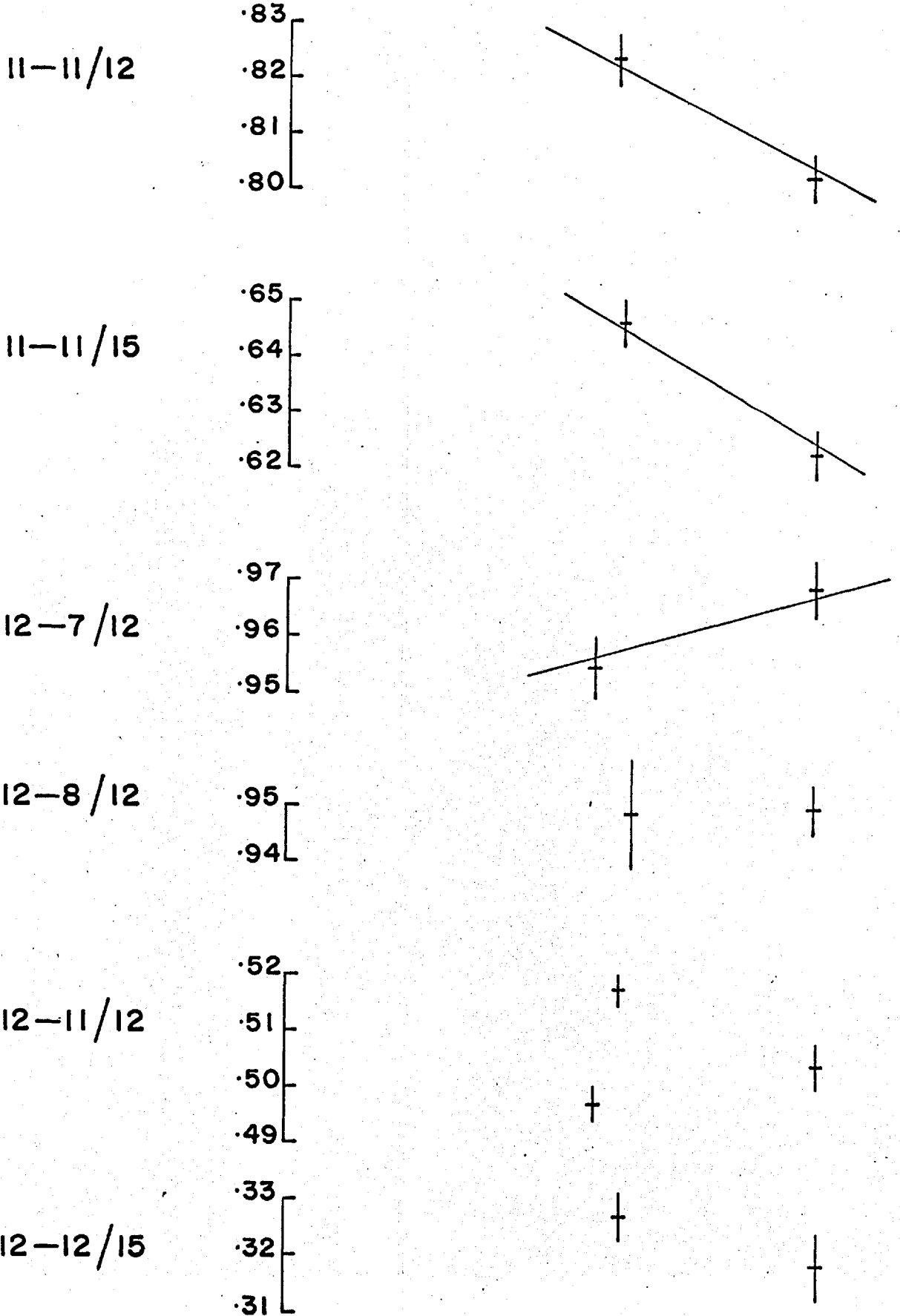


D J F M A M J J A S O N D J F M A M



Line	Distance (ft)	Estimated error (ft)	Date measured
7-4/7	2370.3039		7 Oct 67
	.3074	.0055	23 Aug 68
	.3080	.0029	29 Sep 68
	.3094	.0022	16 Apr 69
7-8	5690.9002	.0047	8 Oct 68
	.8724	.0057	25 Apr 69
7-7/11	7103.4621		6 Oct 67
	.4572	.0095	23 Aug 68
	.4635	.0155	3 Oct 68
	.4752	.0231	16 Apr 69
	.4336	.0038	27 Apr 69
7-7/12	6783.3807	.0063	23 Aug 68
	.3904	.0121	3 Oct 68
	.3994	.0121	16 Apr 69
	.3974	.0067	25 Apr 69
8-4/8	3024.3944	.0010	8 Oct 68
	.3836	.0022	25 Apr 69
8-5/8	3743.3942	.0057	8 Oct 68
	.3954	.0036	25 Apr 69
8-8/9	2530.1835	.0037	25 Apr 69
8-8/12	5408.9794	.0038	8 Oct 68
	.9791	.0036	25 Apr 69
9-5/9	4275.9982	.0004	24 Apr 69
9-8/9	4352.8699	.0043	24 Apr 69
9-9/12	4091.3242	.0021	24 Apr 69
9-9/13	2681.1455	.0032	24 Apr 69
10-10/11	3450.3454	.0017	28 Apr 69
10-10/14	4324.0386	.0022	28 Apr 69
11-6/11	6626.3972	.0347	27 Sep 68
	.4080	.0074	27 Sep 68
	.3680	.0044	20 Apr 69
11-7/11	3552.0412		8 Oct 67
	.0226	.0039	27 Sep 68
	.0066	.0037	20 Apr 69
11-11/12	4138.8234	.0037	27 Sep 68
	.8016	.0036	20 Apr 69

D J F M A M J J A S O N D J F M A M



D J F M A M J J A S O N D J F M A M

15-11/15

94
93

+

+

15-12/15

12
11
10

+

+

Line	Distance (ft)	Estimated error (ft)	Date measured
11-10/11	4586.1486	.0026	28 Apr 69
11-11/15	4976.6459	.0035	27 Sep 68
	.6221	.0042	20 Apr 69
12-7/12	5672.9547	.0052	23 Aug 68
	.9680	.0048	23 Apr 69
12-8/12	6496.9482	.0096	9 Oct 68
	.9492	.0044	23 Apr 69
12-9/12	7435.9151	.0065	23 Apr 69
12-11/12	2933.4966	.0024	23 Aug 68
	.5170	.0026	27 Sep 68
	.5032	.0038	23 Apr 69
12-12/13	3276.4236	.0011	23 Apr 69
12-12/15	4017.3263	.0039	27 Sep 68
	.3178	.0055	23 Apr 69
13-9/13	4182.1099	.0026	24 Apr 69
13-12/13	5291.6175	.0027	24 Apr 69
14-10/14	3005.3611	.0021	27 Apr 69
14-14/16	3406.2421	.0028	27 Apr 69
15-11/15	4530.9301	.0024	26 Sep 68
	.4316	.0035	27 Apr 69
15-12/15	4301.1082	.0091	26 Sep 68
	.1067	.0022	27 Apr 69
15-15/16	2229.1313	.0028	27 Apr 69
16-14/16	6631.5430	.0080	27 Apr 69
	.5384	.0042	27 Apr 69
16-15/16	3811.3852	.0048	27 Apr 69

Note. No estimate of the errors of the 1967 measurements can yet be made.

5.3 Estimation of the Various Errors.

5.3.1 Errors due to cavity and phase settings.

There will be a frequency error if the standard cavity has not reached equilibrium. The field setting up procedure is designed to give the Mekometer as long as possible to reach equilibrium. Nevertheless on some lines there still appears to be a one-way change of distance with time. If this is noticeable from the results the offending readings are ignored.

Experiments have been conducted to investigate the behaviour of the standard cavity while attaining equilibrium. It has been found that the cavity reaches equilibrium by over correcting by up to 20 per cent in the first seven minutes and then more slowly relaxing back to equilibrium in another 13 minutes.

The initial quick frequency change is due to the aluminium outer case of the standard cavity quickly reaching air temperature. This changes the capacity at the ends of the quartz cavity and produces over compensation. As the quartz eventually reaches equilibrium temperature the frequency becomes correct.

If the Mekometer has been kept at an even temperature for a few weeks it is found that the frequency changes take place in sharp jumps. These are caused by the quartz outer line not moving smoothly over the aluminium case. This movement is facilitated by PTFE spacers. These jumps become much less marked if the standard cavity is first cycled through the required temperature range as occurs on field expeditions.

After the cavity has attained equilibrium and the cavity temperature is slowly fluctuating with air temperature the frequency errors will be random and should only introduce a small error to the mean.

A systematic error will result if the frequency cavity temperature calibration is in error. This calibration on each expedition, except the first, has been derived from upwards of 60 frequency measurements spread over a range of 20°C . It is estimated that the calibration curve is known to within 0.13 parts per million for temperatures ranging from -2°C to $+22^{\circ}\text{C}$. The error produced will be negligible in our work.

In frequency measurements the cavity null can only be set to about 0.2 parts per million. On a distance measurement on a calm day it can probably be set slightly better. This is because in frequency measurements a rather unstable oscilloscope pattern has to be held stationary at the same time. On a distance measurement more attention can be given to the cavity setting. If the modulating cavity temperature is fluctuating however the cavity setting may become less precise. The error from this setting will be random.

The phase setting also involves a random error. It is interesting to note however that the first reading is sometimes poor even when the standard cavity has reached equilibrium, as would be the case of measuring a second line from one Mekometer station. This seems to be more noticeable when the line being measured is a poor one. The first readings seem to act as a "sighter". The phase which is randomly varying with time is initially approached from outside the range of deviations. The first reading is taken when the phase

needle is steady on zero. The phase then changes, usually towards its true mean and is followed. These following phase settings should then be inside the actual phase distribution and produce more consistent results.

When the first reading of a set was outside the range defined by the following readings it was ignored. It seems likely that most measurements of this kind will produce first readings which are worse than average. It is believed that this is why the 48 Hour Watch produced such a high scatter in readings. It was the equivalent of a series of first readings.

5.3.2 Errors due to errors in pressure measurement.

The Mekometer physically compensates for pressure changes in the air so that the readings are very insensitive to pressure changes. The pressure need not therefore be known precisely. The knowledge of the difference in pressure between the ends of the line however is important. This is determined from theodolite readings and the correction is good to 0.01 mb for average conditions. This is equivalent to a 0.003 parts per million change in distance correction. The correction will change daily with the air density appropriate to the particular conditions. This change at the most will be two per cent and is ignored.

The same pressure correction is used each time the line is measured so that the changes in line length will not be affected by a slight error in the altitude correction.

5.3.3 Errors due to errors in humidity measurement.

The humidity measurement is generally good to better than 1 mm of Hg, for normal temperatures and rather better at temperatures below about 4°C. This means that the correction is good to 0.05 parts per million and produces a negligible error. The humidity varied only slowly throughout the day and seemed uniform in the area at Reykjanes, but less so at Thingvellir, especially near the lake. The effect of humidity on the refractive index of light is very small so that even at Thingvellir the error would be no more than 0.2 parts per million at the very most.

5.3.4 Geometrical errors.

The angles of elevation of the lines are good to 0.5 minute of arc as determined from the reverse measurement of several lines. This could produce an error of 0.017 mm (0.00006 ft), which is negligible. The same angles are used for all the measurements so that there will be no error produced in estimates of the changes of line lengths.

The tiltmeter readings when repeated on a post had an error with a standard deviation of 0.0008. This is equivalent to an angular error of 30 seconds of arc. This uncertainty is equivalent to a distance error of 0.024 mm at the Mekometer end and 0.007 mm at the reflector end.

If the pillar tilted it would be detected or produce an error of less than 0.15 mm (0.0005 ft).

There is another possible error in the reflector correction. It is assumed that the reflector man can aim the reflector horizontally to within about one degree. This would

produce an error of up to 0.008 mm. If the reflector was five degrees off target the error introduced would be 0.12 mm.

Another end error is that due to the uncertainty of location of the Mekometer on the pillar. The Mekometer mounting bracket has got a three inch spigot on it. Even though the holes in the plates have been machined to within 0.3 thousandths of an inch, it is possible to wobble the spigot in the hole. At the Mekometer end this can produce an error of 0.03 mm which is negligible.

In the same category is the location of the trunion axis on the Mekometer itself. The trunions are on plates which are held by screws on the sides of the Mekometer. One of these plates did not locate uniquely and could be tightened in slightly different positions. This plate was screwed onto the Mekometer in a standard fashion and the resulting error was estimated to be less than 0.1 mm.

5.3.5 Errors due to uncertainty in air temperature.

So far the errors considered have been random, or if systematic not greater than about 0.1 mm. If the error due to temperature fluctuations was random the mean standard deviation and confidence limits could be computed and the results would be self consistent.

Assuming that the computed distances y_i in a given set of n readings are normally distributed about some mean, the best estimate of the mean \bar{y} is given by

$$\hat{\bar{y}} = \frac{1}{n} \sum^i y_i$$

The circumflex accent is used to denote the estimate of a quantity. From a sample such as considered here the true mean may never be known, it can only be estimated. The best estimator of the standard deviation σ is

$$\hat{\sigma} = \sqrt{\frac{\sum (y_i - \bar{y})^2}{n-1}}$$

Clearly the more readings taken, and the smaller the standard deviation, the better will be the estimate of the true mean. For a normal distribution as considered here confidence limits for the estimates may be evaluated.

The $100(1-\alpha)\%$ confidence level is given by

$$\bar{y} \pm (t_{\alpha/2}; n-1) \frac{\hat{\sigma}}{\sqrt{n}}$$

$t_{\alpha/2}; n-1$ is tabulated in any book on statistics under Student's Tables. $n-1$ are the "degrees of freedom" for the estimate. The degrees of freedom are $n-1$ and not n because one parameter has already been estimated from the readings.

90 per cent confidence limits were evaluated for the readings and they did not make sense. With 90 per cent confidence limits it would be expected that a smooth curve through the distances plotted against time should go through about 90 per cent of the evaluated limits, but it did not. This means that either the distances are fluctuating randomly and rather quickly over periods as short as one day, or there is an error which has not been accounted for.

This error is believed to be due to systematic temperature changes along the line which are giving rise to mean temperatures different from those being calculated. To understand the effect various atmospheric structures must be considered.

5.3.5.1 The equilibrium states of the atmosphere.

Meteorologists describe several different states of vertical stability in the atmosphere. They are derived by considering an elemental parcel of air and seeing how it will behave when displaced by some event.

The most unstable state is Autoconvective Instability. This is said to occur when the atmospheric density increases with height. This happens when the temperature decreases with height by more than 3.4°C per 100 m, and will only occur near strongly heated ground. The refractive index of air varies with density so that autoconvective instability will produce ray bending concave upwards. When this occurs mirages are seen. Very strong shimmer will be seen as the less dense air rises and mixes with the denser air causing turbulence. This state only occurs in Iceland on warm sunny days over the black rocks and sand. Mirages are fairly rare and only occur at glancing incidence near the ground.

The next most unstable state is Unstable Equilibrium. In this state air density decreases with height but if a parcel of air is displaced upwards it does work and cools but not sufficiently to lower its density to that of the surrounding air. This means that if some of the air is disturbed by an eddy say, the displaced air will continue travelling upwards disturbing more air. This state occurs for vertical temperature gradients, lapse rates, of 1°C - 3.4°C per 100 m. These conditions will also produce shimmer caused by the turbulent mixing of inhomogeneous air. This state is common in Iceland, occurring over the bare ground whenever the sun is shining directly on it.

Neutral Equilibrium is said to occur when the work done by rising air cools it just enough to keep it neutrally boyant. This is an adiabatic condition which means there is no vertical heat flux. This condition will occur around dusk and dawn. The vertical temperature gradient depends slightly upon humidity, as there is latent heat to take into account, but is nearly 1°C per 100 m.

Stable Equilibrium occurs when the lapse rate is less than 1°C per 100 m. This will happen whenever the ground is cooler than the air above and includes all temperature inversions. This condition is also quite common in Iceland. The bare ground radiates and loses its heat very rapidly and stable equilibrium occurs at around sunset to last until after dawn. Stable equilibrium also occurs over snow and water. Where the water or snow are intermittent however the stable equilibrium may not last for any great height above the snow or water. On sunny days both snow and water produce temperature inversions, that is negative lapse rates, due to cooling by evaporation.

On a sunny day then there will be considerable variation of the vertical temperature gradients. Over bare rock a lapse rate of up to 3°C per 100 m can be expected, over vegetation there would be less, and over water a temperature inversion. In a varied terrain there will also be horizontal temperature gradients which may be considerable near the ground. The extent of these variations will depend upon the time of day or how long the sun has been shining, and also upon the wind strength.

The temperature variations at a single point can also be considerable. Lander and Robinson (1965) measured the temperature over a lawn in Surrey on a June afternoon and in 30 minutes at a height of 0.25 m they observed temperatures varying over 6°C.

5.3.5.2 Ray bending.

With so much temperature variation it might seem that errors could also be introduced by ray bending. With a uniform refractive index gradient it can be shown simply that the light travels in a circular path with a radius of $1/(\text{the refractive index gradient})$. Except under mirage conditions the ray path will be concave downwards. The ray bending will be greatest when the air is most stable. This is why the best conditions for theodolite measurements are the worst for distance measurement and vice versa.

In an atmosphere with no vertical temperature gradient the radius of curvature of a ray path is about 29,000 km. The radius of the earth is about 6,400 km, considerably less. This is one of the reasons you cannot see the back of your head on a clear day. If the refractive index gradient was about five times greater the sun would not set and the earth would look concave.

The arc to chord distance error caused by a radius of curvature of 29,000 km is 8×10^{-5} mm on a line 1 km long, but 0.08 mm on a line 10 km long. Clearly these curvatures will not affect any of the distances, although they would upset theodolite measurements.

One way of estimating the vertical temperature gradients along a line is to measure the vertical angle preferably at both ends. On a line 1 km long the difference in vertical angle as measured at the two ends will be a measure of the vertical refractive index gradient. The difference in angles will vary by 10^{-8} radians for each degree in 100 m temperature gradient. To get the temperature gradient to the nearest degree in 100 m we have to measure the vertical angles to the nearest two seconds of arc. Over the short distances that are being considered our theodolite would not be sensitive enough to produce useful results. On a line 10 km long however the method could produce useful information.

Differences were noted between reverse angles but these were almost entirely due to the earth's curvature.

When the air is very inhomogeneous or on long lines there is a problem with ray bending. The returned light beam is deflected from on its path to the Mekometer. This means that the returned signal is randomly amplitude modulated producing a high scatter in the readings. The problem is common to both the Mekometer and Geodimeter and may be reduced by using a larger reflector.

If the conditions become worse or the line lengthened the returned light may miss the Mekometer altogether. Under these circumstances the returned light appears to go on and off. The working beam diameter is that subtended by the reflector at the Mekometer. The 1 milliradian beam spread is the aiming tolerance. If the air was still, any light reaching the target reflector would be returned. This means that in

10 microseconds the refractive index gradient must change by an amount sufficient to make the working beam miss. A simple calculation will show the order of disturbance involved.

The reflector diameter is 6 cm. Considering a line 2 km long the beam must be deviated by an angle of 3×10^{-5} radians in a path of 2×10^5 cm. This is a radius of curvature of $2/3 \times 10^{10}$ cm or the equivalent of a temperature gradient of 1°C in $2/3 \times 10^4$ cm or about $0.1^\circ\text{C}/\text{km}$. This might seem low but is equivalent to a rate of change of temperature gradient of 20 degrees per cm per second. This confirms the conclusion from work on temperature probes that the smaller the air samples in time and space the more inhomogeneous the air appears to be.

5.3.5.3 Causes of the random scatter in the observed readings.

Random errors arise both from the normal instrument and operator limitations, and atmospheric variations. Some of the causes have been mentioned earlier.

The scatter will always be bounded by the ability to set the phase and frequency. On short lines the phase is more important and on long lines the frequency is more important.

The atmospheric causes of random error vary in importance with the distance being measured. Light going from the Mekometer to the reflector and back again undergoes a random walk in velocity space. This will produce a scatter proportional to \sqrt{D} , where D is the distance being measured. This effect is only important on short lines where the signal to noise ratio is very high.

As the light path increases the signal to noise ratio is decreased. The noise immunity to constant background light

is very high. On a day with shimmer however the background light is not constant but varying rapidly. The ratio of this noise signal strength will vary as D^4 because the signal strength is varying according to an inverse square law, and the noise increasing with D^2 .

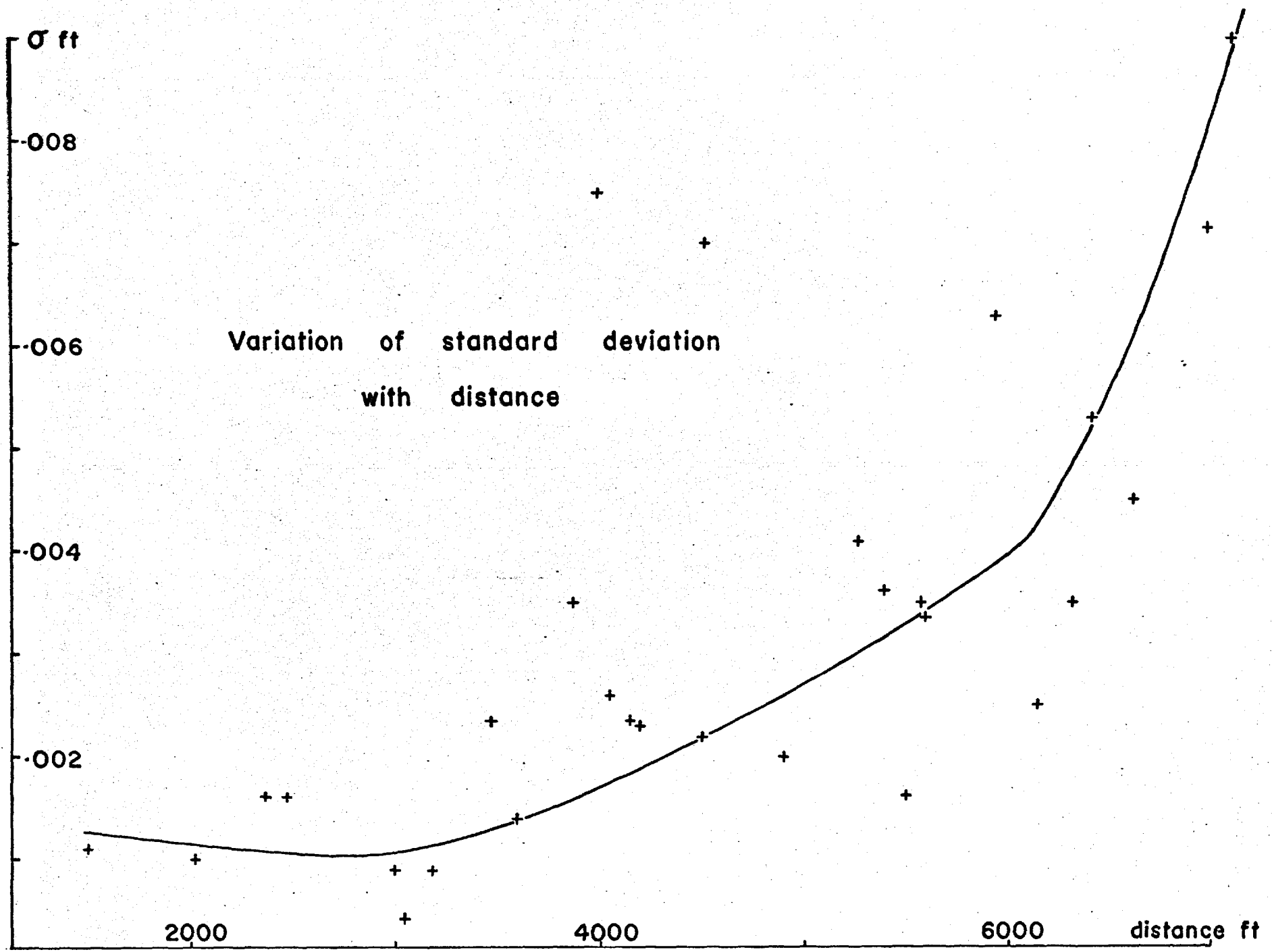
As the light path is further increased the signal itself starts to be amplitude modulated. At first the outgoing and returned beams are randomly focused and defocused and bent slightly. Looking through the Mekometer one sees the returned light come in and out of focus and move about slightly; the light twinkles. At this stage the scatter will vary with a higher power of distance, probably D^6 . The Mekometer still works quite well under these conditions although it will be found best to use the higher time constant for the phase meter.

If the distance is further increased there comes a stage when the returned light appears to go on and off. This is caused by the returned beam missing the Mekometer and sets a working limit on the length of line that can be measured, or the poorness of measuring conditions along the line.

These fluctuations can be reduced by averaging as is done by the Mekometer, the operator and the measurement procedure. An empirical expression for the scatter would be of the form

$$\text{Scatter} = a(\delta T)D^{\frac{1}{2}} + b(\delta T)^2D^4 + c(\delta T)^4D^6 + d \exp(fD)$$

where δT is some measure of the temperature variations. There is no point in trying to fit coefficients to this expression because they will vary from day to day, from line to line, and from operator to operator. To get some idea of how the scatter



is varying, the results from Thingvellir taken during the Autumn of the third field season are plotted, the standard deviation versus distance. This period was notable for generally fine and sunny weather extending over 10 days.

The graph shows that with a few exceptions the results behave as predicted. The scatter possibly decreases until about 3,000 feet. This, it will be remembered, is the most sensitive range of the Mekometer. After 3,000 feet, the scatter increases gently until about 6,000 feet, when the scatter rises steeply. This critical distance is where the returned light starts to flicker.

If the weather had been warmer the critical distance would have been lowered. In mid-summer this critical distance can be as low as 3,000 feet.

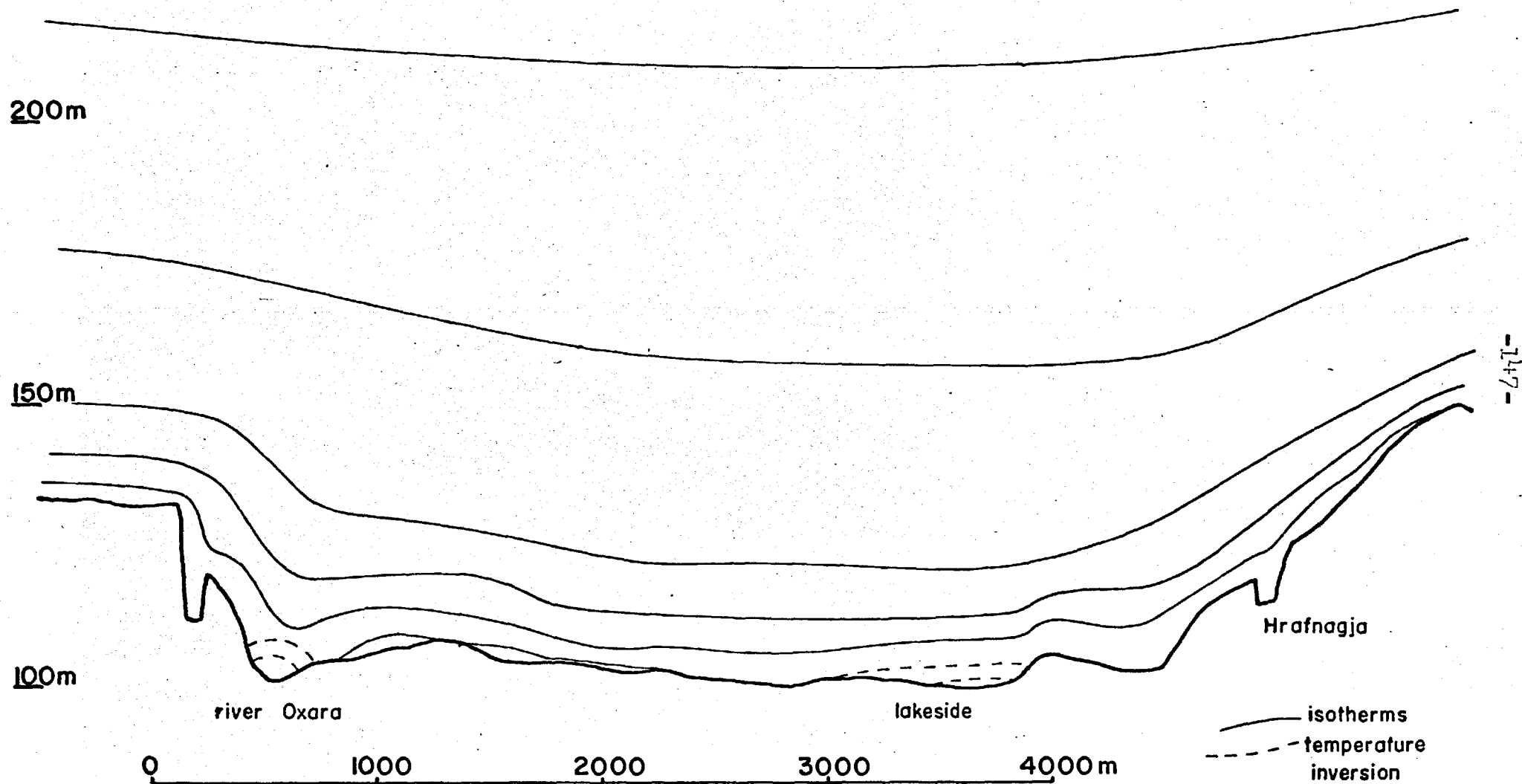
5.3.5.4 Systematic temperature errors.

When the scatter of readings is high the systematic error due to a wrong average temperature is also likely to be high.

The only proper way to resolve this uncertainty is to fly temperature probes along the line. If the line is some way above the ground one probe will give a reasonable estimate of the temperature structure.

Short of this we must approximate the atmospheric structure by some model. Each line has a fixed situation, profile and ignoring snow and seasonal vegetational changes, a fairly constant terrain beneath it. This should give rise to a characteristic pattern of isothermal surfaces. These surfaces would approximate to the ground topography but dip

HYPOTHETICAL ISOTHERMS ACROSS THE GRABEN AT THINGVELLIR



over water and thick vegetation and rise over bare ground. The form of these surfaces may vary with wind direction but not appreciably with wind speed. When the sun is shining the isothermal surfaces should become more closely spaced but not appreciably alter their form.

If this model is valid it would suggest corrections to the distances of the form

$$\delta D = -k \delta T$$

where δD is the correction,

δT is some measure of the temperature changes along the line,

k is a structure constant of the line itself.

The way to test and use this model would be to thoroughly investigate the temperature structure on the line so that an accurate estimate of δD can be found. Some estimate of δT must be chosen, the vertical temperature gradient would be best, if the line is sloping the difference in temperature between the end points may be used. Another measure of δT would be the scatter in the distance readings themselves. From a knowledge of δD and δT , a k can be determined and used to correct other measurements.

Rather than risk introducing bias to the corrections the following reasoning was used to allow for the systematic error based upon the above outlined temperature structure. An investigation was made to see whether the scatter in the readings themselves would be a suitable measure of the temperature variation.

During the fourth field season balloons were used to hoist temperatures probes on several of the lines at Reykjanes.

On some lines the probes gave readings varying up to 1.5°C from the temperatures measured at the ends. Using this information the difference in the line length as computed with, and without, the probe information was found. This difference was then compared with the standard deviations of the readings themselves. On the lines investigated surprisingly close agreement was found between the computed differences and the standard deviations.

Temp. diff. °C	Line length (ft)	Change in computed length (ft)	Standard devn. (ft)
0.8	4464	.0035	.0034
0.75	4344	.0033	.0036
0.4	3809	.0015	.0020
0.3	1155	.0004	.0010
0.5	1740	.0009	.0012
0.4	3259	.0013	.0009
0.4	2564	.0010	.0018
0.4	3389	.0012	.0015
0.25	4773	.0012	.0011

These results suggest that if the distance evaluated using the probe reading is taken as correct, and the standard deviation of the readings as δT , then the structure constant has a value of about unity. The reason for the structure appearing roughly the same for each line is the similar terrain for each.

The considered lines were shot at Reykjanes which is fairly flat and barren. It is also interesting to note that these readings were taken over two days, the first hot, sunny and fairly still, the second cloudy with rain showers and a light wind.

On the basis of this investigation it was decided to add the systematic error $\delta D = 1 \times \delta T$ to the random error. In other words the error on a particular line was estimated to be the 90 per cent confidence limit on the mean of the readings plus the standard deviation of the readings themselves. It was hoped that this would cover the error due to taking the wrong mean temperature. There is in fact a statistical method of testing how well this method is working on some lines. It will be demonstrated in section 5.4.

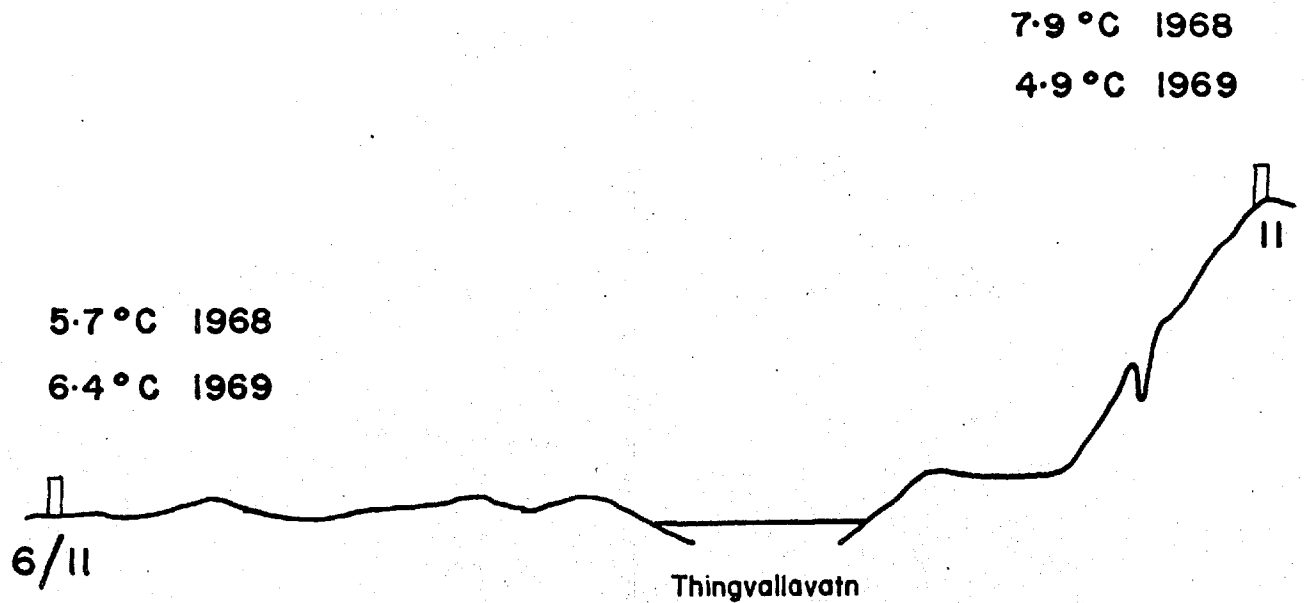
On the expedition during the summer of 1968 probes, flown on kites, were used to a considerable extent. When the wind was strong enough to support a probe on a kite the air was fairly uniform. This gave small temperature differences and fairly small standard deviations so that the readings were not as useful for error investigations. The general behaviour was the same as in the table shown for 1969, but the values of the temperature error and standard deviation are generally lower, and the agreement with the computed change in length not so striking.

For the Thingvellir results the error was estimated in the same manner but with less justification. At Thingvellir the lines were neither over uniform terrain nor flat ground. Most of the lines have only been measured twice so that there is no independent estimate of the errors. The lines at Thingvellir are also much longer than those at Reykjanes which gives room for much greater systematic temperature errors.

Qualitative remarks can be made concerning various measurements but quantitative corrections cannot be determined without further experiment. It is most unfortunate that probe

CHANGING TEMPERATURE

CONDITIONS AT THINGVELLIR



A profile from 6/11 to 11 at Thingvellir showing the differing air temperatures during the two measurements. In 1968 there was a marked temperature inversion.

investigations could not be carried out at Thingvellir. On the last expedition our hydrogen supply was stolen before work was started at Thingvellir.

The first measurements of Thingvellir were during the late summer of 1968, and the second in the spring of 1969. The air was generally warmer during the first measurements. To illustrate some of the difficulties the mean temperatures recorded at the ends of line 11-6/11 are shown for the two measurements. Point 11 is about 100 m above 6/11 and the line is partly over water. The line was first measured at about one hour before sunset. There was a strong temperature inversion over the lake influencing the temperature at point 6/11 which was 2.2°C below that of point 11. The line was next measured during the afternoon and this time the temperature at point 11 was 1.5°C below that at 6/11, a reversal of the previous trend. From these readings it is quite difficult to hazard a guess as to the average temperature along the line. In the first case the average temperature could be as low as 3°C or as high as 7.0°C . In the second case, which is rather more normal, the average temperature should be somewhere between 4.5°C and 6°C . If the temperatures half-way along the line had been known these limits could have been considerably reduced.

The measurements when corrected using the mean of the terminal temperatures suggested that the line had decreased by five parts per million. If the lower temperature limit is used for the first measurement and the upper for the second an increase could be inferred. This is an example of a rather

poor line. It is interesting to note that nearly all lines which were shot over water, including a river, have shown an apparent contraction between their two measurements.

Corrections for the systematic errors in the Thingvellir readings have not been attempted because they would have to be subjective and without check. It is suggested that future measurements at Thingvellir require intermediate temperature stations.

5.3.6 Errors due to equipment faults and operator mistakes.

The errors discussed in this section are particular to a few readings and unlikely to recur.

At the time of the first measurements the standard cavity was still under development and the temperature coefficient had not been finally adjusted. This meant that there existed no unique relationship between cavity temperature and frequency. For this reason the frequency was measured for each line measurement. Despite the difficulty of doing this in the field it is estimated that the frequencies were accurate to 0.7 parts per million and 0.2 parts per million respectively for the first two measurements at Reykjanes. These measurements were of five lines, 6 and 10 days after the 1967 earthquakes.

During the next two expeditions difficulty was experienced in receiving the Droitwich frequency standard, but no error was introduced as the counter frequency was known and stable.

During the early part of the third field season the Mekometer optics slowly became misaligned. This coincided with warm weather and measurement of the desert and interior regions

of the Reykjanes network. This resulted in flicker of the returned light occurring at much shorter distances. The instrument finally became unworkable and a successful attempt was made at realignment in the field.

Later in the same field season very fine atmospheric dust, which is common in Iceland during summer, entered the modulating cavity and caused intermittent arcing. Both of these faults produce random errors.

While working at Thingvellir on the first half of the second field season some of the readings were exactly 0.5 feet in error. This has not been completely explained, but the following are possible causes.

1. The Mekometer was being erroneously operated on high wobble instead of low wobble.
2. The phase was being set on a maximum.
3. There was some switching fault reversing the phase response. A faulty earth on the 100 Hz square wave to one of the wobble systems might produce such a fault.

The lines were all measured and no harm resulted.

The most serious fault occurred during the fourth series of measurements. This was due to UHF pick-up in the phase detection system. An earthing screw for the amplifier and detector board came loose. So great was the pick-up that the system became completely saturated. When this had been fixed slight UHF pick-up was still noticed occasionally.

UHF pick-up can cause a change in the phase meter reading if one of the two modulation frequencies is picked up

more strongly than the other. This would produce a systematic error, so to counteract this field checks were made from time to time by tuning the Mekometer when misaimed, unsymmetrical UHF pick-up would be seen as a meter deflection. As the error produced is essentially that caused by working on a wrong zero the possible magnitude was investigated. The effect of a two division deviation of the phase meter was found for various line lengths.

Mode	Distance (ft)	2 div deflection (ft)
Hi wobble	620	.0026
	1000	.0080
	1380	.0125
Lo wobble	620	.0032
	2050	.0032
	2650	.0031
	4000	.0050
	5000	.0090

It is felt that any deviation of the zero by more than two divisions would have been seen in the field. This happened on two occasions. Once before the earthing screw became completely loose and the second time was on the last day. The pick-up mainly occurred on the units mode and always produced an error of the same sign producing a systematic increase in line length. No evidence of this effect was seen in the readings and it is considered that no undetected errors were caused by the effect

5.4 Determination of Rates of Movement.

The various distances together with estimates of their errors were plotted against time. Most of the lines where the measurements were of sufficient number, or quality, show some trend of movement. Because the changes over one year are generally of the same order of magnitude as the estimated errors it was decided to try and fit straight lines to the measurements, and thus deduce an average rate of growth.

Straight lines were first fitted by eye. The slope error was also estimated by eye but this was rather difficult. In order to eliminate human bias and to evaluate the errors a statistical treatment was used.

We have distances y_i and times x_i when they were measured. We wish to fit a straight line of form $y = a + bx$ to our y_i, x_i . The y_i and x_i are related by $y_i = a + bx_i + e_i$ where e_i is the error or deviation from the straight line of y_i . The x_i are correct. We assume that e_i is one from a sample with zero mean and normal distribution σ_i . We can find least squares estimates of a and b giving a corresponding estimator \hat{y}_i . The circumflex accent is used to denote the estimate of a given quantity. Given a sample of readings y_i, x_i with errors, it will never be known what the true values are, we can only form estimates of them. The estimator of y_i is \hat{y}_i , where

$$\hat{y}_i = \hat{a} + \hat{b} x_i$$

Let the difference between y_i and \hat{y}_i be d_i

$$d_i = y_i - \hat{y}_i$$

The condition for the best estimators \hat{a}, \hat{b} is

$$S = \sum w_i d_i^2 \quad \text{is a minimum,}$$

where $w_i = 1/\sigma_i^2$

ω_i is a weighting factor and this form can easily be shown to give the least error and is the one widely adopted.

$$S = \sum \omega_i (y_i - \hat{a} - \hat{b}x_i)^2$$

is a minimum with respect to \hat{a} and \hat{b}

Setting $\frac{\partial S}{\partial \hat{a}} = 0$ and $\frac{\partial S}{\partial \hat{b}} = 0$ we obtain the normal equations

$$\hat{a} \sum \omega_i + \hat{b} \sum \omega_i x_i - \sum \omega_i y_i = 0$$

$$\hat{a} \sum \omega_i x_i + \hat{b} \sum \omega_i x_i^2 - \sum \omega_i x_i y_i = 0$$

Solving for \hat{b} we get

$$\hat{b} = \frac{\sum \omega_i y_i \sum \omega_i x_i - \sum \omega_i \sum \omega_i y_i x_i}{(\sum \omega_i x_i)^2 - \sum \omega_i \sum \omega_i x_i^2}$$

We can also get an estimate of the variance of \hat{b} since it is a linear sum of the y_i which each are subject to random errors with standard deviations σ_i

$$\text{Putting } X = (\sum \omega_i x_i)^2 - \sum \omega_i \sum \omega_i x_i^2$$

$$Y = \sum \omega_i x_i \quad Z = \sum \omega_i$$

we can write $\hat{b} = \frac{1}{X} \sum (Y - Z x_i) \omega_i y_i$

Note. The variance σ^2 of a sum of quantities with standard deviations σ_i is given by $\sigma^2 = \sum \sigma_i^2$

The estimate of the variance of \hat{b} is then

$$\hat{V}(\hat{b}) = \frac{1}{X^2} \sum (Y - Z x_i)^2 \omega_i^2 \sigma_i^2$$

This simplifies to

$$\hat{V}(\hat{b}) = \frac{1}{X^2} (Z^2 \sum \omega_i x_i - Z Y^2)$$

This tells us how good the estimate of the slope is. We can set confidence limits on the value of \hat{b} .

$$\hat{a} = \frac{\sum \omega_i y_i}{\sum \omega_i} - \hat{b} \frac{\sum \omega_i x_i}{\sum \omega_i}$$

We can now calculate the d_i . Each d_i is drawn from a sample with standard deviation σ_i so that $\frac{d_i}{\sigma_i}$ will be random with a standard deviation σ of unity.

$$\text{i.e. } \frac{\sum w_i d_i^2}{N-2} = \hat{\sigma}^2$$

where N = number of points

2 = the number of estimated parameters. There are $N-2$ degrees of freedom.

By estimating $\hat{\sigma}$ we can see how well the estimates of σ_i fit. If we get a low value of $\hat{\sigma}$ it means that the error estimates are too large. If we accept the model discussed in section 5.3.5.4 this in turn means that the structure constant k is too large.

A program was written to perform this analysis for each line with three or more measurements and the results were as follows. The results are all from Reykjanes.

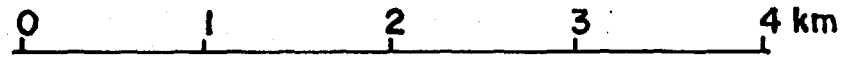
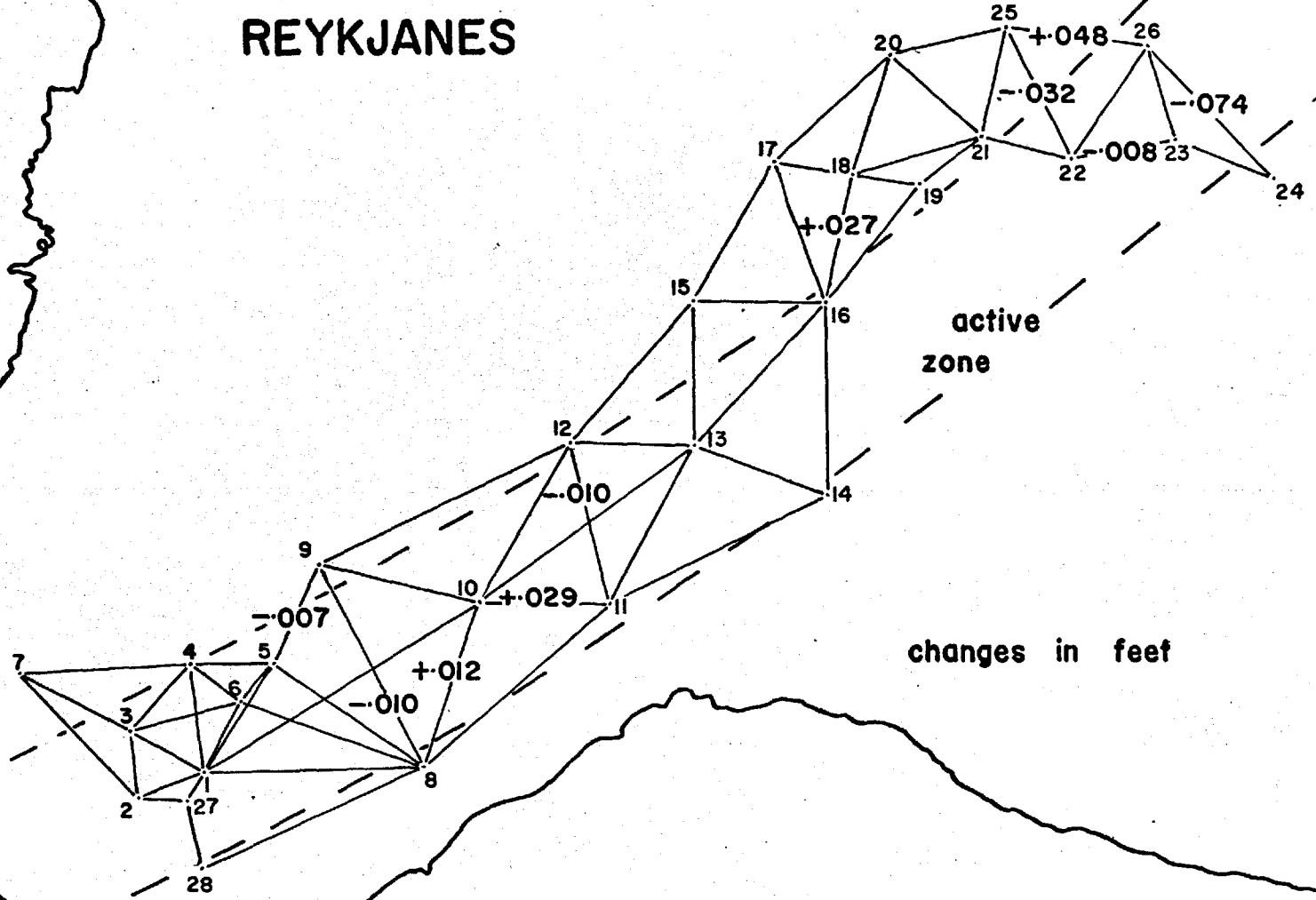
Line	No. of points	Rate of Extn. ft/yr	Standard Devn. of Rate (ft)	$\hat{\sigma}$	Rate by eye ft/yr
1-2	8	0.0026	0.0020	0.3	0.0039
1-3	8	-0.0068	0.0039	0.3	-0.0044
1-4	6	-0.0076	0.0029	0.6	-0.0087
1-5	5	0.0024	0.0023	1.1	0.0052
1-6	6	0.0032	0.0018	0.7	0.0028
1-27	3	0.0038	0.0019	0.1	0.0034
2-3	5	-0.0084	0.0017	0.8	-0.0075
2-7	5	-0.0055	0.0047	0.8	-0.0080
2-27	3	0.0073	0.0034	1.1	0.0072
3-6	4	-0.0129	0.0096	0.7	-0.0122
3-7	5	-0.0036	0.0038	1.0	-0.0040
3-27	3	-0.0155	0.0082	0.5	-0.0114
4-5	5	0.0041	0.0039	0.8	0.0035
4-6	5	-0.0063	0.0033	0.3	-0.0057
5-6	6	0.0107	0.0031	0.3	0.0105
5-8	5	-0.0008	0.0045	1.0	
5-9	4	-0.0067	0.0031	1.4	-0.0078
6-8	4	0.0306	0.0045	1.8	0.0283
8-1	4	0.0141	0.0058	1.2	0.0122
10-8	3	0.0115	0.0069	2.0	0.0056

The line 3-4 was considered as a special case and gave the result -0.0187 ft/year with a standard deviation of 0.0037 ft from 5 points. If we exclude the last reading which seems low we get a $+0.0249$ ft/year with a standard deviation estimated as 0.0095 ft. The reason for treating 3-4 as a special case is that a steam well was opened late in 1968, almost on the line, so that only in high east winds can 3 be seen from 4. Even then the effect will most likely be disturbing. The effect would be that of a large rocket engine firing parallel to the line about two thirds of the way along. The line is now of little value but it might be hoped that the steam will be turned off at some future date. At present the line is of little value and was not used in interpretation.

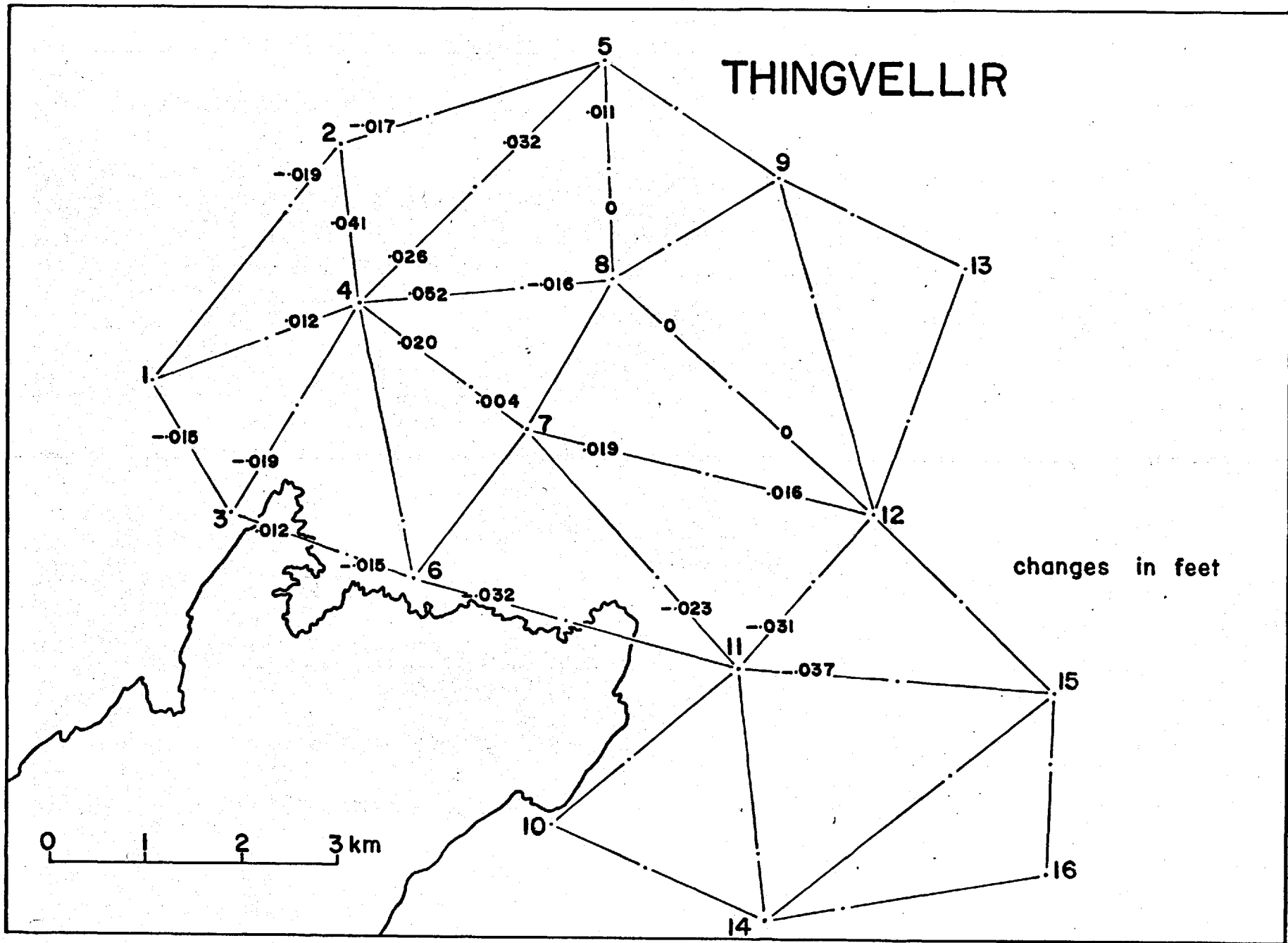
The estimates of $\hat{\sigma}$ are what one would intuitively expect. They measure the amount a particular line deviates from the norm which was considered when making the error estimates. For instance 1-2, 1-3, 4-6 and 5-6 are lines which are parallel to, and only about 10 feet above the ground level for most of their length; these give low values of $\hat{\sigma}$. 1-27 is very short and its standard deviation will be controlled by the phase setting sensitivity rather than atmospheric disturbance.

At the other end of the scale 6-8, and 10-8 are long lines which are high above the ground for most of their length. This sort of behaviour also tends to support the model of temperature structure postulated in section 5.3.5.4. The lines considered span a wide variety of different features, but the value of $\hat{\sigma}$ depends on the change in relief rather than whether the line crosses steam or not.

REYKJANES



THINGVELLIR



Using the values of the standard deviations suggested by the analysis, confidence limits may be put on the rates of movement.

Line	Rate of extensn. (ft/yr)	90% confidence range (ft/yr)	Significant movement ?
1-2	0.0026	0.0013	yes
1-3	-0.0068	0.0022	yes
1-4	-0.0076	0.0036	yes
1-5	0.0045	0.0074	no
1-6	0.0032	0.0021	yes
1-27	0.0038	0.0012	yes
2-3	-0.0084	0.0031	yes
2-7	-0.0055	0.0086	no
2-27	0.0073	0.0236	no
3-6	-0.0129	0.0194	no
3-7	-0.0036	0.0087	no
3-27	-0.0155	0.0026	yes
4-5	0.0041	0.0072	no
4-6	-0.0063	0.0023	yes
5-6	0.0107	0.0020	yes
5-8	-0.0008	0.0100	no
5-9	-0.0067	0.0125	no
6-8	0.0306	0.0235	yes
8-1	0.0141	0.0202	no
10-8	0.0115	0.0868	no

Although some of the lines do not show significant movement they show consistent trends which are significant. Also some of the lines which have only been measured twice show movement although at present there is no method of estimating reliable error limits. These values are taken from the graphs of distance against time and are shown on the network maps.

CHAPTER 6

INTERPRETATION AND CONCLUSIONS

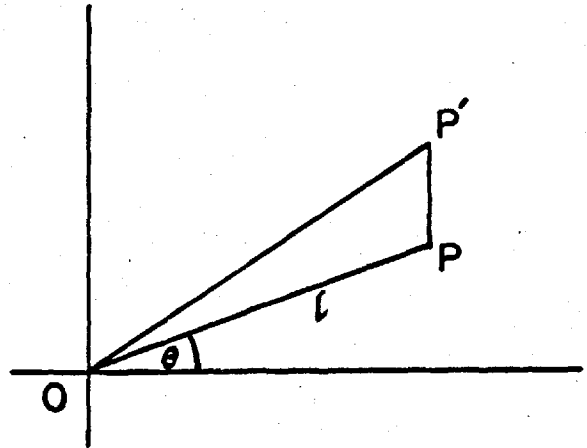
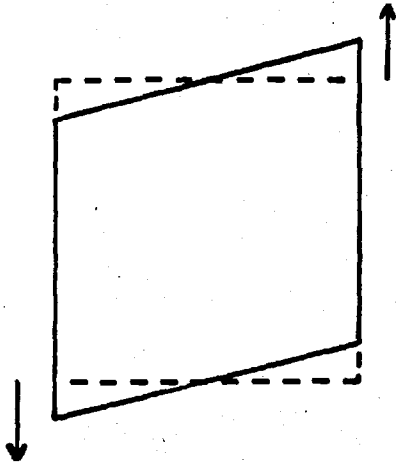
When seeking an interpretation of the measured movements consistent trends must be looked for. The movements may be restricted to a narrow zone or line as would be the case of movement along a fault line, or may be extended over some area. Some movements would not be acceptable. Lines on the horizontal plane must obey plane geometry before and after movement. For instance one triangle cannot contract in an area of general expansion.

6.1 Reykjanes Interpretation.

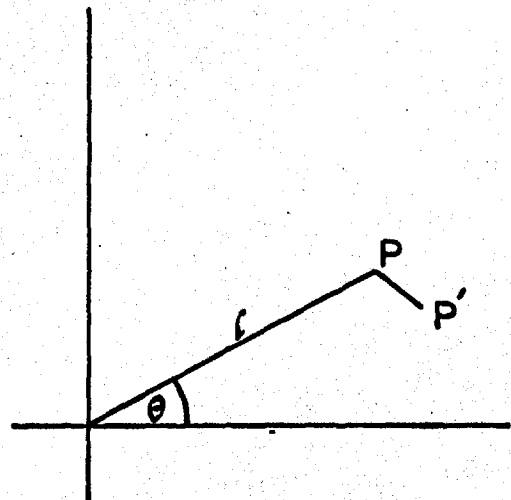
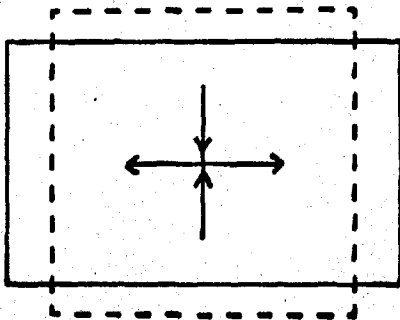
Looking at the southern end of the Reykjanes network there is obvious extension in a north-easterly direction and contraction at right angles to it. This suggests a shear. Geologists distinguish between two types of shear, simple and pure. For small changes the two are equivalent. This may be shown by considering the changes in line length caused by each.

6.1.1 Fitting a shear.

With simple shear consider a line of length l making an angle θ with the direction of zero extension. Relative to O the point P moves to P' . The simple shear is the transformation



SIMPLE SHEAR



PURE SHEAR

which makes the length $PP' = \tau l \cos \theta$ where τ is a constant. The change in the line length OP is $\delta l \approx \tau l \cos \theta \sin \theta$ for small changes.

A pure shear is defined by extension in one direction and contraction at right angles to it. The ratio of extension to contraction may be defined for different circumstances, but for small changes it may be considered unity. For a line OP of length l making an angle θ with the direction of maximum extension, P moves to P' in such a manner that PP' is made up of two components, $al \cos \theta$ in the direction of maximum extension and $-al \sin \theta$ perpendicular to it. The change in line length δl is given by

$$\delta l = al (\cos^2 \theta - \sin^2 \theta)$$

If we rotate the axes used for the simple shear expression through 45° we get

$$\delta l \approx \frac{\tau l}{\sqrt{2}} (\cos^2 \theta - \sin^2 \theta)$$

showing that the two shears are equivalent.

A shear of this form was fitted to the various estimates of rates of change of line length. The shear taking place during one year was considered. Estimates have been made of the rates of extension \hat{r}_i and their standard deviations $\hat{\sigma}_i$ on lines of length l_i and bearing θ_i . The magnitude and direction of a shear is least squares fitted to these results. The expression for the line length changes is not linear in the shear magnitude and bearing so a least squares fit of magnitude was found for each of several chosen bearings. The sum of the residuals squared and weighted was calculated for each assumed bearing and the bearing minimising this sum was found. This

process although tedious by hand is quite efficient on a computer.

Let the bearing of each line of length l_i be θ_i relative to a chosen direction of maximum shear. The estimate of r_i is then given by

$$\hat{r}_i = \hat{a} l_i (\cos^2 \theta_i - \sin^2 \theta_i)$$

To find \hat{a} we minimise the sum

$$S = \sum \omega_i (\hat{r}_i - r_i)^2$$

where $\omega_i = 1/\sigma_i^2$

Setting $\partial S / \partial \hat{a} = 0$ we obtain

$$\hat{a} = \frac{\sum \omega_i r_i (\cos^2 \theta_i - \sin^2 \theta_i)}{\sum \omega_i (\cos^2 \theta_i - \sin^2 \theta_i)}$$

Using this value of \hat{a} we also calculate S .

By repeating this calculation for one degree changes of assumed shear bearing the minimum value of S with respect to \hat{a} and bearing is found.

To find the significance of the result the computer's power for repetitive calculation is again used. An analytic solution to find the standard deviations of \hat{a} and the bearing would be very cumbersome.

The error in a function F of variables $a, b, c \dots$ with errors $\delta a, \delta b, \delta c \dots$ is given by

$$\delta F = \frac{\partial F}{\partial a} \delta a + \frac{\partial F}{\partial b} \delta b + \frac{\partial F}{\partial c} \delta c + \dots$$

This is the familiar Taylor expansion which expresses δF as a linear function in $\delta a, \delta b$ etc. We calculate

$$\left(\frac{\partial F}{\partial a}\right) \sigma_a, \left(\frac{\partial F}{\partial b}\right) \sigma_b$$

by changing in turn each r_i by σ_i and recomputing \hat{a} and the

bearing. From this we get the errors δ_i in \hat{a} and the bearing due to one standard deviation change of r_i .

Since these errors will be independent they should add randomly. Therefore we may estimate the standard deviation of \hat{a} as $\sqrt{\sum \delta_i^2}$ and similarly for the bearing.

This analysis was carried out for the lines within the polygon formed by points 1, 27, 2, 3, 4, 5, 6. This area was chosen because it contains the lines for which there are sound extension rate estimates and it is in what seems a disturbed zone.

6.1.2 The shear fit results.

The results are as follows.

The deformation in the direction of maximum extension is 5.0 parts per million with 90 per cent confidence limits ± 0.65 parts per million.

The bearing of the direction of maximum extension is 53.0° with 90 per cent confidence limits $\pm 4.5^\circ$.

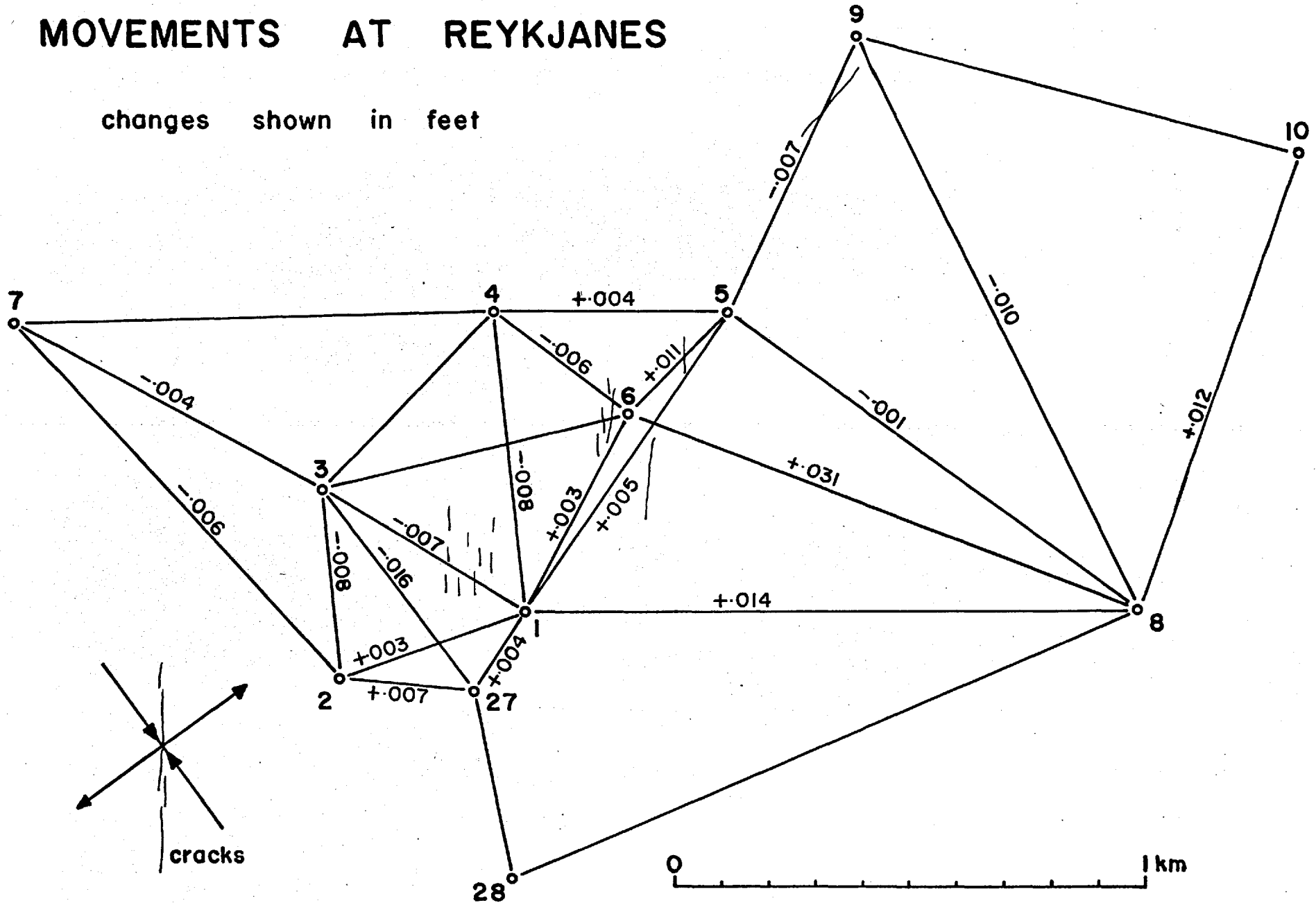
The bearing of the direction of maximum compression is -37.0° with 90 per cent confidence limits $\pm 4.5^\circ$.

The individually fitted line rates were as follows.

Line	Fitted rate	Measured rate
1-2	0.0059 ft/yr	0.0026 ft/yr
1-27	0.0022	0.0038
1-3	-0.0061	-0.0068
1-4	-0.0053	-0.0076
1-5	0.0101	0.0045
1-6	0.0051	0.0032
2-27	0.0006	0.0073
2-3	-0.0031	-0.0084
3-27	-0.0091	-0.0155
4-5	0.0027	0.0041
4-6	-0.0049	-0.0063
5-6	0.0047	0.0107

MOVEMENTS AT REYKJANES

changes shown in feet



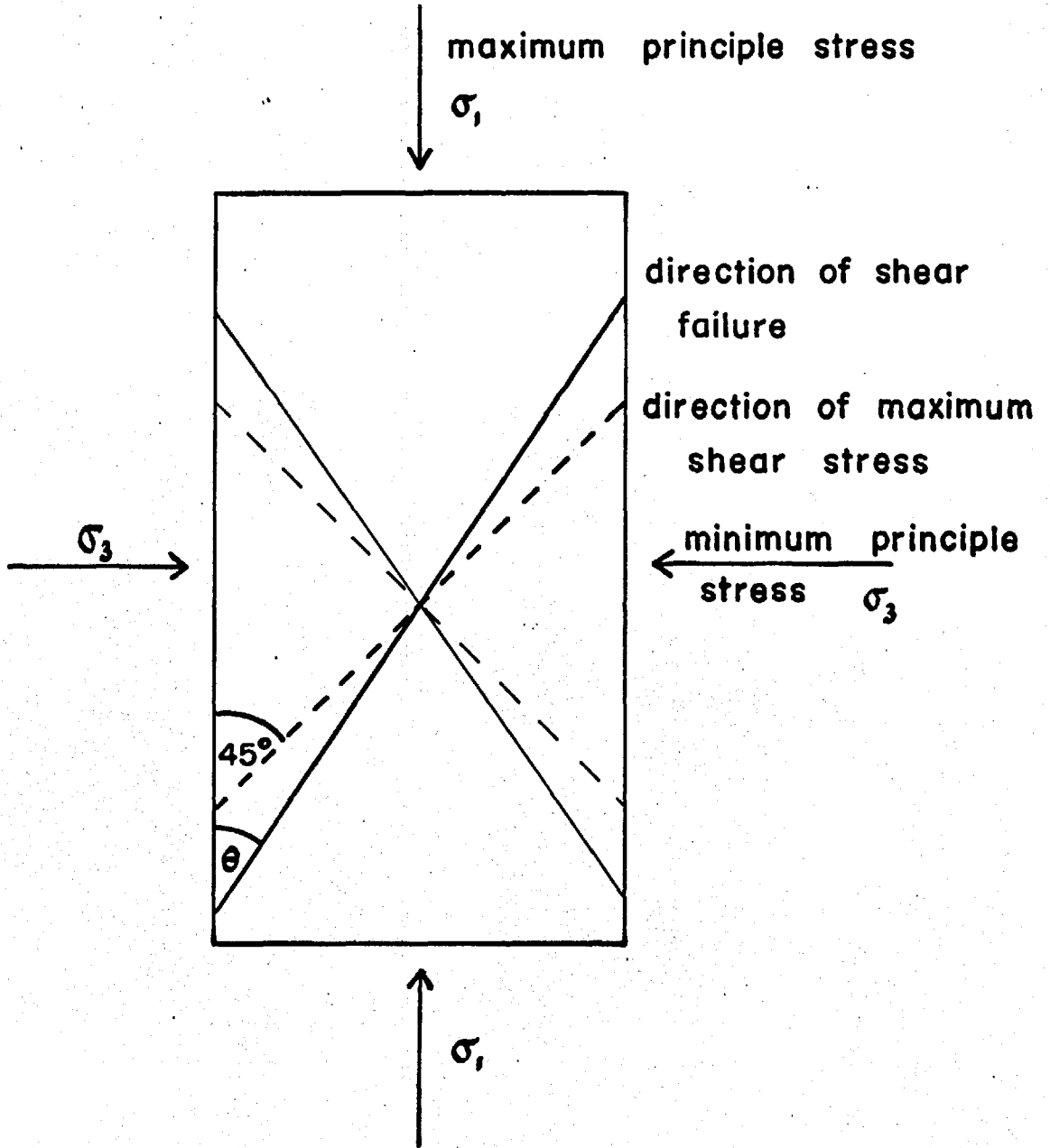
The measured and computed rates agree surprisingly well. Even if the measurements were perfect discrepancies between the measured and fitted values would still be expected because there was cracking on the ground. The strain would not be expected to be uniform over a given area but concentrated along any cracks.

It is interesting to note that the deformations found between the first two measurements just after the 1967 earthquakes were all of an opposite sense to subsequent motion. The first two measurements were 5 and 10 days respectively after the main quakes. These early readings are open to criticism on the grounds of poor measuring technique and using the pillars only one day after they were built. These changes were small and not significant statistically but the fact that each line measured reversed its trend may indicate a period of relaxation immediately after the earthquake. In this period the elastic components of the rock strain may have been partially recovered.

6.1.3 Interpretation of the faulting.

Small cracks appeared on the ground caused by the 1967 earth tremors and their general directions are shown together with the computed directions of maximum extension and contraction. There was some en echelon formation of the cracks suggesting left lateral movement. The cracks have a bearing 0 ± 10 degrees. They thus make an angle of $37^\circ \pm 14^\circ$ with the direction of maximum compression.

From this result an estimate of a quantity known as the coefficient of internal friction of the rock can be made



BEHAVIOUR OF A HOMOGENEOUS

BLOCK UNDER STRESS

using the Navier-Coulomb criterion of brittle failure. A discussion of this may be found in any book on rock mechanics. A simple treatment is given by Price (1966).

The criterion for failure along a surface is

$$\tau = S + \mu_i n$$

where τ is the shear stress acting along the shear surface,

S is the cohesive strength of the rock,

μ_i is the coefficient of internal friction,

and n is the normal stress acting on the shear surface.

This criterion is based upon a simple intuitive model where the force on a rock has to overcome the inherent cohesive strength and then a friction force between the rock particles which will vary with normal pressure as does sliding friction.

By considering the principle stresses acting on an element of rock the normal and shear stresses on any given plane can be computed. The maximum shearing stress occurs at 45 degrees to the direction of maximum compression in the plane containing the maximum and minimum principal compressions. Compressive stresses will be considered positive as seems conventional when dealing with rock stresses.

The angle at which failure will occur will be that for which $\tau - \mu_i n$ is a maximum. This occurs when $\tan 2\theta = 1/\mu_i$; where θ is the angle that the fault plane makes with the direction of maximum stress. Another way of expressing this result is to use the angle of internal friction ϕ_i , where $\mu_i = \tan \phi_i$. Using this we get the result that $\theta = 45 - \phi_i/2$. This shows that the shear plane will make an angle of less than 45° with the maximum stress. The shear plane makes an angle of $\phi_i/2$ with the direction of maximum shear.

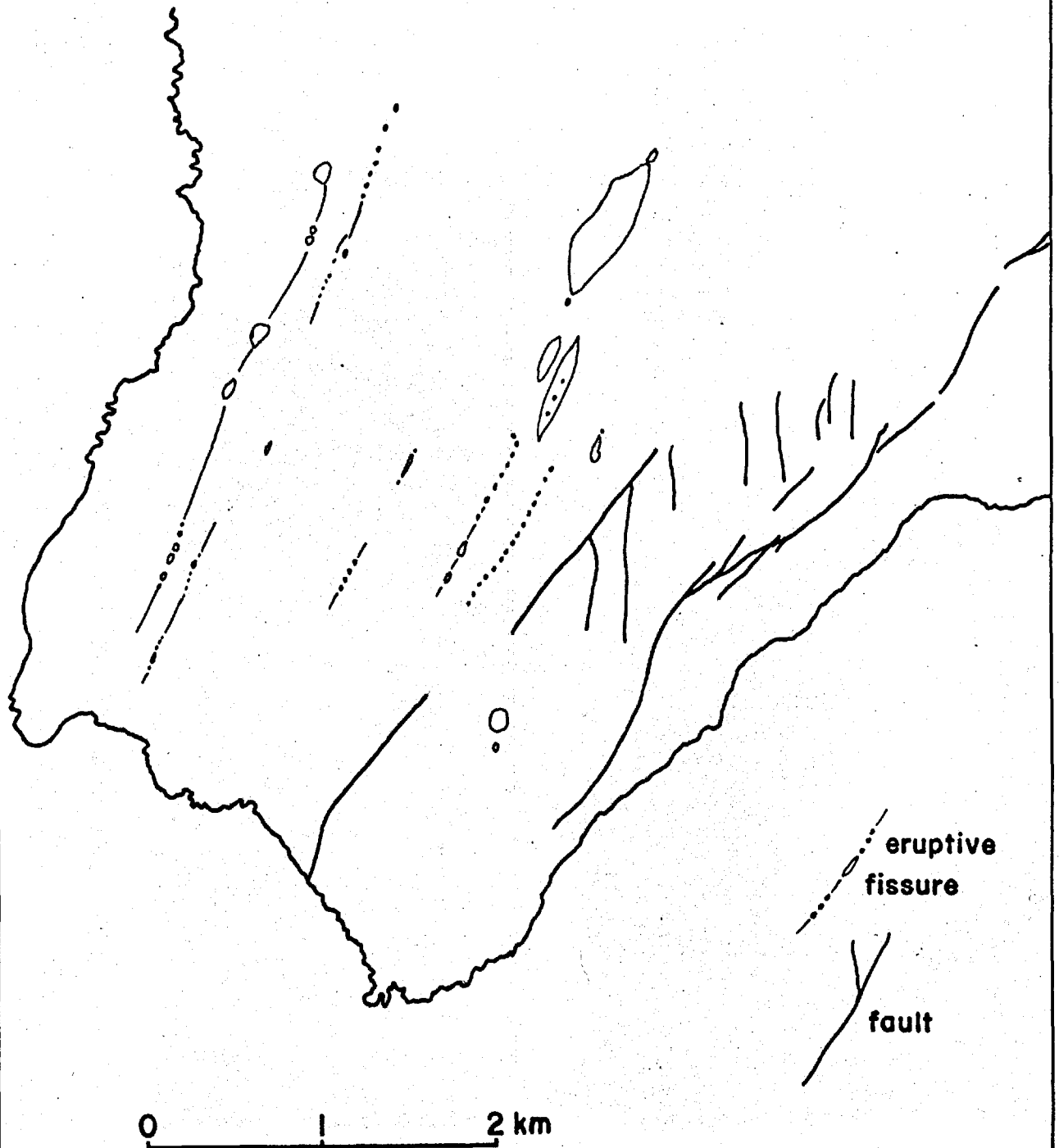
Our results give a value of $\mu_s = 0.29$ or an angle of friction $\phi_s = 16 \pm 28^\circ$. This angle of friction is lower than values obtained by laboratory tests on most rocks. The result is in agreement however with the findings of Ambraseys (1969) who has studied the energy released during earthquakes. Ambraseys explained a value of $\phi_s = 20^\circ - 30^\circ$ by earthquakes occurring on already sheared zones. The Reykjanes peninsula is an earthquake zone which has been heavily fissured and sheared. Basalt in Iceland is seen to be heavily jointed by cooling cracks. It is reasonable to suppose that faulting takes place along these joints giving low values of ϕ_s . It could also be expected that the rock has been considerably weakened in Reykjanes since it is a thermal area.

The area covered by the southern part of the Reykjanes network therefore seems to be subject to a maximum compressive stress in a direction with bearing -37° and a minimum stress at right angles to this. This is giving a maximum linear deformation of 5.0 parts per million and producing cracks which strike at 37° to the maximum stress.

The absence of the complementary set of cracks suggests that the deformation is by a simple shearing process rather than pure shear. The rocks do not show anisotropy which would also give a preferred direction of cracking, although it cannot be stated what the properties might be at depth.

Looking beyond to other parts of the network it can be seen that there is significant extension on line 6-8. Line 1-8 also appears to be extending. This suggests a continuation of the deformation at least part of the way towards point 8.

FAULT MAP OF REYKJANES



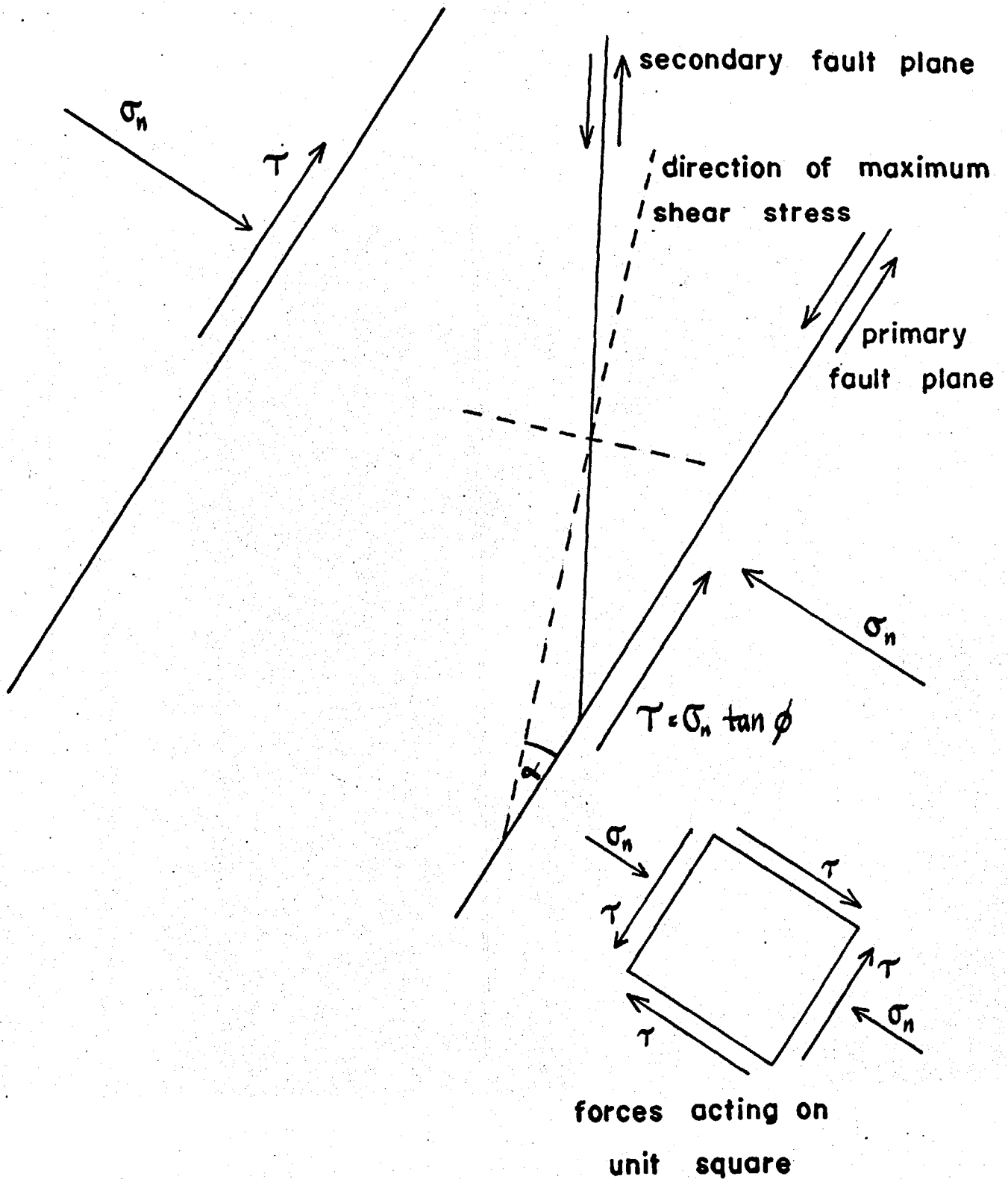
Other lines which seem likely to have changed are 10-11, 18-16, 25-26, which show an increase, and 12-11, 25-22, 26-24, which show a decrease. The changes along all these lines with the exception of 18-16 are consistent with the type of movement suggested for the southern part of the network. The line 18-16 is suspicious as it is the poorest line for measurement in an area where the two repeated measurements indicate little or no movement.

It will be noticed that the movements appear to be taking place on a zone which is on the eastern part of the network. From aerial photographs of the area a distinct pattern of faults can be seen. Unfortunately we have no aerial photograph of the 1967 cracks. The fissures are shown on the map taken from the aerial photographs. There are the north-south cracks which are secondary to larger faults which trend in a direction about 50° east of north. These larger faults are in the direction of the geological trend which is such a notable feature of nearly all of the active zone in southern Iceland. This is the direction of palagonite ridges and their feeder dykes, and the direction of all the large fissures both eruptive and open.

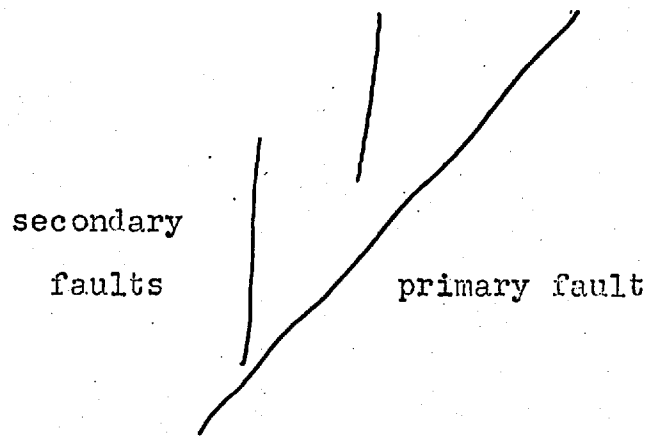
It is believed that the measured movement is caused by the disturbance of the general tectonic forces by these large faults. This disturbance occurs because only limited shear stress can be transmitted across a fault.

To investigate this phenomenon we follow a treatment due to McKinstry (1953). McKinstry investigated the forces acting on a slab of material between two shear planes. The

SECONDARY FAULTING



second shear plane is not necessary for the treatment but is used as a source of equilibrium forces.



Let the shear and normal stresses on the primary shear planes be T and σ_n . The shear stress T_α acting on a plane making an angle α with the primary shear is given by

$$T_\alpha = \sigma_n \cos\alpha \sin\alpha + T \cos^2\alpha - T \sin^2\alpha$$

The direction of maximum shear is obtained by equating $\partial T_\alpha / \partial \alpha = 0$.

This gives

$$\tan 2\alpha = \frac{\sigma_n}{2T} = \frac{1}{2 \tan\phi}$$

where ϕ is the angle of friction along the primary shear.

By using the average bearing of the secondary faults seen on the photographs, $4^\circ \pm 5^\circ$, a more precise estimate of ϕ may be obtained from the fitted strain. Using this value

$\phi_i = 8^\circ \pm 9^\circ$ is obtained. Putting ϕ equal to this angle of internal friction, two values of α namely $37^\circ \pm 10^\circ$ and $127^\circ \pm 10^\circ$ are obtained. The secondary shears should make angles of $\phi_i/2$ with these directions, i.e. the secondary shears should make angles of $41^\circ \pm 5^\circ$ and $123^\circ \pm 15^\circ$ with the primary fault plane. It is the first set which occurs at Reykjanes.

From the photographs the angles between the primary and secondary faults vary between 33° and 47° so the agreement with the calculated values is surprisingly good.

6.2 Generalisations from the Reykjanes Results.

These calculations are really only descriptive at the very best. In the first place the Navier-Coulomb criterion was assumed to derive a value of ϕ_i . This was equated with the angle of friction along the primary fault. In general, one would expect the angle of sliding friction to be less than the angle of internal friction although in jointed rocks there may not be much difference.

The vertical dimension has been ignored through lack of knowledge. For wrench faults, and constant values of ϕ_i , this will not matter. For some rocks however ϕ_i is not constant with varying normal stress, ϕ_i might be expected to increase with depth. For deep wrench faults this would tend to produce an en echelon pattern at the surface. There is slight evidence of this on the large fault at the east of the peninsula. A higher value of ϕ_i should probably be used when considering the larger faults.

Since the earth's crust is not a homogeneous body caution must be exercised when applying particular results to other areas, especially in Iceland where there is considerable variation of physical properties between different lavas. On the other hand, in a region of lava flows the rock is fairly isotropic in the horizontal plane and the differences will occur vertically except in a region of dyke swarms. Also, the

values of parameters derived in the field are more likely to be valid for similar situations than those derived under special conditions in the laboratory.

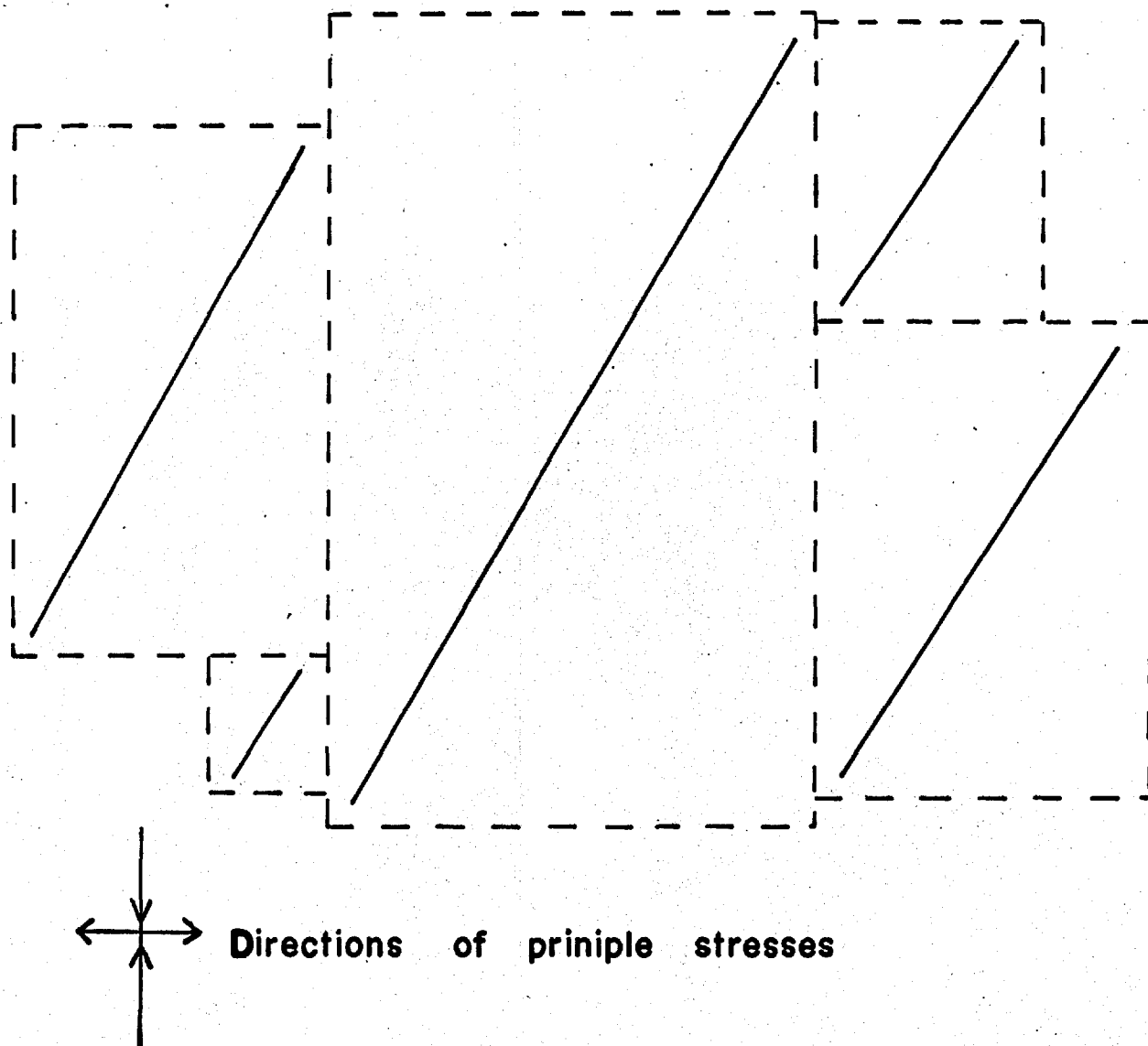
Using the previous result the stress field causing the primary faults with bearing 50° may be postulated. There should be maximum compression in a direction with bearing 13° and minimum compression perpendicular to it, causing extension in a direction with bearing 103° .

Most previous workers have assumed that the fissures in Iceland, particularly those at Thingvellir, are caused by tension perpendicular to the fault plane. This can happen in rock, but usually only at the axes of anticlines or synclines, but is unlikely in Iceland. Furthermore, if the tension were perpendicular to a fault it might be expected that all the tension in the surrounding area might be relieved by that fault, but in fact many parallel faults are found sometimes only separated by a few metres. It is thought that these faults are produced not by any special mechanism but by the usual failure criteria for rock.

A horizontally stressed portion of crust would not produce the high density of faults evident in southern Iceland. It might be expected that the stress field causing the primary faulting would be relieved laterally in the directions of the principal stresses by a distance of the same order as the components of the faults in those directions. The faults would be expected to be spaced as shown.

Clearly, in Iceland, in many regions the faults are much more densely spaced than this. The observed faulting is

FAULT DENSITY

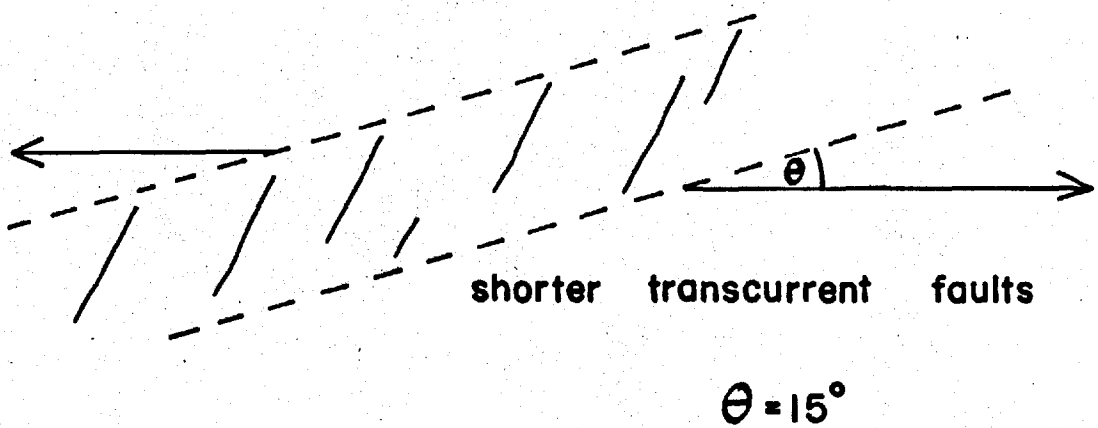
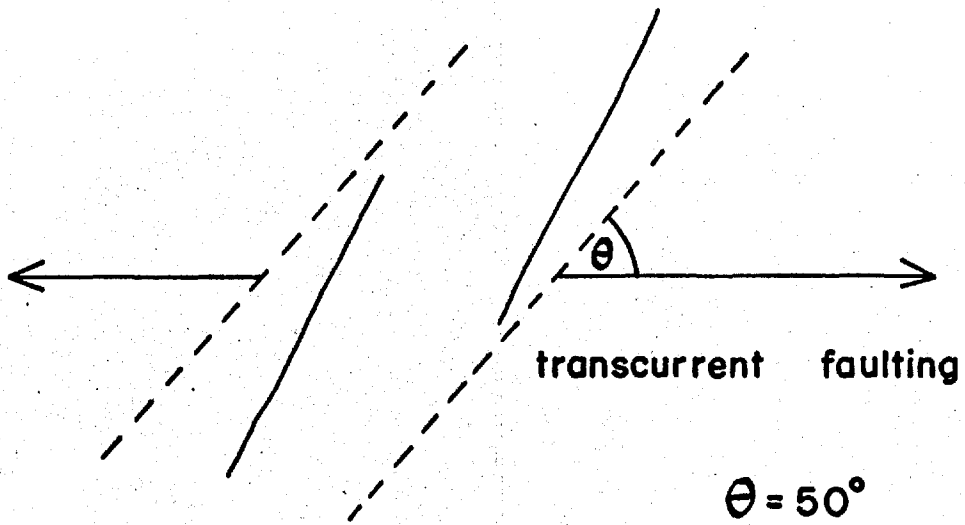
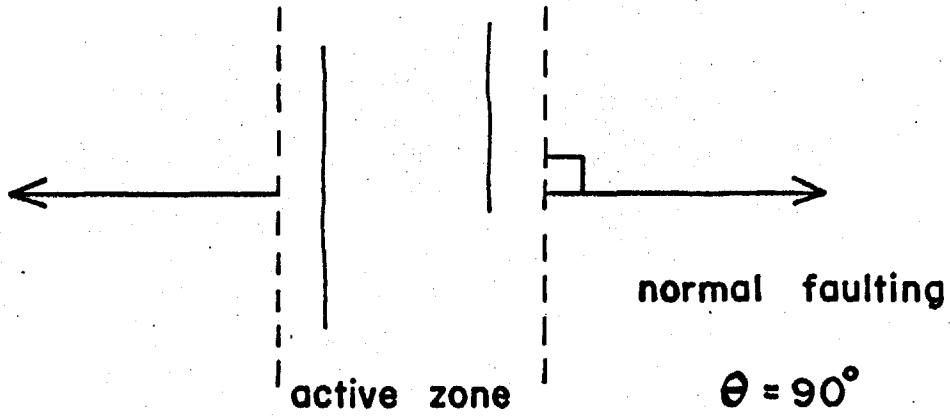


A diagram showing the expected fault density in a uniformly stressed plane.

not readily explained by a two-dimensional model which is equivalent to assuming that the faults are of infinite depth. The high fault density is most likely caused by shear forces being transmitted from below. As depth increases, the pressure and temperature increase, rendering the rock more plastic. At depth, the crustal movement will be by a plastic mechanism. An indication of the depth at which this might occur may be obtained from earthquake studies. Ward et al (1969) recorded micro-earthquakes in Iceland and found that from over 1,000 events most were shallower than 4 km depth, only seven were deeper than 5 km, and only one deeper than 15 km. This would indicate that most of the faulting takes place in the upper 4 km of crust. It is thought that the shearing forces required for the high fault density are transmitted from about 4 km depth. Iceland may be pictured as a brittle crust bonded onto a more plastic basement.

The constancy of the direction of primary faulting, and hence the constancy of the directions of the principal stresses over large areas is direct evidence for the ideas put forward by the theory of rigid plate tectonics (McKenzie, 1967). From the direction of the primary faults in southern Iceland we would expect the extension to take place in a direction east-west.

It is of interest to consider how the ideas of plate tectonics and simple fault theory might explain some of the features in Iceland. The plate boundaries are zones of weakness. These boundaries are marked by the active volcanic zones of Iceland and are extremely narrow in width. If we take



The effects on faulting of the angle θ between plate boundaries and their directions of separation.

post glacial activity and fissuring as marking the extent of the zones it can be seen that the zones are only 5-10 km wide.

Let us consider the effects of the angle θ between the plate boundaries and the direction of plate motion.

For $\theta = 90^\circ$ we would expect mainly normal faulting to develop. By the principle of least energy the faults would favour development along the zones of greatest weakness. This would tend to discriminate against wrench faults, which should make angles of 50° to 68° with the direction of motion depending upon the angle of friction. We would expect graben structures to be formed in the zone.

For $\theta = 50^\circ$ we would expect mainly wrench faults. These wrench faults can be long since they are nearly along the direction of maximum weakness. The motion will tend to open the faults to form open fissures. If this opening extends deep enough the pressure on the rock at depth will be reduced. If the pressure gradient is sufficient, the deep warm rock may become unstable. A reduction in pressure will cause it to become more fluid. If this enables it to relieve the pressure even more, the process will gather momentum and an eruption will result.

The ground between two large faults will be able to subside to form a graben-like structure. The separation in Iceland is sufficiently fast to cause a deficiency of material along the active zone. This produces a gravity low and subsidence along the zone. Precise levelling by Tryggvason (1968) suggests that this subsidence is still continuing at Thingvellir. This subsidence will also cause the horizontal lavas adjacent to the zone to dip towards the zone.

THE TECTONICS OF S.W. ICELAND

Reykjanes

Thingvellir

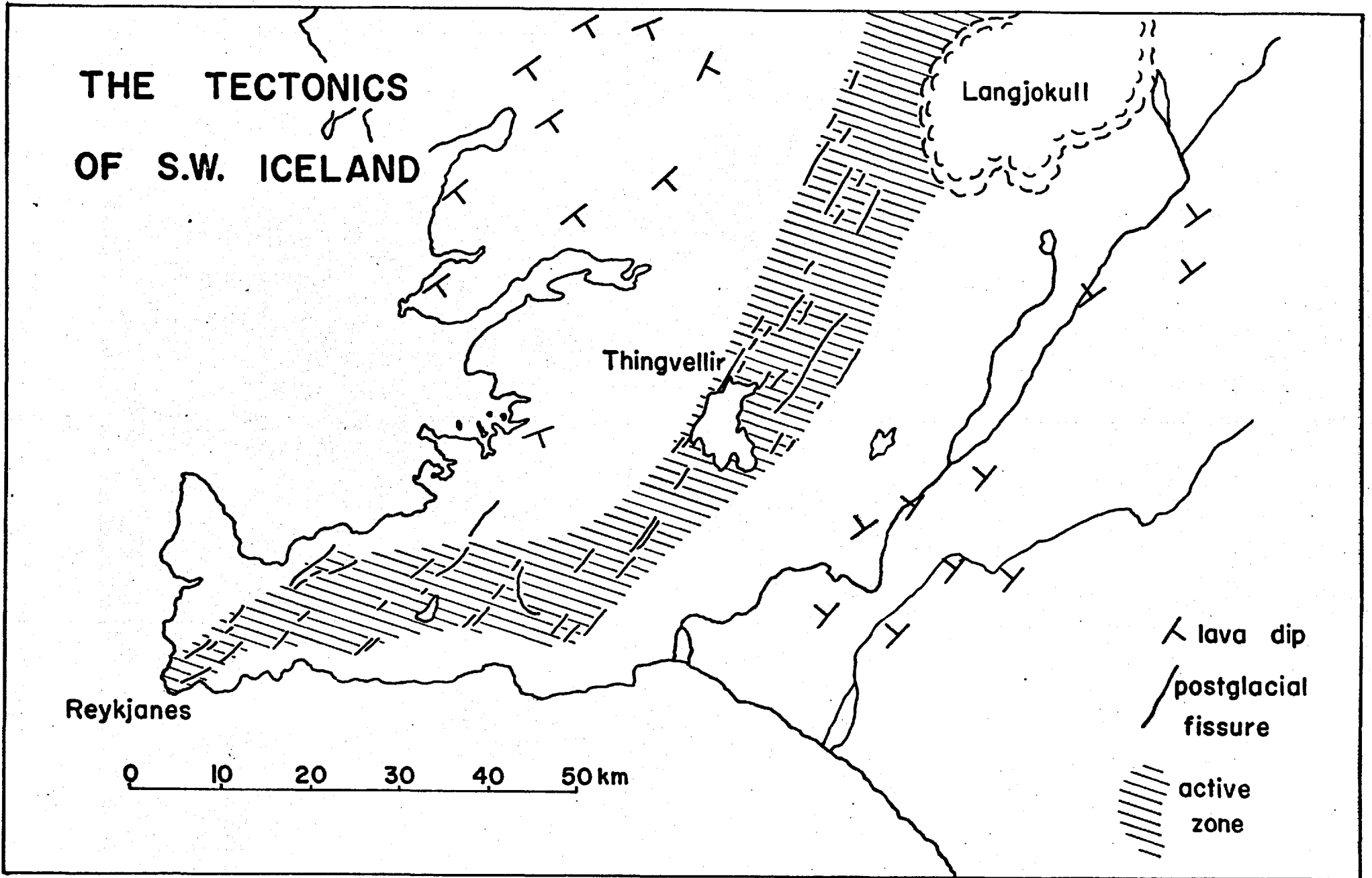
Langjokull

0 10 20 30 40 50 km

^ lava dip

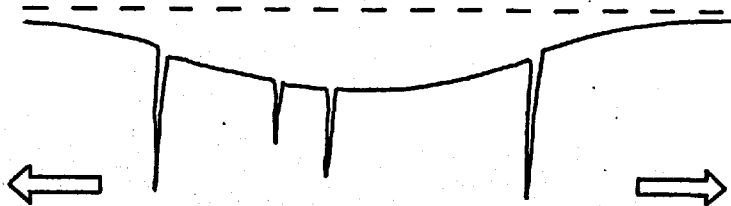
/ postglacial
fissure

||||| active
zone



It is considered that the idea of extension approximately east-west across a zone with bearing 50° explains many of the features observed at Thingvellir.

If the direction of motion makes a smaller angle with the plate boundary wrench faulting would still be expected.



For $\theta = 15^\circ$ the faults would be expected to be shorter as they are crossing the zone of weakness. The extension is spread across a greater distance of the zone so that the opening of the fissures will not be as great.

The subsidence will also be less well marked as it will take place over a greater area. Graben-like structures will not be so easily formed, as the faults are shorter. The dipping of the lavas will also be less pronounced.

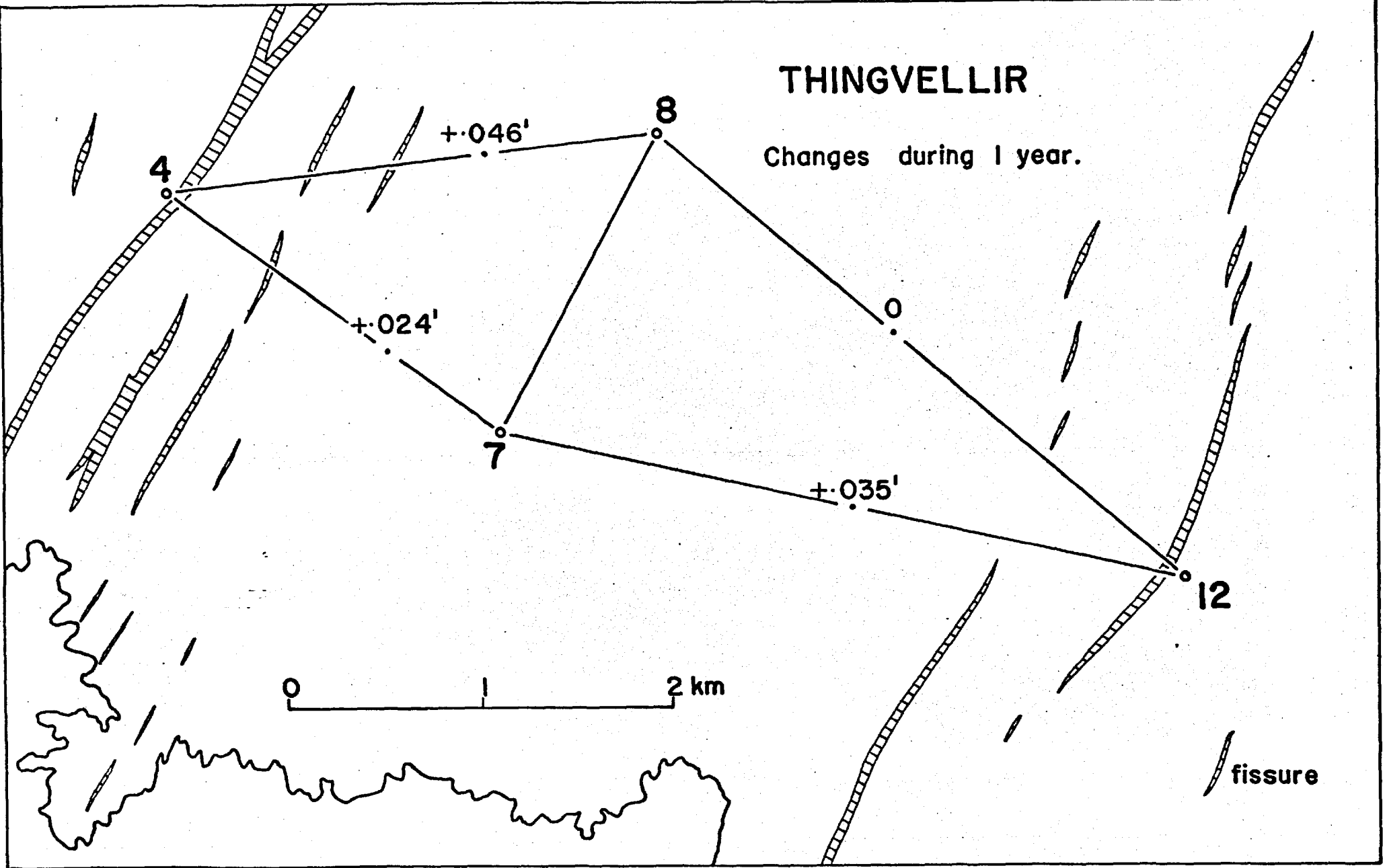
The above situation is thought to apply to the zone between Reykjanes and Hengill. An ocean survey of a similar region would term it a Leaky transform fault (Menard, 1969).

6.3 Interpretation of the Thingvellir Results.

The Thingvellir results are neither of sufficient number nor quality to allow any reasonable interpretation to be made. The lines by the lake are considered to be extremely unreliable.

THINGVELLIR

Changes during 1 year.



fissure

Two paths across the valley have been measured which are over two kilometres from the lake. These are 4-7-12 and 4-8-12. They both show extension. The two path extensions are .046 ft and .059 ft respectively. Looking at the individual extensions also suggests that the extension is greatest in an east-west direction rather than perpendicular to the faults.

It is hoped that further measurements will resolve the movements at Thingvellir.

6.4 The Horizontal Tectonics of Iceland.

It has been suggested that many of the features of south-western Iceland may be explained by an east-west separation across the post glacial volcanic zone. At Reykjanes deformations were measured of five parts per million extending over a zone 2 km wide. If this is the total limit of the present active zone it suggests a present day separation rate of one centimetre per year. This is in agreement with the order of spreading rates suggested by magnetic anomaly work (Heirtzler, 1966) and estimates of rates of extension across open fissures by Bodvarsson and Walker (1964).

The fissure orientation suggests a similar motion might be taking place along the eastern zone. From the frequency of recent eruptions, for example Laki 1783 and Surtsey 1963, it might be supposed that the separation is still taking place.

It seems most probable that the motion across the northern zone is also east-west. This would be by normal faulting. If the western plate is continuous to the west of

THE PLATES OF ICELAND

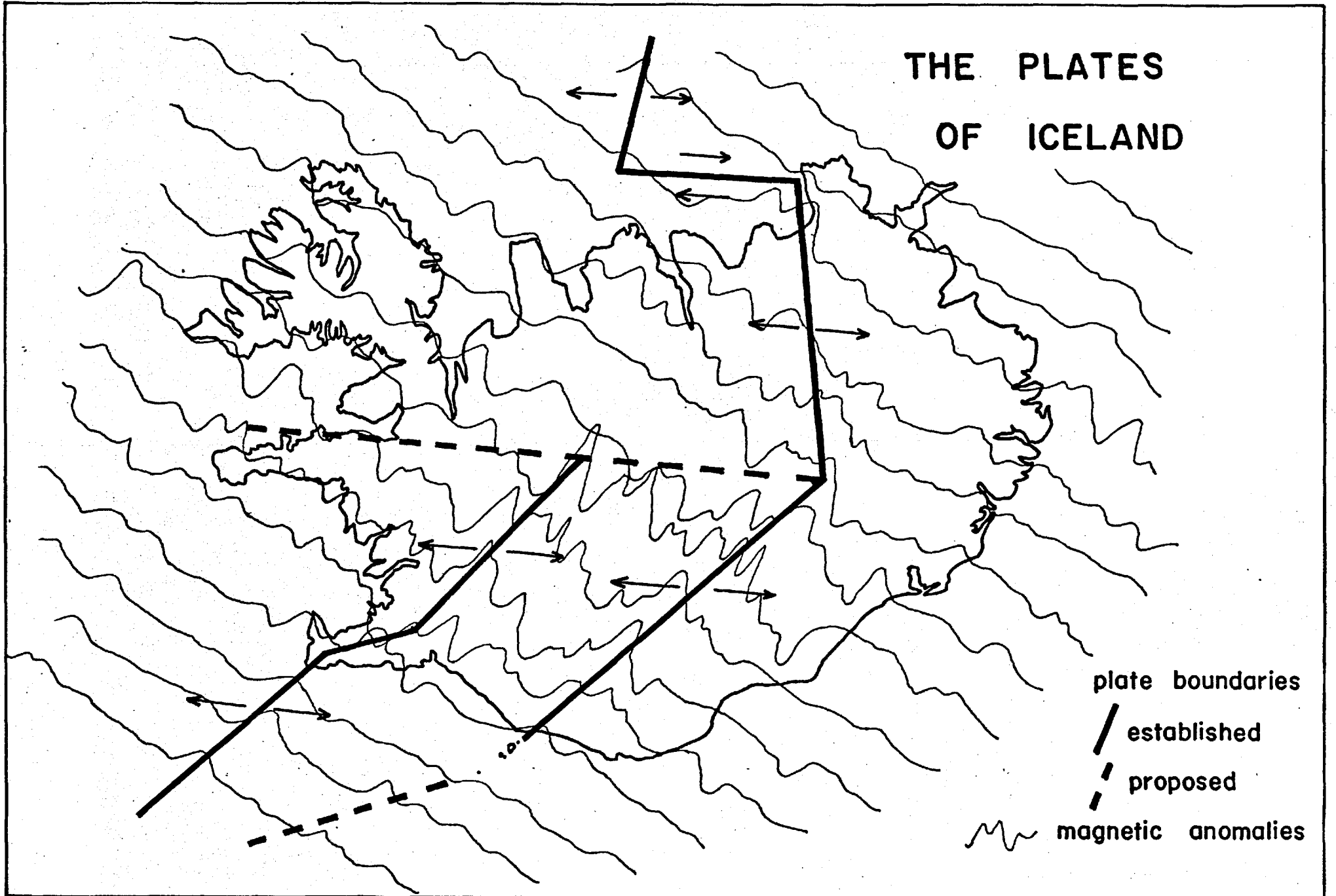


plate boundaries
/ established
- - - proposed
~ magnetic anomalies

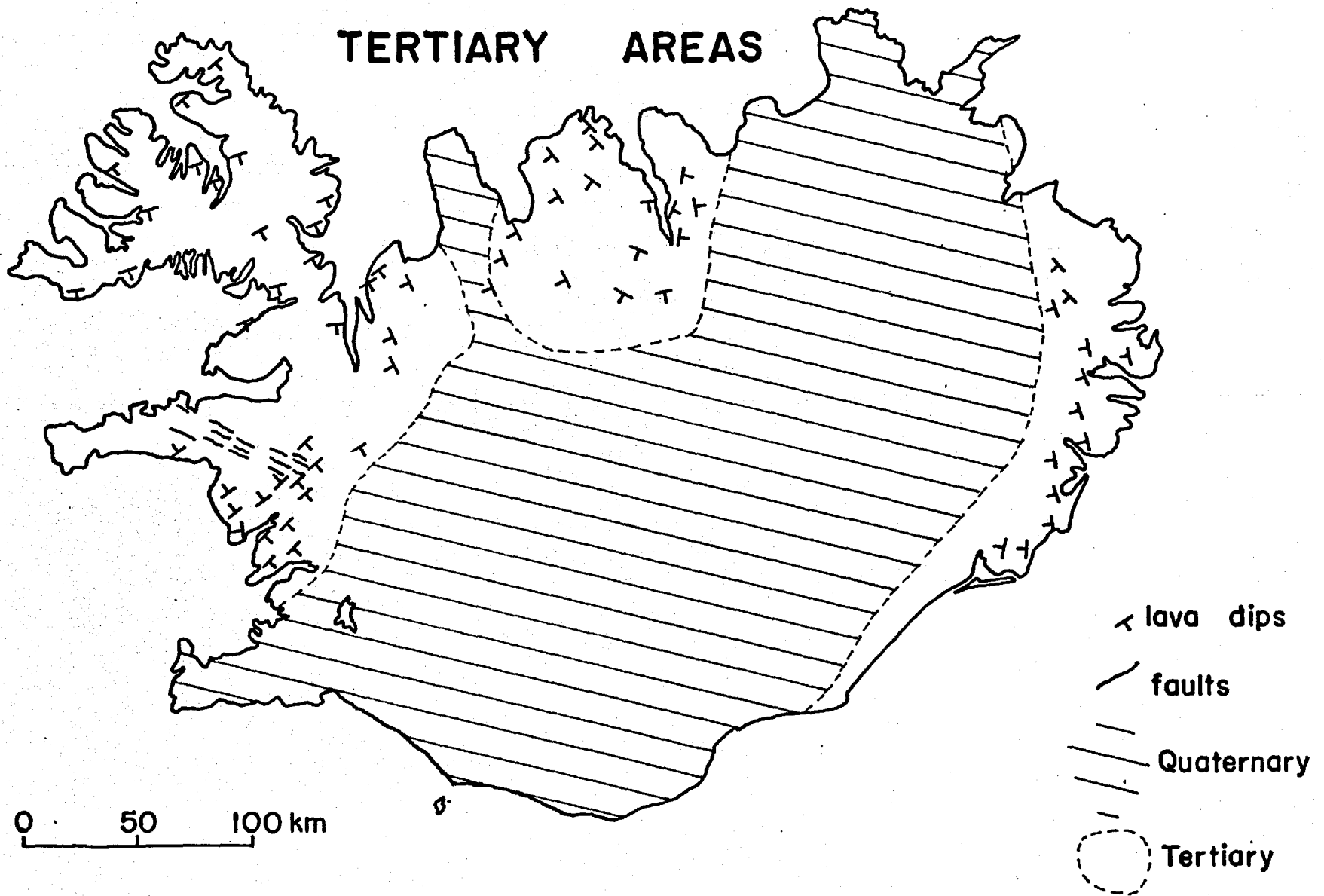
Iceland it will mean that the extension across the northern branch should be equal to the sum of the extensions across the two southern zones. There is however no evidence for this. The rate of extension seems to be about the same as determined by both magnetic work and the measurement of open fissures.

There are two ways in which this difficulty might be explained. The separation might be greater to the south because Iceland is opening by a rotary mechanism with little movement at the north and larger movement at the south.

Another explanation could be that there is a trans-current fault running from near Askja to the Snaefellsness peninsula. This line could conceal a fault because it lies under sand near Askja and under ice and moraine for much of the rest of its length. The reasons for suspecting this line are that there have been several isolated post glacial lava eruptions along it. Also it crosses several large volcanoes including Snaefells, north Langjökull, Hofsjökull and Trolladyngja. It is suggested that an investigation of the recent lava fields, on this line, for faulting might be profitable. This could most easily be done from aerial photographs.

In general it does not appear that it is necessary to assume that spreading is always perpendicular to the fault zone of a mid-ocean ridge, as workers on sea-floor spreading have so far done. Spreading perpendicular to the fault zone does not seem to explain the features observed in Iceland. The change in direction of the active zone in mid-Iceland would require compression to the west or separation to the east to form a

TERTIARY AREAS



three rift system similar to those proposed by Raff (1968) for the S.E. Pacific. There is no evidence for either of these features.

It seems that oblique faults as described fit the observed features more closely. A leaky transform fault is then the case of a very oblique fault.

The most favourable directions for the spreading relative to the active zone are likely to be 90° and 67° - 53° by means of normal and wrench faults respectively. Other directions are possible but would not be expected to be stable in the long term.

If oblique spreading takes place generally some of the directions and rates of spreading inferred from magnetic anomaly work may be in error.

6.5 The Origins of Iceland.

Iceland at the present time seems to behave consistently with its position on a mid-ocean ridge or zone of plate separation. Its separation rate seems to fit well with other parts of the Mid-Atlantic Ridge. There are about 60,000 miles of mid-ocean ridge on the earth; if Iceland is typical one might expect similar islands elsewhere. Iceland is unique however, characterised by its exceptional productivity of lava.

The reason for this may be its position on the Wyville-Thompson ridge which runs from western Scotland and Northern Ireland through the Faeroes and Iceland to Greenland. This ridge was volcanically active during the Tertiary. Western Scotland and Northern Ireland have many basic dykes

striking north-east south-west (Holmes, 1965). The Wyville-Thompson ridge clearly marks a zone of crystal weakness during the Tertiary. It is tempting to suggest that this ridge was a mid-ocean ridge during the early Tertiary. The orientations of the dykes is consistent with east-west extension. It is suggested that magnetic profiles across this ridge should be investigated to give information concerning its past.

During the mid-Tertiary Iceland may have been like the Faeroes. If the plate boundaries changed and took up their present positions Iceland would be expected to be the site of a very major crustal weakness, which would build up into a sizable island. The transition from one set of eruptive zones to another would be complex and the two zones in southern Iceland might be a product of this. It is further thought that the anomalous dips of the old lavas in Iceland are best explained by a north-west south-east trending active zone. These old Tertiary lavas occur in the north-west and west of Iceland. The Icelandic geologist Sigurdsson (1967) working on this area found that dykes and fractures suggested NW-SE compression and hence presumably NE-SW extension.

6.6 Conclusions.

The Mekometer has been successfully used for measuring horizontal strains as small as one part in 10^6 . The accuracy of measurement is at present limited by the temperature determination along the light path. It is thought that the temperature correction should be able to be improved to produce results good to 0.5 parts per million on most lines.

A shearing deformation with a maximum extension of 5.0 ± 0.7 parts per million in a direction $53^\circ \pm 5^\circ$ east of north was measured in an area at Reykjanes. No evidence has been found to suggest that the motion has not occurred at a constant rate during the period of observation, except perhaps immediately after the 1967 earthquakes, when the motion may have been reversed. The surface cracks in this area are consistent with this deformation. The forces required for this deformation could be caused by shearing between the major south-west striking faults.

The major faults and fissures can be explained as being due to various portions of Iceland moving apart from each other in an east-west extension. This is thought to be the origin of vulcanism in Iceland at the present time, and explains the directions of dip of quaternary lavas.

By postulating a mid-ocean ridge running north-west south-east in the early Tertiary an origin of Iceland due to present day processes can be envisaged.

REFERENCES

- Ambraseys, M. Recent Faults and Fault Patterns. A paper given in Symposium on Crustal Movement held at Imperial College, March 1969.
- Badgley, P.C. Structural and Tectonic Principles. Harper and Row, 521 pp.
- Barrel, H. The Dispersion of Air Between 2500A and 6500A. J. Opt. Soc. Am., 41, 5, 1951.
- Bengt, Edlen. The Dispersion of Standard Air. J. Opt. Soc. Am., 43, 5, 1953.
- Bodvarsson, G. and G.P.L. Walker. Crustal Drift in Iceland. Geophys. J. Roy. Astr. Soc., 8, 285-300, 1964.
- Bott, M.H.P. Terrestrial Heat Flow and the Mantle Convection Hypothesis. Geophys. J., 14, 413, 1967.
- Bradsell, R.H. The Electronic Principles of the Mekometer II. Electronic Eng., 38, 459, 1966.
- Bullard, E., J.E. Everette and A.G. Smith. The Fit of Continents Around the Atlantic. Phil. Trans. Roy. Soc. London A., 258, 41, 1965.
- Decker, R.L. Measurement of Horizontal Ground Surface Deformation in Iceland. Trans. Am. Geophys. Union, 49, 114, 1968.
- Dietz, R.S. Continental and Ocean Basin Evolution by Spreading of the Sea Floor. Nature, 190, 854, 1961.
- Ewing, M., J. Ewing and M. Talwani. Sediment Distribution in the Oceans. Bull. Geol. Soc. Am., 75, 17, 1964.
- Froome, K.D. Precision Determination of the Velocity of Electromagnetic Waves. Nature, 181, 4604, 1958.

- Froome, K.D. and R.H. Bradsell. A New Method for the Measurement of Distances up to 5,000 ft by Means of a Modulated Light Beam. *J. Sci. Instr.*, Vol. 43, pp 129-133, 1966.
- Froome, K.D. and R.H. Bradsell. N.P.L. Mekometer III. *Allgemeine Vermessungs Nachrichten*, Heft 4, 1968.
- Funnel, Crustal Spreading and Palaeontology. A paper given in a Symposium on Crustal Movement held at Imperial College, March 1969.
- Gerke, K. Ein Beitrag zur Bestimmung rezenter Erdkrusterbewegungen *Festschrift (Grossman)*, pp 66-78, Wittwer, Stuttgart, 1967.
- Heirtzler, J.R., X. Le Pichon and J.G. Baron. Magnetic Anomalies over the Reykjanes Ridge. *Deep Sea Research*, 13, 427-445, 1966.
- Hess, H.H. History of the Ocean Basins. *Petrological Studies*, Geol. Soc. Am., New York, 1962.
- Holmes, A. Principles of Physical Geology. Thomas Nelson and Sons Ltd., 1944.
- Isacks, B., J. Oliver and L.R. Sykes. Seismology and the New Global Tectonics. *J. Geophys. Res.*, 73, 18, 1968.
- Kasahara, K., A. Okada, M. Shibano, K. Sasaki, S. Matsumoto and M. Hirai. Electro-Optical Measurement of Horizontal Strains Accumulating in the Swarm Earthquake Area (4). *Bull. Earthquake Res. Inst. Tokyo*, 46, 3, 1968.
- Le Pichon, X. Sea-Floor Spreading and Continental Drift. *J. Geophys. Res.*, 73, 3661, 1968.
- Mason, R.G. and A.D. Raff. Magnetic Survey off the West Coast of North America 32°N Latitude to 42°N Latitude. *Bull. Geol. Soc. Am.*, 72, 1259, 1961.
- McKenzie, D. and R.L. Parker. The North Pacific : An Example of Tectonics on a Sphere. *Nature*, 216, 1276, 1967.